NASA TN D-1771

TECHNICAL NOTE

D-1771

SOME CONTROL PROBLEMS ASSOCIATED WITH EARTH-ORIENTED SATELLITES

By Vernon K. Merrick

Ames Research Center
Moffett Field, Calif.

NATIONAL AERONAUTICS AND SPACE ADMINISTRATION
WASHINGTON

June 1963

NATIONAL AERONAUTICS AND SPACE ADMINISTRATION

TECHNICAL NOTE D-1771

SOME CONTROL PROBLEMS ASSOCIATED WITH EARTH-ORIENTED SATELLITES

By Vernon K. Merrick

SUMMARY

A stability and control analysis is made of a class of inertia-wheel-controlled earth satellites whose orientation is controlled relative to a set of orthogonal axes, two of which are the local earth vertical and the normal to the orbital plane. The NASA Nimbus meteorological satellite is a typical example.

It is demonstrated for a restricted but nevertheless important sub-class of these satellites, defined by a particular inertia distribution, that the stability about the local earth vertical (yaw) and the stability of the vehicle angular momentum are independent of each other. This fact is used to extract many fundamental dynamical properties of the system, in particular, the influence, on stability, of the orientation and time constant of the yaw sensing gyro. Furthermore, the analysis gives some insight into the role of gravity torques and into the inherent difficulties involved in the removal of angular momentum from the vehicle.

Performance data for a satellite similar to Nimbus, obtained from digital and analog studies, are used to supplement the stability analysis and to demonstrate transient responses following control commands.

INTRODUCTION

An important class of satellites is one whose mission requirements can be adequately met only by a configuration which is stabilized so that a line fixed in it lies along the local earth vertical or close to it. Such a satellite is usually termed an "earth-oriented satellite" or simply an "earth pointer." Perhaps the most widely discussed type of earth-oriented satellite control system is one which uses a combination of inertia wheels for momentum storage and mass expulsion for momentum removal. Research into the behavior of this type of system has been reported by Roberson in references 1 and 2 and Cannon in reference 3. The work of these investigators has yielded considerable insight into the general dynamical properties of earth-oriented satellites controlled in this way.

The studies reported here are also concerned with the problems and behavior of earth-oriented satellites controlled by inertia wheels. The aim, however, is somewhat different from that of the previously mentioned authors in that a specific type of inertia-wheel control system is investigated in considerable detail. The primary aim of this control system is to provide full three-axis stabilization of the satellite relative to a set of orbit-fixed axes and in addition some measure of angular control (yaw control) about the earth-pointing axis. The essential features of the control system are that it has three inertia wheels with mutually orthogonal spin axes, each inertia wheel receiving signals from a separate attitude sensor. The sensors for the two axes located in the local horizontal plane (pitch and roll axes) are horizon scanners and for the earth-pointing axis (yaw axis) the sensor is a single-degree-of-freedom gyro.

The report is divided into two major sections. The first deals with general theoretical considerations and the second with computed results, both digital and analog, obtained on a typical example of this type of control system. The numerical data used for the example were representative of the Nimbus meteorological satellite at one stage in its development.

The theoretical section commences with considerations basic to a complete understanding of the behavior of the system. Included are some general results for very small and very large control system gains, a discussion of the best gyro orientation from a steady-state point of view and some steady-state results for large angles of yaw. They are followed by an analysis of the linearized equations describing the satellite system both from the stability and steady-state aspects. It is here that the main contributions of the report are to be found. The theoretical part of the report is completed with an analysis which demonstrates the feasibility of minimizing the effects of certain control system failures, in particular, a complete failure of the yaw channel.

The section of the report containing the computed results on a typical satellite is organized so that the topics are introduced in roughly the same order as in the theoretical section. These results are used to strengthen the theoretical arguments and to reveal problems not readily apparent from the theoretical analysis.

SYMBOLS

Reference Frames

All reference frames are right-hand systems.

$\bar{o}_i$ orbital reference frame; $\bar{o}_1$, along the velocity vector of the center of mass, $\bar{o}_2$ normal to the orbital plane, $\bar{o}_3$ along the local vertical, positive towards the center of the earth (See fig. 1.)

$\bar{b}_i$ vehicle principal axes of inertia; $\bar{b}_1$ along roll, $\bar{b}_2$ along pitch, $\bar{b}_3$ along yaw

$\overline{m}_i$ "marked" reference frame, oriented with respect to the $\overline{b}_i$ frame through a constant small error angle matrix

$\overline{d}_i$ actual satellite fixed reference frame of the gyro, oriented with respect to the $\overline{m}_i$ frame through a small error angle matrix

$\overline{s}_{xi}$ actual satellite fixed reference frame of roll sensor, oriented with respect to the $\overline{m}_i$ frame through a small error angle matrix

$\overline{s}_{yi}$ actual satellite fixed reference frame of pitch sensor, oriented with respect to the $\overline{m}_i$ frame through a small error angle matrix

$\overline{c}_i$: $\overline{c}_1 = \overline{IRA}$, $\overline{c}_2 = \overline{ORA}$, $\overline{c}_3 = \overline{SRA}$ reference frame fixed relative to gyro case

$\overline{g}_i$: $\overline{g}_1 = \overline{IA}$, $\overline{g}_2 = \overline{OA}$, $\overline{g}_3 = \overline{SA}$ reference frame fixed relative to gyro gimbal, oriented with respect to the $\overline{c}_i$ frame through the gimbal angle matrix

Angles

(ψ,φ,θ) Euler sequence angles for rotations about the yaw, roll, and pitch axes, respectively

θ_g gyro gimbal angle; angle orienting the $\overline{g}_i$ frame with respect to the $\overline{c}_i$ frame

C_{ij} elements of the direction cosine matrix orienting the gyro fixed reference frame $\overline{c}_i$ with respect to the $\overline{d}_i$ frame

C_{ij}' elements of the direction cosine matrix orienting the gyro fixed reference frame $\overline{c}_i$ with respect to the $\overline{m}_i$ frame

m_{ij} elements of the direction cosine matrix orienting the $\overline{m}_i$ frame with respect to the $\overline{o}_i$ frame

$()_{m/o}$, $()_{d/m}$, $()_{m/b}$, etc. for right-hand rotations in measuring the position of the $\overline{m}_i$ frame with respect to the $\overline{o}_i$ frame, etc.

Angular Rates

$\omega_1,\omega_2,\omega_3$ inertial angular velocity components of the satellite as measured in the $\overline{m}_i$ reference frame

$\omega_{w_1},\omega_{w_2},\omega_{w_3}$ angular velocities of the roll, pitch, and yaw inertia wheels, respectively, measured in the $\overline{m}_i$ reference frame

Inertias

$\left[I_{ij}\right]$ — inertia matrix for the satellite system (with rotating components at rest with respect to the satellite) as measured in the $\bar{m}_i$ reference frame

$\begin{bmatrix} I_1 & 0 & 0 \\ 0 & I_2 & 0 \\ 0 & 0 & I_3 \end{bmatrix}$ — principal inertia matrix, that is, inertia matrix in the $\bar{b}_i$ frame

I_g — polar moment of inertia of a single-degree-of-freedom gyro gimbal

J_1, J_2, J_3 — vehicle inertia parameters in the $\bar{b}_i$ frame;

$$J_1 = \frac{I_2 - I_3}{I_1} \quad , \quad J_2 = \frac{I_1 - I_3}{I_2} \quad , \quad J_3 = \frac{I_2 - I_1}{I_3}$$

Angular Momenta

h_{iw} — variable-speed flywheel angular momenta in $\bar{m}_i$ reference frame

h_{iK} — constant-speed flywheel angular momenta in $\bar{m}_i$ reference frame

H_r — gyro rotor angular momentum about its spin axis

Miscellaneous

C_D — gyro damping coefficient

M_g — gyro torque generator term

K — gyro torque generator feedback constant

ΔM_g — spurious torques about the gyro gimbal axis

$K_\varphi, K_\theta, K_\psi$ — roll, pitch, and yaw control channel gains

ω_o — orbital angular velocity

$\sum T_i$ — torques about the $\bar{m}_i$ reference frame from sources other than wheels or gyros

τ_g — gyro time constant

τ_m — motor flywheel time constant

DESCRIPTION OF THE SATELLITE CONTROL SYSTEM

A schematic block diagram of the satellite control system is shown in sketch (a). Continuous attitude control of the satellite is through the action

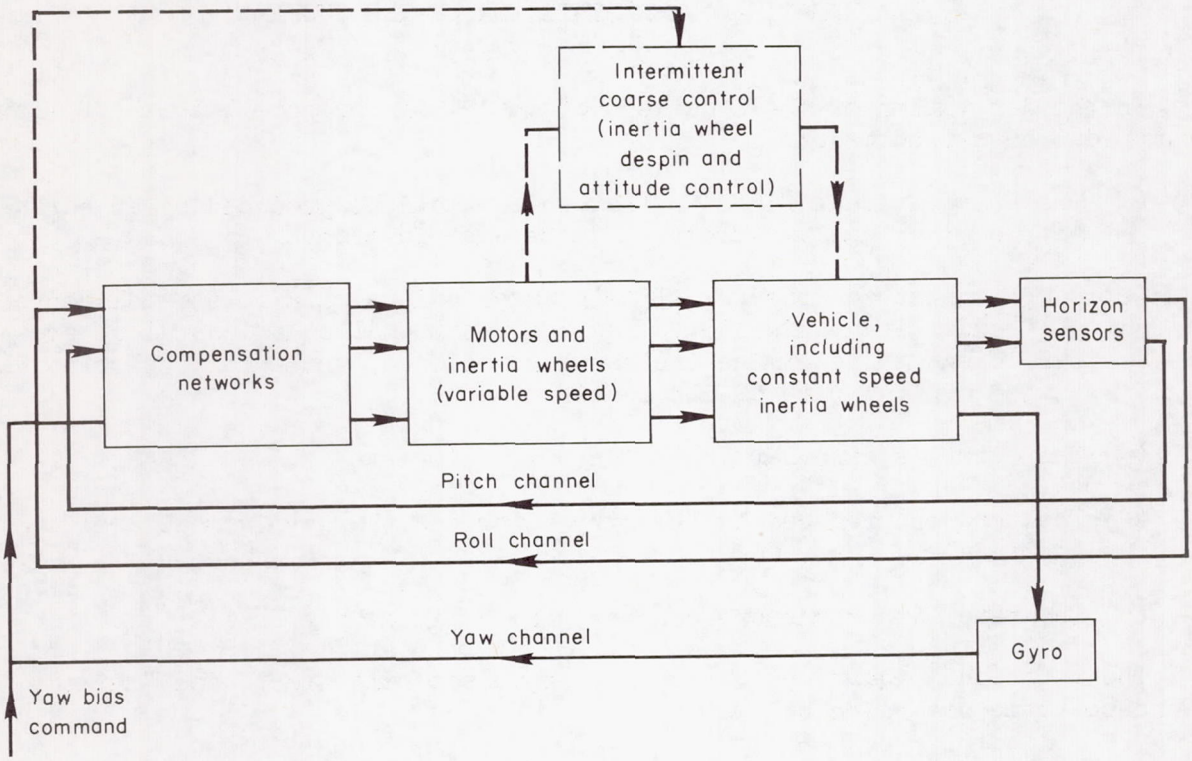

Sketch (a).- Block diagram of satellite control system.

of variable-speed inertia wheels nominally alined along three mutually orthogonal, body-fixed axes. These body axes will subsequently be referred to as the "marked" axes system and are alined as closely as possible to the principal axes of inertia of the satellite. Pitch and roll attitude signals are provided by earth horizon sensors. These signals are passed through compensation networks before being used as command signals to the pitch and roll inertia-wheel motors. The method of measuring angle of yaw makes use of the signal from a single-axis gyro oriented so that it senses a component of the orbital angular velocity proportional to angle of yaw. The output signal from the gyro is passed to compensation networks before being used as the command to the yaw inertia-wheel motor.

The part of sketch (a) shown dotted depicts an additional control system which operates only intermittently and is used both to despin the inertia wheels and to limit the possible attitude deviations of the vehicle. It is not specified further since in this report the concern is only with the continuously operating inertia-wheel part of the over-all control system.

A provision is made in the control system, shown in sketch (a), to inject command or "yaw bias" signals into the yaw control channel. In the case of the Nimbus satellite, this type of command is used to point a solar array at the sun when the sun is not in the orbital plane of the satellite.

MATHEMATICAL REPRESENTATION OF THE SYSTEM

In the derivation of the equations of motion of the satellite the following assumptions have been made:

(1) The gravitational field is that which would be produced by an earth with a spherically symmetrical mass distribution.

(2) Coupling between the satellite's translational and rotational degrees of freedom is negligible. Thus the rotational equations alone are sufficient to determine the angular motion of the satellite relative to the orbital path of its center of mass.

(3) The orbit is circular.

(4) The torques produced by the gyro rotor and the gyro gimbal are negligible.

(5) The satellite structure behaves like a rigid body.

The rotational equations of motion, expressed relative to the "marked" reference frame, are given below:

$$\underbrace{\begin{bmatrix} I_{11}\dot{\omega}_1 + \omega_2\omega_3(I_{33} - I_{22}) + I_{12}\dot{\omega}_2 + I_{13}\dot{\omega}_3 + \omega_1\omega_2 I_{31} - \omega_1\omega_3 I_{21} + I_{23}(\omega_2^2 - \omega_3^2) \\ I_{22}\dot{\omega}_2 + \omega_1\omega_3(I_{11} - I_{33}) + I_{21}\dot{\omega}_1 + I_{23}\dot{\omega}_3 + \omega_2\omega_3 I_{12} - \omega_1\omega_2 I_{32} + I_{13}(\omega_3^2 - \omega_1^2) \\ I_{33}\dot{\omega}_3 + \omega_1\omega_2(I_{22} - I_{11}) + I_{31}\dot{\omega}_1 + I_{32}\dot{\omega}_2 + \omega_3\omega_1 I_{23} - \omega_3\omega_2 I_{13} + I_{21}(\omega_1^2 - \omega_2^2) \end{bmatrix}}_{\text{Rigid vehicle}}$$

$$= \underbrace{-\begin{bmatrix} \dot{h}_{1W} \\ \dot{h}_{2W} \\ \dot{h}_{3W} \end{bmatrix} - \begin{bmatrix} \omega_2 h_{3W} - \omega_3 h_{2W} \\ \omega_3 h_{1W} - \omega_1 h_{3W} \\ \omega_1 h_{2W} - \omega_2 h_{1W} \end{bmatrix}}_{\substack{\text{Variable-speed} \\ \text{flywheels}}} + 3\omega_o^2 \underbrace{\left\{ \begin{bmatrix} -J_1 I_1 \varphi_{m/o} \\ -J_2 I_2 \theta_{m/o} \\ 0 \end{bmatrix} + \begin{bmatrix} J_1 I_1 \varphi_{m/b} \\ J_2 I_2 \theta_{m/b} \\ 0 \end{bmatrix} \right\}}_{\text{Gravity torques}} - \underbrace{\begin{bmatrix} \omega_2 h_{3K} - \omega_3 h_{2K} \\ \omega_3 h_{1K} - \omega_1 h_{3K} \\ \omega_1 h_{2K} - \omega_2 h_{1K} \end{bmatrix}}_{\substack{\text{Constant-speed} \\ \text{flywheels}}} + \underbrace{\begin{bmatrix} \Sigma T_1 \\ \Sigma T_2 \\ \Sigma T_3 \end{bmatrix}}_{\substack{\text{Torques from sources} \\ \text{other than} \\ \text{wheels or} \\ \text{gyros}}} \qquad (1)$$

The equation of motion of the combined gimbal and rotor of the single-degree-of-freedom gyro is:

$$I_g\ddot{\theta}_g + C_D\ddot{\theta}_g = \left\{-I_g(C_{21}\dot{\omega}_1 + C_{22}\dot{\omega}_2 + C_{23}\dot{\omega}_3) + H_r[(C_{11} - C_{31}\theta_g)\omega_1 + (C_{12} - C_{32}\theta_g)\omega_2 + (C_{13} - C_{33}\theta_g)\omega_3]\right\} - I_g[(-\psi_{d/m}C_{22} + \theta_{d/m}C_{23})\dot{\omega}_1 + (\psi_{d/m}C_{21} - \varphi_{d/m}C_{23})\dot{\omega}_2 + (-\theta_{d/m}C_{21} + \varphi_{d/m}C_{22})\dot{\omega}_3] + H_r[(-\psi_{d/m}C_{12} + \theta_{d/m}C_{13})\omega_1 + (\psi_{d/m}C_{11} - \varphi_{d/m}C_{13})\omega_2 + (-\theta_{d/m}C_{11} + C_{12}\varphi_{d/m})\omega_3] + M_g \tag{2}$$

where, in general, $M_g = -K\theta_g + \Delta M_g$.

The relationship between the inertial angular velocities (ω_1, ω_2, and ω_3) and the Euler angles and Euler angle rates are given by the following expressions:

$$\left.\begin{aligned}
\omega_1 &= \dot{\varphi}_{m/o}\cos\theta_{m/o} - \dot{\psi}_{m/o}\sin\theta_{m/o}\cos\varphi_{m/o} - \omega_o(\sin\varphi_{m/o}\sin\theta_{m/o}\cos\psi_{m/o} + \cos\theta_{m/o}\sin\psi_{m/o}) \\
\omega_2 &= \dot{\theta}_{m/o} + \dot{\psi}_{m/o}\sin\varphi_{m/o} - \omega_o\cos\varphi_{m/o}\cos\psi_{m/o} \\
\omega_3 &= \dot{\psi}_{m/o}\cos\theta_{m/o}\cos\varphi_{m/o} + \dot{\varphi}_{m/o}\sin\theta_{m/o} - \omega_o(-\cos\theta_{m/o}\sin\varphi_{m/o}\cos\psi_{m/o} + \sin\theta_{m/o}\sin\psi_{m/o})
\end{aligned}\right\} \tag{3}$$

Equations (1), (2), and (3) are well known and many derivations of various forms of them have been published (see, e.g., ref. 1).

The equations closing the roll, pitch, and yaw control loops are assumed to be of the following general form:

$$\text{Roll} \qquad h_{1w} = K_\varphi F_\varphi(s)\varphi_{sx/o} \tag{4}$$

$$\text{Pitch} \qquad h_{2w} = K_\theta F_\theta(s)\theta_{sy/o} \tag{5}$$

$$\text{Yaw} \qquad h_{3w} = K_\psi F_\psi'(s)\left(-\frac{\theta_g}{G}\right) \tag{6}$$

where

$$G(\text{gyro constant}) = \frac{H_r}{K - H_r\omega_o C_{32}}$$

and

$$\theta_g(\text{gyro gimbal angle}) = \frac{G[(C'_{11}s+C'_{13}\omega_o)\varphi_{m/o}+C'_{12}s\theta_{m/o}+(C'_{13}s-C'_{11}\omega_o)\psi_{m/o}+M_g-C'_{12}\omega_o]}{1+\tau_g s}$$

The development of the gyro gimbal expression from equation (2) is given in detail in appendix A. The quantities K_φ, K_θ, and K_ψ are the control loop gains, and the transfer functions $F_\varphi(s)$, etc., represent the combined behavior of the horizon sensors, inertia-wheel motors, and compensation networks. It is assumed that the transfer functions $F_\varphi(s)$, etc., are rational algebraic functions of the Laplace transform variable s.

GENERAL DYNAMICAL BEHAVIOR OF THE SATELLITE

Sources of Coupling Between the Degrees of Freedom

An important problem that exists for all earth-oriented satellites is caused by the set of axes, relative to which the satellite is to be stabilized, rotating with respect to inertial space. In the notation of figure 1, the roll and yaw axes rotate relative to inertial space with orbital angular velocity, while the pitch axis remains fixed relative to inertial space. Therefore, any disturbance in the orbital plane which is constant relative to inertial space has oscillatory components along both the roll and yaw axes and, clearly, these components are 90° out of phase. It follows that the rotation of the reference frame itself causes coupling between the roll and yaw degrees of freedom.

In general, the gyro in the control system of sketch (a) will produce a signal which consists of a relatively complex mixture of yaw, roll, and pitch information, the proportions of each being dictated by the gyro orientation within the satellite. It follows that the gyro must tend to introduce coupling between the degrees of freedom although, in some cases, it may be sufficiently weak to be neglected in the analysis. An important special case of this type of control system, and one which will be treated in some detail later in this report, is a system in which the gyro is oriented so that its input axis is located in the roll-yaw plane of the satellite. In this case it is always possible to a first approximation to treat the stability and transient response of the combined roll and yaw degrees of freedom separately from the pitch degree of freedom.

The Roll of Gravity Torques

Gravity torques play a particularly important role in the dynamics of earth-oriented satellites. This can be demonstrated in the following very general way. Let $\bar{G}$ be the vector gravity torque acting on the satellite, and $\bar{\omega}_o$ the vector angular velocity of the orbital reference frame relative to inertial space. The rotational equations of motion of the satellite are:

$$\dot{\bar{H}} + \bar{\omega}_o \times \bar{H} = \bar{G} \qquad (7)$$

It is assumed here that no external torques other than gravity torques act on the satellite. The vectors $\bar{H}$, $\bar{G}$, and $\bar{\omega}_o$ expressed in terms of their components along the $\bar{o}_1$, $\bar{o}_2$, $\bar{o}_3$ directions (orbital reference frame) are:

$$\bar{H} = \bar{o}_1 H_1 + \bar{o}_2 H_2 + \bar{o}_3 H_3 \tag{8}$$

$$\bar{G} = \bar{o}_1 G_1 + \bar{o}_2 G_2 + \bar{o}_3 G_3 \tag{9}$$

$$\bar{\omega} = -\bar{o}_2 \omega_o \tag{10}$$

Thus equation (4) resolved along the $\bar{o}_1$, $\bar{o}_2$, $\bar{o}_3$ directions becomes

$$\dot{H}_1 - \omega_o H_3 - G_1 = 0 \tag{11}$$

$$\dot{H}_2 - G_2 = 0 \tag{12}$$

$$\dot{H}_3 + \omega_o H_1 - G_3 = 0 \tag{13}$$

If the gravity torque terms G_1 and G_3 were missing from the equations, then equations (11) and (13) would represent an undamped sinusoidal oscillation of orbital frequency $\omega_o/2\pi$ in the momentum components H_1 and H_3. This leads to the conclusion that if the satellite system is to be damped, then gravity torques must be present.

The Effect of Magnitude of the Gain

The selection of the final compensation networks and gains required for satisfactory dynamic behavior of the class of satellite control systems under discussion, as with most multivariable, multigain control systems, is somewhat a matter of trial and error. In this case, however, it is possible to deduce some important general properties of the system by examining its behavior as the gain parameters K_φ, K_θ, and K_ψ simultaneously tend to either very small or to very large values.

When the gains all tend to zero, the system is completely uncontrolled, that is, h_{1w}, h_{2w}, and h_{3w} are all zero. A considerable amount of work has been carried out elsewhere on the subject of the uncontrolled motion of a satellite and it is not proposed to repeat this work here except to quote the main results. These are that the energy transferred to a satellite from an outside disturbance remains constant in the absence of further disturbances (i.e., the motion is undamped) and furthermore the motion is completely governed by the torques produced by gravity gradients (gravity torques).

Perhaps more interesting is the case when the gains K_φ, K_θ, and K_ψ are all very large. It can be readily seen from equations (4), (5), and (6) that the

set of variables describing the motion of the satellite body (i.e., $\varphi_{m/o}$, $\theta_{m/o}$, $\psi_{m/o}$) and their derivatives must all be small compared to the inertia-wheel angular momenta h_{1w}, h_{2w}, and h_{3w}. When the gains tend to infinitely large values, the equations of motion (eqs. (1)) become[1]

$$I_{23}\omega_o^2 = -\dot{h}_{1w} + \omega_o h_{3w} + 3\omega_o^2 J_1 I_1 \varphi_{m/b} + \omega_o h_{3K} \tag{14}$$

$$0 = -\dot{h}_{2w} + 3\omega_o^2 J_2 I_2 \theta_{m/b} \tag{15}$$

$$-I_{21}\omega_o^2 = -\dot{h}_{3w} - \omega_o h_{1w} - \omega_o h_{1K} \tag{16}$$

These equations fall naturally into two independent groups, one containing the pitch equation (eq. (15)) and the other containing the roll and yaw equations. The pitch equation when integrated yields

$$h_{2w} = 3\omega_o^2 J_2 I_2 \theta_{m/b} t \tag{17}$$

where it is assumed that $h_{2w} = 0$ when $t = 0$. This equation indicates that the pitch wheel speed increases linearly with time at a rate proportional to the pitch control axis misalinement angle $\theta_{m/b}$. The implications of this are discussed in a later section on control axes misalinements.

The roll and yaw equations when integrated yield

$$h_{1w} = A \cos(\omega_o t + \epsilon) - h_{1K} + \omega_o I_{21} \tag{18}$$

$$h_{3w} = A \sin(\omega_o t + \epsilon) - h_{3K} - \omega_o(3J_1 I_1 \varphi_{m/b} - I_{23}) \tag{19}$$

where A and ϵ are constants depending on the initial conditions. It follows from equations (18) and (19) that there is an undamped sinusoidal oscillation in the roll and yaw inertia wheels and they are exactly 90° out of phase with each other. This implies that any energy from external disturbances that is imparted to the roll and yaw degrees of freedom is transferred entirely to the roll and yaw inertia flywheels where it remains indefinitely. Since, with both zero and infinite gains, the system has a mode of oscillation with zero damping, then (for given compensation networks, inertia-wheel-motor time constant, and gyro time constant and provided the system is stable for all finite nonzero values of the gains) there must be a set of finite gains which result in the maximum damping of the system.

---

[1]Equations (14), (15), and (16) are derived in the following way: The quantities $\varphi_{m/o}$, $\theta_{m/o}$, $\psi_{m/o}$ and their derivatives are put equal to zero in equations (3). This yields $\omega_1 = 0$, $\omega_2 = -\omega_o$, $\omega_3 = 0$ which are then substituted into equations (1).

Gyro Orientation Within the Satellite

Examining the steady-state gyro output signal, $\theta_{g(steady)}$, (the error signal used to drive the yaw inertia-wheel motor) will give some indication of the influence of input axis orientation on the ability of the gyro to control the satellite yaw attitude. An expression for $\theta_{g(steady)}$ when the vehicle orientation angles are small can readily be obtained from equation (A6) by setting the Laplace transform variable s equal to zero, that is,

$$\theta_{g(steady)} = \frac{H_r}{K - H_r\omega_o C_{32}}\left(C'_{13}\omega_o\varphi_{m/o} - C'_{11}\omega_o\psi_{m/o} + \frac{\Delta M_g}{H_r} - C'_{12}\omega_o\right)$$

or

$$\theta_{g(steady)} = \frac{-C'_{11}\psi_{m/o} - C'_{12} + C'_{13}\varphi_{m/o} + (\Delta M_g/H_r\omega_o)}{(K/H_r\omega_o) - C_{32}} \tag{20}$$

where the quantity ΔM_g represents any spurious torque acting about the gyro gimbal axis and the quantity K is the torque generator feedback gain when the gyro is operating in the rate mode ($K = 0$ when the gyro is operating in the integrating mode).

The interesting point about equation (20) is that, provided C_{32} is nonzero, it shows there is no fundamental difference in the steady-state behavior of the integrating and rate gyros. This is due entirely to the fact that the frame of reference relative to which the satellite is to be stabilized is itself rotating relative to inertial space with orbital angular velocity ω_o.[2] This becomes very apparent if ω_o is made equal to zero in equation (20). The steady-state gimbal angle for a rate gyro is then equal to zero or $\Delta M_g/K$, depending on whether or not ΔM_g is zero, while for the integrating gyro it is equal to $(-C'_{11}\psi_{m/o} - C'_{12} + C'_{13}\varphi_{m/o})/-C_{32}$ or infinity, depending on whether or not ΔM_g is zero.

An immediate deduction from equation (20) is that, if the gyro signal is to be used to control angle of yaw, then C'_{11} must not be zero. An interesting and perhaps unexpected implication of this is that a gyro operating in the integrating mode, oriented with its input axis along the satellite earth pointing axis ($\bar{m}_3$ or yaw axis) is unsatisfactory as a yaw control device since C'_{11} is zero. In addition, in the case of the gyro operating in the integrating mode, it is necessary that C_{32} not be zero.

---

[2]This is also the reason a constant spurious torque acting about the gimbal axis of a gyro operating in the integrating mode does not necessarily cause it to drift away until it reaches the stops, as would happen if the reference frame were not rotating. Instead the gimbal angle reaches the steady-state value indicated by equation (20); that is, if $\psi_{m/o} = \varphi_{m/o} = 0$, the value is

$$\frac{-C'_{12} + (\Delta M_g/H_r\omega_o)}{-C_{32}}$$

A desirable, though not strictly necessary, condition is C'_{12} equal to zero. A nonzero value results in a steady-state output signal (gimbal angle) from the gyro even with $\psi_{m/o}$ and $\varphi_{m/o}$ both zero. Although this steady-state signal could be removed from the yaw channel by applying a constant bias, it is doubtful whether it is worth considering because it is shown in a later section that a nonzero C'_{12} has no beneficial effects on over-all system stability. To meet the zero C'_{12} condition, the gyro input axis must be located in the $\bar{m}_1\bar{m}_3$ or roll-yaw plane of the satellite. In practice it is only possible to set C_{12} equal to zero (or locate the gyro input axis in the $\bar{d}_1\bar{d}_3$ plane). The value of C'_{12} may then differ slightly from zero if the gyro reference frame ($\bar{d}_i$ frame) and the control or marked reference frame ($\bar{m}_i$ frame) are misalined. Thus if C_{12} is zero, then by equation (A2), C'_{12} is given by $\psi_{d/m}C_{11} - \varphi_{d/m}C_{13}$.

Perhaps the simplest orientation, for the gyro operating in either mode, is when C_{11} is unity, $-C_{32}$ is unity,[3] and C_{12} and C_{13} are both zero. With this orientation the gyro input axis lies along the $\bar{d}_1$ or roll axis of the gyro reference frame and the spin axis lies along the negative $\bar{d}_2$ axis. The gimbal angle expression (eq. (20)) then reduces to

$$\theta_{g(\text{steady})} = \frac{-\psi_{m/o} - \psi_{d/m} - \theta_{d/m}\varphi_{m/o} + (\Delta M_g/H_r\omega_o)}{(K/H_r\omega_o) + 1} \tag{21}$$

There may, of course, be objections to this orientation from the point of view of over-all system stability. This question is deferred to a later section. It is possible, however, to predict a possible objection to this orientation for an integrating gyro if it is required to rotate the satellite through large angles of yaw, say of the order of 30° or more. It can be seen from equation (21) that with K equal to zero the gyro gimbal angle must be approximately equal to the angle of yaw, which is clearly incompatible with current gyro gimbal angle limitations of about 6°. Overcoming this problem, without recourse to special gyros, necessitates reducing the value of C_{11}/C_{32} from unity to something of the order of 0.2. This can be arranged by rotating the gyro input axis in the roll-yaw plane so that it makes an angle of about 78° with the roll axis. With this orientation, however, the value of C_{13}/C_{32} is increased from zero to 0.98, so that the part of the steady-state gyro signal proportional to angle of roll becomes about five times greater than that proportional to angle of yaw. Thus, not only can the integrating gyro input axis orientation be severely limited by the yaw bias requirement, but noise becomes an increasingly important consideration since the controlling signal in yaw is so much weaker.

The gyro used in the rate mode does not suffer from problems introduced by the yaw bias requirement to the same extent as the integrating gyro. It can be seen from equation (21) that if K is made sufficiently large, the gimbal angle can be made small relative to the angle of yaw.

---

[3]It is shown in appendix A that for a gyro operating in the integrating mode it is essential to have C_{32} negative.

ANALYSIS OF THE LINEARIZED EQUATIONS

Stability of the Linearized Equations

It is proposed, from the outset, to simplify the subsequent analysis by making the following two assumptions:

(1) There are no misalinements between the marked axes and the principal axes of inertia and between the horizon sensor axes and the marked axes.

(2) There is a constant-speed inertia wheel alined along the pitch axis only ($h_{1K} = h_{3K} = 0$).

Although the analysis is therefore not completely general, it nevertheless serves to indicate many of the main stability characteristics that exist with the type of system under consideration in this report.

The linearized kinematic equations corresponding to equations (3) are:

$$\left.\begin{aligned} \omega_1 &= \dot{\varphi}_{m/o} - \omega_o\psi_{m/o} \\ \omega_2 &= \dot{\theta}_{m/o} - \omega_o \\ \omega_3 &= \dot{\psi}_{m/o} + \omega_o\varphi_{m/o} \end{aligned}\right\} \tag{22}$$

Substituting equations (22) into equations (1) and carrying out the usual linearizing procedures yields

$$\left.\begin{aligned} I_1\ddot{\varphi}_{m/o} - 4\omega_o^2(I_3 - I_2)\varphi_{m/o} - \omega_o(I_1 - I_2 + I_3)\dot{\psi}_{m/o} + \dot{h}_{1w} - \omega_o h_{3w} \\ - h_{2K}(\dot{\psi}_{m/o} + \omega_o\varphi_{m/o}) &= \sum T_1 \\ I_2\ddot{\theta}_{m/o} + 3\omega_o^2(I_1 - I_3)\theta_{m/o} + \dot{h}_{2w} &= \sum T_2 \\ I_3\ddot{\psi}_{m/o} + \omega_o^2(I_2 - I_1)\psi_{m/o} + \omega_o(I_1 - I_2 + I_3)\dot{\varphi}_{m/o} + \omega_o h_{1w} + \dot{h}_{3w} \\ + h_{2K}(\dot{\varphi}_{m/o} - \omega_o\psi_{m/o}) &= \sum T_3 \end{aligned}\right\} \tag{23}$$

The control equations (see eqs. (4), (5), (6)) become

$$h_{1w} - K_\varphi F_\varphi(s)\varphi_{m/o} = 0 \tag{24}$$

$$h_{2w} - K_\theta F_\theta(s)\theta_{m/o} = 0 \tag{25}$$

$$h_{3w} + K_\psi F_\psi(s)[(C'_{11}s + C'_{13}\omega_o)\varphi_{m/o} + C'_{12}s\theta_{m/o} + (C'_{13}s + C'_{11}\omega_o)\psi_{m/o} + \Delta M_g - C'_{12}\omega_o] = 0 \qquad (26)$$

where

$$F_\psi(s) = \frac{F_\psi'(s)}{1 + \tau_g s} \qquad (27)$$

Equations (23), (24), (25), and (26) form the complete system of linearized equations.

It is convenient, at this stage, to change the time scale from t to τ where $\tau = \omega_o t$. This procedure implies that the Laplace transform variable, s, in equations (23) to (26) must be replaced by $\omega_o s'$, where s' is the Laplace transform variable corresponding to the new time scale, τ. The characteristic equation of the complete system expressed in the Laplace transform variable s' can then be written in the following form:

$$\begin{vmatrix}
\left[I_1 s'^2 - 4(I_3 - I_2)\frac{h_{2K}}{\omega_o}\right] & 0 & \left[-(I_1 - I_2 + I_3)s' - \frac{h_{2K}s'}{\omega_o}\right] & s' & 0 & -1 \\
 & \left[I_2 s'^2 + 3(I_1 - I_3)\right] & & 0 & s' & 0 \\
\left[(I_1 - I_2 + I_3)s' + \frac{h_{2K}s'}{\omega_o}\right] & 0 & \left[I_3 s'^2 + (I_2 - I_1) - \frac{h_{2K}}{\omega_o}\right] & 1 & 0 & s' \\
\frac{-K_\varphi F_\varphi(\omega_o s')}{\omega_o} & 0 & 0 & 1 & 0 & 0 \\
0 & \frac{-K_\theta F_\theta(\omega_o s')}{\omega_o} & 0 & 0 & 1 & 0 \\
K_\psi F_\psi(\omega_o s')(C'_{11}s' + C'_{13}) & K_\psi F_\psi(\omega_o s')C'_{12}s' & K_\psi F_\psi(\omega_o s')(C'_{13}s' - C'_{11}) & 0 & 0 & 1
\end{vmatrix} = 0 \qquad (28)$$

The determinant of equation (28) can be simplified by the following steps:

(a) multiply row 1 by s'

(b) add row 3 to row 1

(c) divide row 3 by s'

(d) multiply row 5 by s'

(e) subtract row 5 from row 2

(f) multiply column 4 by $[(I_2 - I_1) - (h_{2K}/\omega_o)]$

(g) subtract column 4 from column 3

(h) subtract row 6 from row 3

to

$$\left[I_2 s'^2 + 3(I_1 - I_3) + \frac{K_\theta F_\theta(\omega_o s')s'}{\omega_o}\right] \begin{vmatrix} s'\left[I_1 s'^2 - 3(I_3 - I_2) + I_1\right] & 0 & s'^2 + 1 \\ \left(I_1 - I_2 + I_3 + \frac{h_2 K}{\omega_o}\right) - K_\psi F_\psi(\omega_o s')(C'_{11}s' + C'_{13}) & I_3 s' - K_\psi F_\psi(\omega_o s')C'_{13}s' - C'_{11} & \frac{1}{s'} \\ \frac{-K_\varphi F_\varphi(\omega_o s')}{\omega_o} & -\left[(I_2 - I_1) - \frac{h_2 K}{\omega_o}\right] & 1 \end{vmatrix} = 0 \tag{29}$$

Expanding the determinant about the second column yields

$$I_2 s'^2 + 3(I_1 - I_3) + \frac{K_\theta F_\theta(\omega_o s')s'}{\omega_o} = 0 \tag{30}$$

and

$$\left[I_3 s' - K_\psi F_\psi(\omega_o s')(C'_{13}s - C'_{11})\right]\left\{s'\left[I_1 s'^2 - 3(I_3 - I_2) + I_1\right] + \frac{K_\varphi F_\varphi(\omega_o s')(s'^2 + 1)}{\omega_o}\right\}$$

$$+ \left[(I_2 - I_1) - \frac{h_2 K}{\omega_o}\right]\left\{-4(I_3 - I_2) - \frac{h_2 K}{\omega_o} - \left[(I_3 - I_2) + \frac{h_2 K}{\omega_o}\right]s'^2 + K_\psi F_\psi(\omega_o s')(C'_{11}s + C'_{13})(s'^2 + 1)\right\} = 0 \tag{31}$$

An examination of equations (30) and (31) reveals that they are independent of C'_{12}. It follows that the stability of the system is independent of the angle between the gyro input axis and the $\bar{m}_1\bar{m}_3$ or roll-yaw plane. In other words, there are no stability improvements to be gained by skewing the gyro input axis out of the $\bar{m}_1\bar{m}_3$ plane.

Since equation (30) contains only one gain parameter, K_θ, the characteristics of the stability in pitch can be readily obtained by standard root locus techniques. On the other hand, equation (31), representing the roll-yaw stability, contains two gain parameters K_φ and K_ψ; therefore standard root locus techniques do not readily indicate the important features. If, however, the additional assumption[4] is made that

$$(I_2 - I_1) - \frac{h_{2K}}{\omega_o} = 0 \tag{32}$$

then equation (31) factors into two equations; thus

$$I_3 s' - K_\psi F_\psi(\omega_o s')(C'_{13} s' - C'_{11}) = 0 \tag{33}$$

$$s'\left[I_1 s'^2 - 3(I_3 - I_2) + I_1\right] + \frac{K_\varphi F_\varphi(\omega_o s')(s'^2 + 1)}{\omega_o} = 0 \tag{34}$$

Equations (33) and (34) each contain only a single gain parameter and both are therefore amenable to treatment by standard root locus techniques.

While the assumption represented by equation (32) restricts the treatment of stability considerably, the class of satellites which satisfy the assumption is important. If, for example, the control system does not include a constant speed pitch inertia wheel ($h_{2K} = 0$), then a satellite configuration satisfying equation (32) must have inertial symmetry about its earth-pointing axis. Even if equation (32) is not completely satisfied, equations (33) and (34) provide a sound basis for considering the kind of problems and type of behavior likely to be encountered. In fact, it will be shown subsequently that the stability of the Nimbus satellite is closely approximated by equations (33) and (34) although the assumption of equation (32) is not completely satisfied.

Equations (30), (33), and (34) can be rewritten in a form more suitable for root locus analysis; thus,

---

[4]The significance of this assumption is that it removes all torques of a purely gyroscopic origin from the yaw equation. It is interesting to note that this can always be achieved by choosing the appropriate value of h_{2K}. For further insight into the significance of this decoupling parameter, see appendix B.

$$1 + \frac{K_\theta F_\theta(\omega_o s')s'}{\omega_o I_2(s'^2 + 3J_2)} = 0 \tag{35}$$

$$1 - \frac{K_\psi F_\psi(\omega_o s')(C'_{13}s' - C'_{11})}{I_3 s'} = 0 \tag{36}$$

$$1 + \frac{K_\varphi F_\varphi(\omega_o s')(s'^2 + 1)}{\omega_o I_1 s'(s'^2 + 1 + 3J_1)} = 0 \tag{37}$$

It is now proposed to examine, in some detail, the implications of equations (35), (36), and (37).

Root loci of equation (35).- First consider the case where no compensation is provided; the transfer function $F_\theta(\omega_o s')$ will then be that of the motor flywheel in the pitch channel and can be approximated by a simple lag, that is, $F_\theta(\omega_o s') = 1/[1 + \tau_m(\omega_o s')]$. The type of root locus obtained depends on the sign of the gravity torque parameter, J_2. The root locus diagrams for J_2 positive or negative are shown in sketch (b).[5] If J_2 is positive (stable gravity

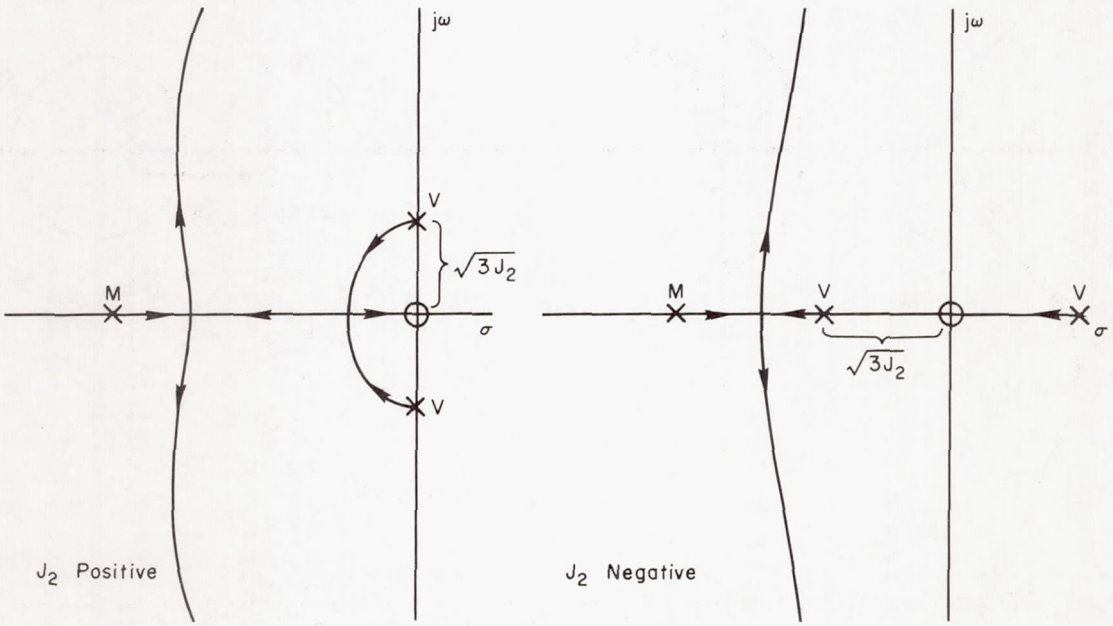

Sketch (b).- Root locus of $1 + \left(\frac{K_\theta}{\omega_o I_2}\right) \frac{1}{1 + \tau_m(\omega_o s')} \frac{s'}{(s'^2 + 3J_2)} = 0$

[5]In all root locus diagrams the poles and zeros may be identified by the following code:

V	open loop poles
M	pole associated with motor flywheel
G	pole associated with gyro lag
G.O	zero associated with gyro orientation
C	poles and zeros associated with compensation networks

torques), then the pitch channel is stable for all finite positive values of the gain parameter K_θ and there is a value of the gain which gives the optimum damping. When J_2 is negative (unstable gravity torques), the pitch channel is unstable for all finite values of the gain. The stability when J_2 is either positive or negative can very easily be improved by the inclusion of passive compensation. If, for example, the compensation is of the often used lead-lag type, that is,

$$F(\omega_o s') = \frac{1}{1 + \tau_m(\omega_o s')} \left[\frac{1 + \tau_\theta(\omega_o s')}{1 + \alpha\tau_\theta(\omega_o s')}\right]$$

then with suitable values for τ_θ and $\alpha\tau_\theta$ the root locus diagrams can be made to appear as in sketch (c). By judicious choice of the lead-lag parameters, the

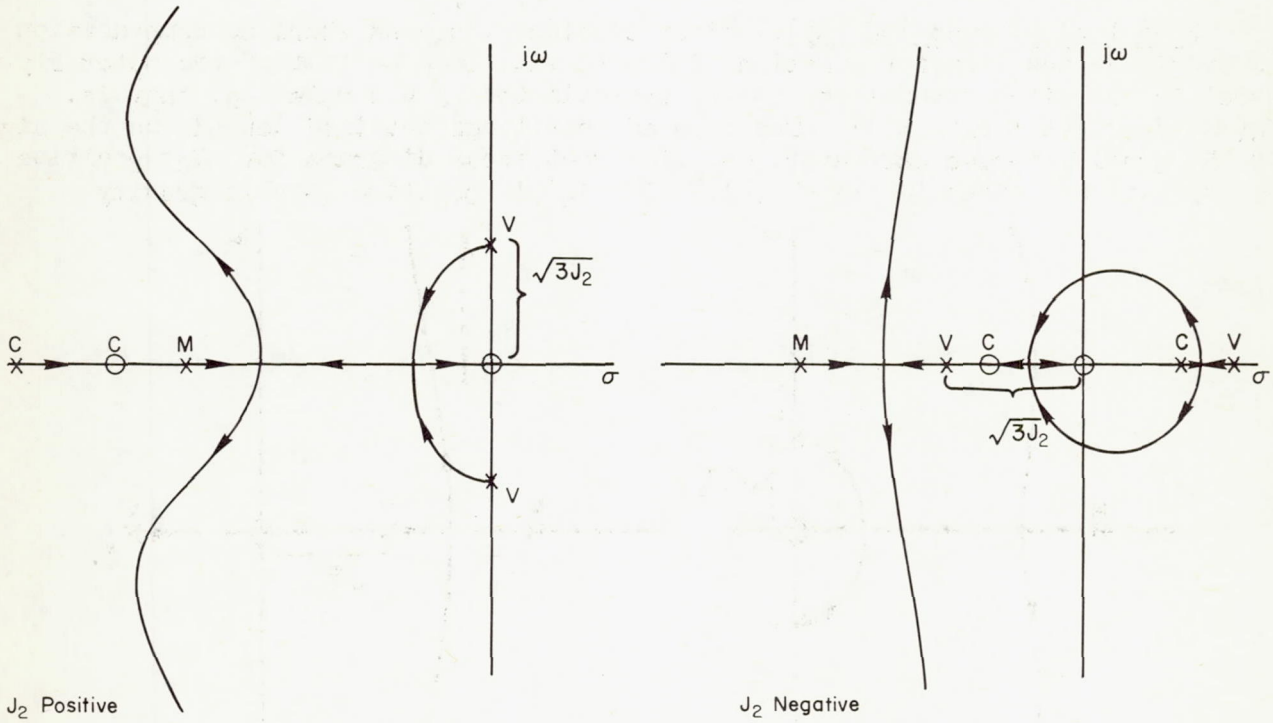

Sketch (c).- Root loci of $1 + \left(\frac{K_\theta}{\omega_o I_2}\right) \frac{1}{1 + \tau_m(\omega_o s')} \left[\frac{1 + \tau_\theta(\omega_o s')}{1 + \alpha\tau_\theta(\omega_o s')}\right] \frac{s'}{(s'^2 + 3J_2)} = 0$

optimum damping of the system with J_2 positive can be improved substantially. When J_2 is negatave, it can be seen that the stability can be improved so that there is a range of values of the gain parameter for which the system will be stable even though the damping, in general, will be low.

Root locus of equation (36).- The types of root locus diagrams representing the solutions of equation (36) can be divided into two classes corresponding to $C'_{13} \neq 0$ and $C'_{13} = 0$. When $C'_{13} \neq 0$, the equation can be written in the form

$$1 - \left(\frac{K_\psi C'_{13}}{I_3}\right) F_\psi(\omega_o s') \frac{[s' - (C'_{11}/C'_{13})]}{s'} = 0 \qquad (38)$$

and when $C'_{13} = 0$, in the form

$$1 + \left(\frac{K_\psi C'_{11}}{I_3}\right) \frac{F_\psi(\omega_o s')}{s'} = 0 \qquad (39)$$

First consider the case where no compensation is provided. The transfer function $F_\psi(\omega_o s')$ can be written in the form

$$F_\psi(\omega_o s') = \frac{1}{1 + \tau_m(\omega_o s')} \frac{1}{1 + \tau_g(\omega_o s')}$$

where τ_m is the motor flywheel time constant and τ_g is the gyro time constant. The root loci of equation (38) are shown in sketch (d) for C'_{11}/C'_{13}

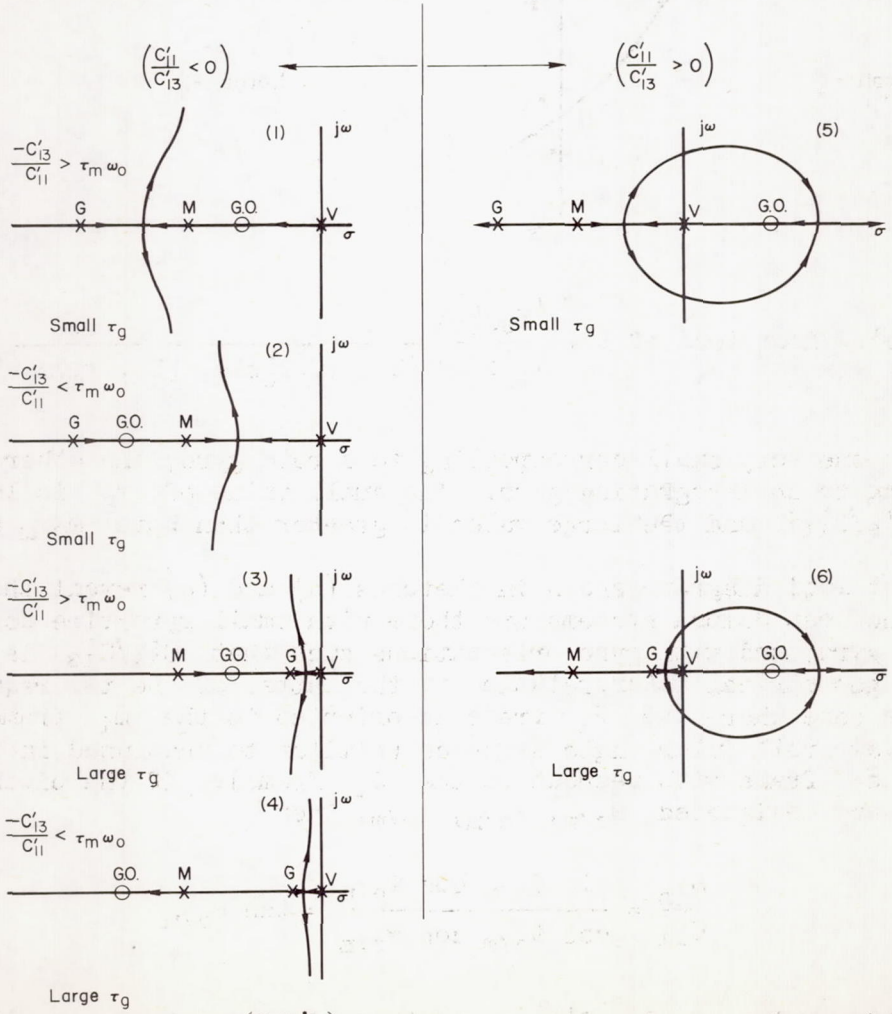

Sketch (d).- Root loci of $1 - \left(\frac{K_\psi C'_{13}}{I_3}\right) \frac{1}{1 + \tau_m(\omega_o s')} \frac{1}{1 + \tau_g(\omega_o s')} \frac{[s' - (C'_{11}/C'_{13})]}{s'} = 0$

negative and positive. The case where C'_{11}/C'_{13} is negative is subdivided into two cases corresponding to $-C'_{13}/C'_{11} < \omega_o\tau_m$ and $-C'_{13}/C'_{11} > \omega_o\tau_m$. The root loci of equation (39) (i.e., $C'_{13} = 0$) are shown in sketch (e). Two values of τ_g are

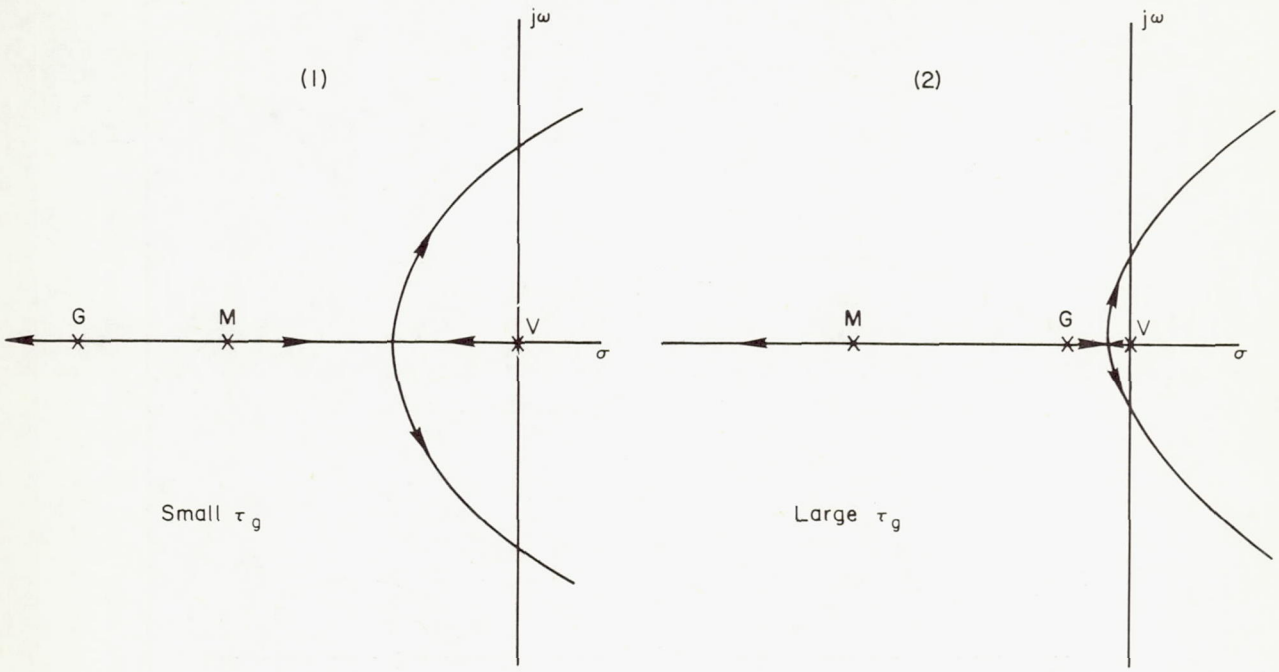

Sketch (e).- Root loci of $1 + \left(\frac{K_\psi C'_{11}}{I_3}\right) \frac{1}{[1 + \tau_m(\omega_o s')]} \frac{1}{[1 + \tau_g(\omega_o s')]} \frac{1}{s'} = 0$

considered: one very small corresponding to a rate gyro, the other very large corresponding to an integrating gyro. The small value of τ_g is less than both $\omega_o\tau_m$ and $|C'_{13}/C'_{11}|$ and the large value is greater than both $\omega_o\tau_m$ and $|C'_{13}/C'_{11}|$.

The root loci diagrams shown in sketches (d) and (e) reveal the important fact that the best damped systems are those with small gyro time constants (i.e., rate gyro) and with gyro orientations such that C'_{11}/C'_{13} is negative. To obtain a geometrical interpretation of the latter of the two requirements, consider the case where the $\bar{c}_i$ frame is oriented to the $\bar{m}_i$ frame by a standard pitch, yaw, roll Euler angle sequence (similar to that used in appendix D to orient the $\bar{c}_i$ frame with respect to the $\bar{d}_i$ frame). If the pitch, yaw, and roll angles are designated $\theta_{c/m}$, $\psi_{c/m}$, $\varphi_{c/m}$, then

$$\frac{C'_{13}}{C'_{11}} = \frac{\sin\theta_{c/m}\cos\psi_{c/m}}{\cos\theta_{c/m}\cos\psi_{c/m}} = \tan\theta_{c/m} \tag{40}$$

Thus a negative value of C'_{11}/C'_{13} means that $\theta_{c/m}$ must lie in either the second or fourth quadrants. It makes no difference which of these two quadrants

is selected, provided a K_ψ of the correct sign is used. Sketch (f) gives a pictorial idea of a gyro oriented with its input axis in the fourth quadrant, when K_ψ must be positive for stability.

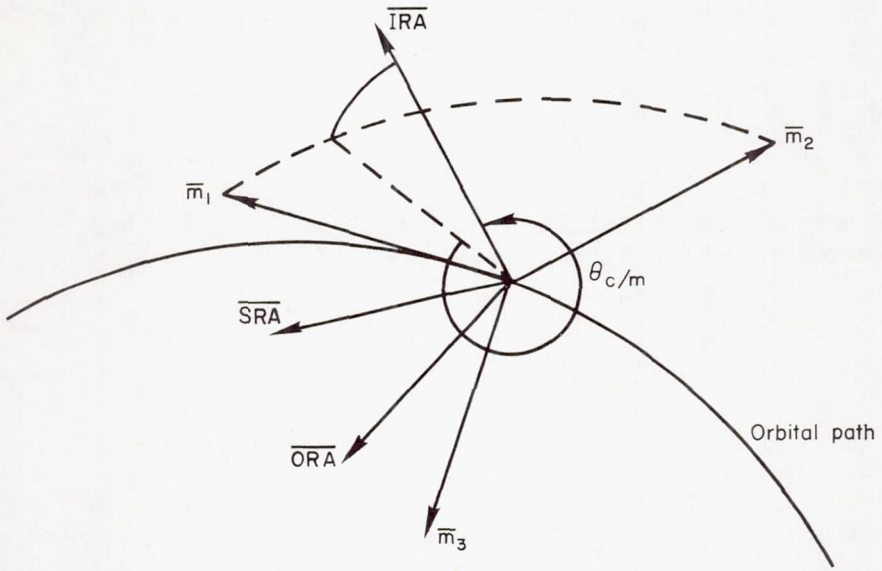

Sketch (f).- Stable gyro orientation.

To obtain a gyro signal which has the component proportional to the angle of yaw $\psi_{m/o}$ a maximum, it has been shown that the input axis must be located along the $\overline{d}_1$ axis (see eq. (21) and related discussion). The advantage of obtaining the strongest yaw signal is, of course, that the influence of noise and signal threshold limits is minimized. With an orientation of this type, C_{11} is unity and C_{12} and C_{13} are both zero. The expressions for C'_{13} and C'_{11} obtained from equation (A2) are

$$C'_{13} = -\theta_{d/m}$$

$$C'_{11} = 1$$

Therefore

$$\frac{C'_{13}}{C'_{11}} = -\theta_{d/m}$$

If $\theta_{d/m}$ is less than or equal to zero, then C'_{13}/C'_{11} is greater than or equal to zero, and it can be seen from sketches (d) and (e) that the system has an oscillatory instability for values of the gain parameter greater than some critical value. To guard against the possibility of an instability due to gyro misalinement (i.e., $\theta_{d/m}$), the gyro input axis must be oriented at an angle, $\theta_{c/m}$, as in sketch (f), so that

$$\tan \theta_{c/m} < 0$$

or, since $\tan \theta_{c/m}$ need be only slightly less than zero,

$$\theta_{c/m} < 0$$

Since $\theta_{c/m} = \theta_{c/d} - \theta_{d/m}$,[6] this criterion for stability may be written as

$$\theta_{c/d} < \theta_{d/m}$$

The least value of $\theta_{d/m}$ may be written as $-|\theta_{d/m}|_{max}$ where $|\theta_{d/m}|_{max}$ is the estimated maximum numerical value for the misalinement error angle $\theta_{d/m}$. Hence the criterion for stability becomes

$$\theta_{c/d} < -|\theta_{d/m}|_{max} \tag{41}$$

In the case of the integrating gyro (large τ_g), it can be seen from sketch (d) that, in general, a large value of $-C'_{13}/C'_{11}$ yields better stability characteristics than a small value. In other words a large value of $-\theta_{c/m}$ is desirable (direction of $-\theta_{c/m}$ as in sketch (f)). It is interesting that this condition is compatible with the integrating gyro orientation conditions (established earlier in the section dealing with gyro orientation) necessary to meet the yaw bias requirement.

Even if the gyro orientation is favorable and the time constant small, the damping factors of the oscillatory roots at high gain may be unacceptably low for some applications. This can be improved by adding lead-lag compensation in a manner similar to that indicated in sketch (c) for the pitch channel.

Root loci of equation (37).- Again consider first the case where no compensation is provided. The transfer function $F_\varphi(\omega_o s')$ is then the simple lag function assumed to represent the motor flywheel dynamics. The type of root locus obtained depends on the sign of the gravity torque parameter J_1. The root locus diagrams for J_1 positive and negative are shown in sketch (g). The system with J_1 positive has a convergent mode of oscillation lying in the frequency band $\omega_o/2\pi$ to $\omega_o\sqrt{1 + 3J_1}/2\pi$; whereas with J_1 negative, such that $0 > J_1 > -1/3$, the mode of oscillation in this frequency band is divergent. If J_1 is in the range $-1/3 > J_1 \geq -1$, the divergent mode may be oscillatory or nonoscillatory depending on the value of K_φ. If J_1 is zero (no gravity torques), the poles and zeros on the imaginary axis become coincident and there is an undamped sinusoidal oscillation of orbital frequency $\omega_o/2\pi$ for all values of the gain K_φ. This is in agreement with the general conclusions given earlier in the report. It should also be noted, again in agreement with earlier conclusions, that, as the gain is made very large, the system tends to possess an undamped sinusoidal oscillation of orbital frequency.

---

[6]The negative sign for $\theta_{d/m}$ occurs because $\theta_{c/m}$ and $\theta_{c/d}$ are rotations about the $\bar{c}_2$ axis while $\theta_{d/m}$ is a rotation about the $\bar{d}_2$ axis and by the convention adopted in appendix D, $\bar{c}_2 = -\bar{d}_2$.

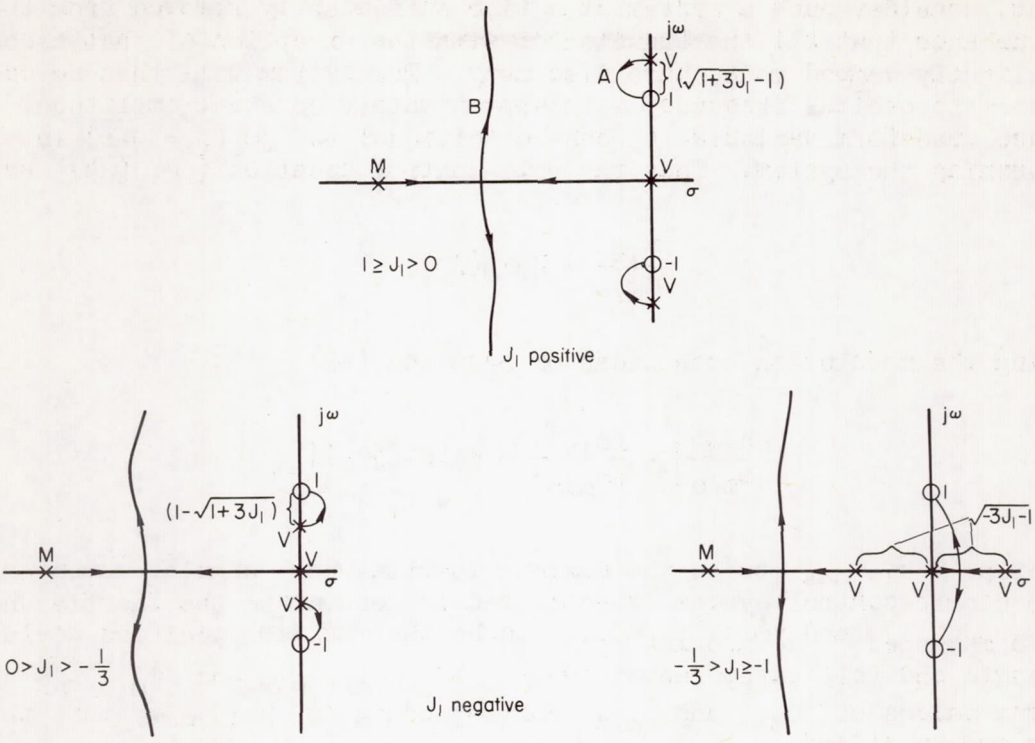

Sketch (g).- Root loci of $1 + \left(\frac{K_\varphi}{I_1\omega_o}\right) \frac{1}{[1 + \tau_m(\omega_o s')]} \frac{(s'^2 + 1)}{s'(s'^2 + 1 + 3J_1)} = 0$

It is shown in appendix B that equation (34) governs the transport of roll-yaw angular momentum between the satellite and its orbit. (When the transport of angular momentum is from the satellite to the orbit, the process is usually termed "momentum dumping.") It is clearly desirable to maintain the angular momentum of the satellite (including the inertia wheels) as small as possible within the framework of other satellite performance requirements. It can be seen from sketch (g) that the best system from the momentum dumping point of view is the one with the largest positive value of J_1 (e.g., a long slender cylinder with its axis earth pointing). With J_1 negative, momentum dumping is not possible with an uncompensated inertia-wheel control system. It is not possible to materially improve a system with J_1 between 0 and -1/3 even with very general forms of passive compensation. It is theoretically possible to improve a system with J_1 between -1/3 and -1 by cancelling the unstable pole with a zero, but it is doubtful that the resulting system would be practical. Even with J_1 positive it is very difficult to materially improve the maximum damping (given by point A of sketch (g)). Furthermore, the gain corresponding to the maximum damping is relatively small and for many systems may not be compatible with the demands of other performance requirements. If these requirements dictate a high value for K_φ then the momentum dumping capability will be extremely low and there is little that can be done to improve it. However, the fact that one of the roots of the characteristic equation is almost undamped does not necessarily mean that the system is unsatisfactory. To demonstrate

this point, consider such a system at a time sufficiently removed from the time of a disturbance that all the transients, with the exception of that associated with the lightly damped mode, have died away. The system will then be oscillating at close to orbital frequency with approximately constant amplitude, so that the Laplace transform variable s can be set equal to $j\omega_o (j = \sqrt{-1})$ in the equations governing the system. Thus the roll control equation (eq. (24)) becomes

$$\frac{h_{1w}}{\varphi_{m/o}} = K_\varphi F_\varphi(j\omega_o) \tag{42}$$

or equating the modulus on both sides of equation (42)

$$\left|\frac{h_{1w}}{\varphi_{m/o}}\right| = \frac{|h_{1w}|}{|\varphi_{m/o}|} = K_\varphi |F_\varphi(j\omega_o)| \tag{43}$$

We now define $|h_{1w}|_{max}$ to be the maximum inertia-wheel angular momentum, at which the coarse control system is activated to desaturate the inertia wheel, and $|\varphi_{m/o}|_{max\ spec}$ and $|\dot{\varphi}_{m/o}|_{max\ spec}$ to be the maximum specified deviations of roll angle and roll rate, respectively. If $|\varphi_{m/o}|_{max}$ and $|\dot{\varphi}_{m/o}|_{max}$ are the maximum values of $\varphi_{m/o}$ and $\dot{\varphi}_{m/o}$ corresponding to $|h_{1w}|_{max}$, then the following are specified:

$$|\varphi_{m/o}|_{max} < |\varphi_{m/o}|_{max\ spec} \tag{44}$$

$$|\dot{\varphi}_{m/o}|_{max} < |\dot{\varphi}_{m/o}|_{max\ spec} \tag{45}$$

but since the motion is sinusoidal with circular frequency ω_o

$$|\dot{\varphi}_{m/o}|_{max} = \omega_o |\varphi_{m/o}|_{max} \tag{46}$$

Thus inequalities (44) and (45) may be restated in the following form:

$$|\varphi_{m/o}|_{max} < \left\{\text{greatest of } |\varphi_{m/o}|_{max\ spec} \text{ and } \frac{|\dot{\varphi}_{m/o}|_{max\ spec}}{\omega_o}\right\}$$

or from equation (43)

$$K_\varphi > \left\{\text{greatest of } \frac{|h_{1w}|_{max}}{|F_\varphi(j\omega_o)|\,|\varphi_{m/o}|_{max\ spec}} \text{ and } \frac{\omega_o |h_{1w}|_{max}}{|F_\varphi(j\omega_o)|\,|\dot{\varphi}_{m/o}|_{max\ spec}}\right\} \tag{47}$$

Therefore if K_φ is large enough to produce a system with small damping in the sense discussed previously, then inequality (47) is a necessary condition that the system will be satisfactory in meeting the specifications. In a similar manner to the above, an inequality connecting K_ψ with $|h_{3w}|_{max}$, $|\psi_{m/o}|_{max\ spec}$ and $|\dot{\psi}_{m/o}|_{max\ spec}$ can be derived which must also be satisfied. It is not proposed to go into the details of this since the expressions involved are long and not particularly revealing.

If, in order to meet the specifications, a very high value of K_φ is required, then it may be desirable to improve the damping factor of the pair of oscillatory roots located on the branch marked B of the root locus diagram shown in sketch (g). This can be accomplished by the addition of simple lead-lag compensation applied in a manner similar to that indicated in sketch (c) for the pitch channel.

The effect on stability of $(I_2 - I_1)$ and h_{2K}.- If the system does not satisfy equation (32), even approximately, then it is necessary to consider the complete characteristic equation (eq. (31)) in determining the stability of the system. Unfortunately as with most multivariable problems of this kind it is very difficult, if not impossible, to deduce any general properties of the system by methods currently available. Several specific examples have been evaluated in which it appears that small negative values of $(I_2 - I_1)/I_3 = J_3$ and small positive values of $h_{2K}/\omega_o I_3$ result in a system with a maximum momentum dumping capability which is slightly better than that which would be predicted by equation (37), although always at the expense of the damping of other modes. Larger values of $-J_3$ and $h_{2K}/\omega_o I_3$ eventually result in a decrease of the momentum dumping capability below that predicted by equation (37). With very large values of $h_{2K}/\omega_o I_3$, the dynamics of the constant speed wheel tend to dominate the over-all stability of the system and always result in an almost undamped oscillation of orbital frequency which tends to create large amplitude roll and yaw deviations. Thus for the type of satellite system considered here any improvement due to the use of a constant speed wheel is always small and probably not worth the additional mechanical complications.

A possible way of improving the roots of equation (37) for the cases where J_3 is nonzero, but small, is to replace the imaginary poles by the corresponding true open loop poles derived from the open loop characteristic equation

$$s'^4 + s'^2(1 + 3J_1 + J_1J_3) + 4J_1J_3 = 0 \qquad (48)$$

The Influence of Axes Misalinement

Two types of axes misalinement can occur and can influence the behavior of the satellite significantly:

(a) Angular misalinements of the axes system selected as the reference for control information (known as the marked or control axes).

(b) Angular misalinements of the sensors relative to the marked axes system.

It is usual to attempt to aline the control axes so that they are coincident with the principal axes of inertia of the satellite. If some orientation other than this is selected, then in its equilibrium attitude, the satellite generally has torques acting on it as a result of the action of the gravity gradient. These gravity torques have to be countered by the control system and the only way this can be achieved is to continuously change the speed of the inertia wheels. This situation is undesirable for two basic reasons. First, there is a tendency to reduce the life of the inertia-wheel units and, second, an additional burden is placed on the coarse control system (and its energy supply) through the increased likelihood of the inertia wheels attaining saturation speed.

The difficulty of accurately determining the location of the principal axes of inertia of the satellite makes it almost impossible to completely avoid the problems outlined above. In addition, the uncertainty of the location of the principal axes can introduce important stability problems, as will be demonstrated subsequently. Opinions differ somewhat on the question of attainable accuracy with which the principal axes can be determined, and, certainly, the type of configuration is an important factor. It appears, however, that the control system design should allow for the possibility of a control axis misalinement of at least 3° and possibly as much as 5°.

Misalinement of the sensors can result from manufacturing errors and structural distortion. Their effect is to produce both attitude errors and inertia-wheel speed biases. In general, however, the influence of these misalinements is largely overshadowed by that due to the control axes misalinements.

It is possible to obtain a quantitative idea of the influence of misalinements by considering the steady-state equilibrium of the system. The steady-state equations governing the static equilibrium of the system can be derived from equations (1), (3), (4), (5), and (6). These equations take on a simplified and more meaningful form when linearized, a process which is justifiable in the present circumstances since no external torques are assumed and the misalinement angles are, in general, small. The equations are given below.

Roll
$$\left(-\frac{h_{2K}}{\omega_o I_1} + 4J_1\right)\varphi^s_{m/o} - \frac{h^s_{3w}}{I_1\omega_o} = 4\varphi_{m/b}J_1 \tag{49}$$

Pitch
$$J_2\theta^s_{m/o} = J_2\theta_{m/b} \tag{50}$$

Yaw
$$\left(-\frac{h_{2K}}{\omega_o I_3} + J_3\right)\psi^s_{m/o} + \frac{h^s_{1w}}{I_3\omega_o} = J_3\psi_{m/b} \tag{51}$$

Roll control
$$\frac{K_\varphi\varphi^s_{m/o}}{\omega_o} - \frac{h^s_{1w}}{\omega_o} = \frac{-K_\varphi\varphi_{sx/m}}{\omega_o} \tag{52}$$

Pitch control
$$K_\theta\theta^s_{m/o} - h^s_{2w} = -K_\theta\theta_{sy/m} \tag{53}$$

Yaw control
$$K_\psi C'_{13}\varphi^s_{m/o} - K_\psi C'_{11}\psi^s_{m/o} - \frac{h^s_{3w}}{\omega_o} = 0 \tag{54}$$

where the suffix s means the steady-state value of the variable. It should be noted here that misalinements of the gyro orientation enter the equations only through the terms C'_{11} and C'_{13}. Thus gyro misalinements do not of themselves introduce any steady-state attitude angles and inertia-wheel speeds although they do influence the value of those derived from other sources of misalinement.

It follows directly from equations (50) and (51) that in the case of pitch

$$\theta^s_{m/o} = \theta_{m/b} \tag{55}$$

and

$$h^s_{2w} = K_\theta(\theta_{m/b} + \theta_{sx/m}) \tag{56}$$

provided

$$J_2 \neq 0$$

Equation (55) merely states that, in equilibrium, the principal axes of inertia in roll and yaw always point along the roll and yaw axes of the orbital reference frame (i.e., $\bar{b}_1 = \bar{o}_1$ and $\bar{b}_3 = \bar{o}_3$). As the pitch gain K_θ is increased, equation (56) indicates that the steady-state-pitch wheel speed increases. If the gain is high, however, the wheel speed will probably saturate before it reaches the steady-state value given by equation (56) and will therefore have to be desaturated by the coarse control system. For high values of the gain the rate of increase of wheel speed with time tends to the asymptotic value (corresponding to an infinite gain) given by equation (17). Thus for high gain systems, equation (17) provides a rapid approximate estimate for the time interval between wheel desaturations for a given pitch misalinement angle.

The steady-state roll and yaw angles ($\varphi^s_{m/o}$ and $\psi^s_{m/o}$) and the associated inertia-wheel angular momenta h^s_{1w} and h^s_{3w} can be obtained by solving the simultaneous equations (49), (51), (52), and (54). The general results are not presented here since the expressions are not particularly revealing. When the gains K_ψ and K_φ are infinite, the general expressions reduce to the following

$$\left.\begin{aligned}
\varphi^s_{m/o} &= -\varphi_{sx/m} \\
h^s_{1w} &= I_3 J_3 \omega_o \left(\varphi_{sx/m}\frac{C'_{13}}{C'_{11}} + \psi_{m/b}\right) - h_{2K}\varphi_{sx/m}\frac{C'_{13}}{C'_{11}} \\
\psi^s_{m/o} &= \frac{-C'_{13}}{C'_{11}}\varphi_{sx/m} \\
h^s_{3w} &= -I_1\omega_o 4J_1(\varphi_{sx/m} + \varphi_{m/b}) + h_{2K}\varphi_{sx/m}
\end{aligned}\right\} \tag{57}$$

The important properties indicated by equations (57) are that the inertia-wheel speeds are bounded (note that the pitch wheel speed is unbounded when K_θ tends to infinity) and the steady-state angles $\varphi^s_{m/o}$ and $\psi^s_{m/o}$ are dependent only on the sensor misalinements which are usually very small (of the order of $1/10^o$). These facts illustrate a general point noted earlier in connection with stability, namely, that misalinements in pitch have a much more significant effect on the behavior of the system than have misalinements in roll and yaw.

The Influence of Control System Failure

The desired lifetime of a satellite is usually of the order of months and in some extreme cases, years. The multiplication of components to achieve the desired reliability is often very costly in weight. In some cases, however, it is possible, after a component fails, to rearrange the operation of the remaining components so that stability is maintained with some degradation of performance. Clearly, it is desirable to exploit such circumstances to the maximum since this may provide a way of improving system reliability for only a small weight penalty.

The stability of the roll and yaw degrees of freedom can always be arranged to be dependent on each other. The condition for this is that the system must <u>not</u> satisfy equation (32), or the system parameter must satisfy the equation

$$\frac{(I_2 - I_1)}{I_3} - \frac{h_{2K}}{\omega_o I_3} = K \qquad (\text{where } K \neq 0)$$

This raises the possibility, in the event of a roll or yaw channel failure, of activating a constant speed wheel to adjust the value of K so that the resulting system is stable. Furthermore, if the value of h_{2K} required to produce the desired value of K is not too large, there is the possibility of using the pitch control inertia wheel to provide the value of h_{2K}, using the remainder of its speed capability for pitch control in the usual way. It should be noted that the coupling between any of the degrees of freedom can be changed by changing the values of h_{1K}, h_{2K}, and h_{3K}. For example, it may be possible to minimize the effect of a pitch channel failure by selecting appropriate values for either h_{1K} or h_{3K} or both, which can be provided by the roll and yaw control wheels, respectively. However, in all but the case considered here (i.e., varying h_{2K}) the analysis appears to be rather intractable from the point of view of yielding general conclusions and the feasibility of these schemes can only be determined for specific satellite configurations.

In the subsequent discussion on the influence of a control channel failure, it is assumed that the system prior to failure has those design features which have been shown to be desirable in the previous discussion. In particular the following are assumed:

$$\left.\begin{array}{l} J_1 > 0 \\ \dfrac{C'_{11}}{C'_{13}} < 0 \\ \tau_g \quad \text{small} \end{array}\right\} \tag{58}$$

Failure of the yaw control channel.- The stability of the roll-yaw motion with the yaw control channel inoperative may be obtained from equation (31) by setting K_ψ equal to zero. The resulting equation may be written in the following form, suitable for a root locus investigation:

$$1 + \frac{K_\varphi}{I_1\omega_o} \frac{F_\varphi(\omega_o s')s'(s'^2+1)}{s'^4+s'^2\left[1+3J_1+\left(J_3 - \frac{h_{2K}}{\omega_o I_3}\right)\left(J_1 - \frac{h_{2K}}{\omega_o I_1}\right)\right] + \left(J_3 - \frac{h_{2K}}{\omega_o I_3}\right)\left(4J_1 - \frac{h_{2K}}{\omega_o I_1}\right)} = 0 \tag{59}$$

It is shown in appendix C that the best open loop stability (i.e., $K_\varphi = 0$) is obtained when h_{2K}/ω_o satisfies the condition

$$\frac{h_{2K}}{\omega_o} \geq [\text{both } (I_2 - I_1) \text{ and } 4(I_2 - I_3)]$$

The open loop poles are then all located on the imaginary axis and are, of course, symmetrically disposed relative to the real axis. The two poles on the positive imaginary axis are located so that one is always equal to or less than j and the other always greater than or equal to $j\sqrt{C}$, where C is given by the expression

$$C = \left(J_3 - \frac{h_{2K}}{\omega_o I_3}\right)\left(4J_1 - \frac{h_{2K}}{\omega_o I_1}\right)$$

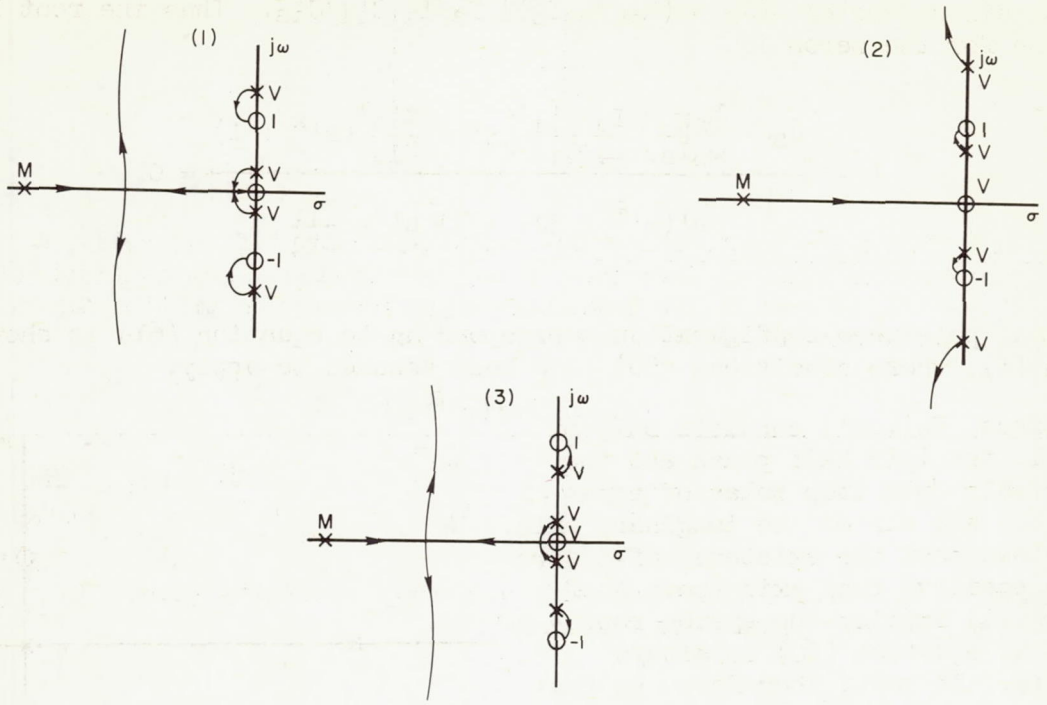

Sketch (h).- Root loci of equation (59).

The three types of root loci that can be obtained are shown in sketch (h) where $F_\varphi(\omega_o s')$ has been assumed to be a simple lag function approximating the motor flywheel dynamics. It can be seen that a stable system is achieved only if there is an open loop pole on either side of each of the zeros located at the points $s' = \pm j$ (i.e., sketch (h)1 and 2). This can be arranged by selecting an appropriate value for h_{2K}/ω_o (for example, any value for which $C \geq 1$ would be satisfactory). The value of $K_\varphi/I_1\omega_o$ corresponding to maximum damping of the system represented by either 1 or 2 of sketch (h) is always relatively low (i.e., comparable with its value at point A of sketch (g)). Hence if the original system has high gain, this method of overcoming the effect of a yaw channel failure is not very satisfactory, since two almost neutrally stable roots occur, one at $s' = \pm j$, the other at $s' = 0$. Whereas the neutrally stable root of orbital frequency ($s' = \pm j$) can be tolerated in the original system (since most of the system angular momentum is always stored in the inertia wheels) after the system has a failure there is no yaw wheel to store the yaw angular momentum which must therefore appear in the form of large yaw angles and yaw rates.

Failure of the roll control channel.- The characteristic equation for a system with a roll channel failure is given below (eq. (31) with $K_\varphi = 0$)

$$1 - \frac{K_\psi C'_{13}}{I_3} \frac{F_\psi(\omega_o s')\left[s'(s'^2 + 3J_1 + 1)\left(s' - \frac{C'_{11}}{C'_{13}}\right) - \left(J_3 - \frac{h_{2K}}{\omega_o I_3}\right)\frac{I_3}{I_1}\frac{C'_{11}}{C'_{13}}\left(s' + \frac{C'_{13}}{C'_{11}}\right)(s'^2 + 1)\right]}{s'^4 + s'^2\left[1 + 3J_1 + \left(J_3 - \frac{h_{2K}}{\omega_o I_3}\right)\left(J_1 - \frac{h_{2K}}{\omega_o I_1}\right)\right] + \left(J_3 - \frac{h_{2K}}{\omega_o I_3}\right)\left(4J_1 - \frac{h_{2K}}{\omega_o I_1}\right)} = 0 \qquad (60)$$

The zeros of equation (60) may be obtained in the form of a root locus diagram with a gain parameter $-[J_3 - (h_{2K}/\omega_o I_3)]\, I_3/I_1\, C'_{11}/C'_{13}$. Thus the root locus equation for the zeros is

$$1 - \frac{\left(J_3 - \frac{h_{2K}}{\omega_o I_3}\right)\frac{I_3}{I_1}\frac{C'_{11}}{C'_{13}}\left(s' + \frac{C'_{13}}{C'_{11}}\right)(s'^2 + 1)}{s'(s'^2 + 3J_1 + 1)\left(s' - \frac{C'_{11}}{C'_{13}}\right)} = 0 \qquad (61)$$

A typical pole-zero configuration corresponding to equation (61) is shown in sketch (i), where conditions (58) have been assumed to apply.

Since $F_\psi(\omega_o s')$ consists only of poles in the left half plane and the most stable open loop poles of equation (60) are all on the imaginary axis, it follows that the existence of a zero on the positive real axis (zero A of sketch (i)) implies the system represented by equation (60) is always unstable. It must, therefore, be concluded that the scheme as outlined is not, in general, satisfactory in the event of a roll wheel failure. It is possible to visualize a modification to the scheme whereby additional compensation is switched in after a roll wheel failure. Such modifications are, however, outside the scope of this report.

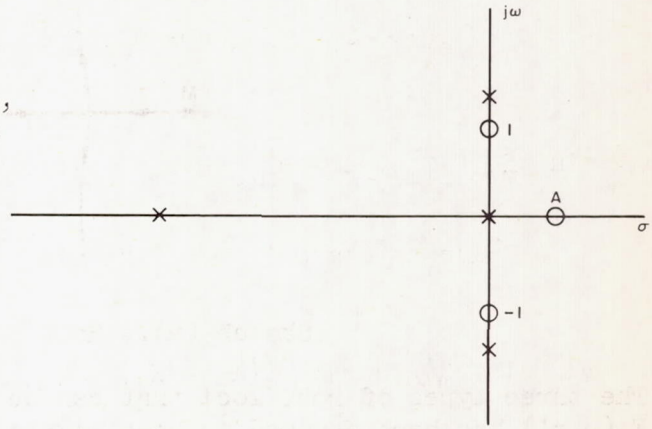

Sketch (i).- Typical pole-zero configuration for equation (61).

Steady-State Behavior at Large Angles of Yaw

For some purposes it may be required to rotate the satellite to some yawed position while maintaining the pitch and roll attitudes close to zero. One example of this is the previously mentioned yaw bias requirement for Nimbus. Yet another example could be a requirement to point, in a given direction, an antenna which is rigidly fixed to the main body of the satellite. An important property of the type of system under discussion is that if the yaw angle is large, then the nonlinearities and couplings inherent in the system produce steady-state pitch and roll attitudes which differ from zero. (It is assumed here that no provision is made to inject command signals to the roll and pitch channels.) The error involved in these angles is dependent on the angle of yaw, the inertia distribution of the satellite and the roll and pitch channel gains. In order to calculate the steady-state roll and pitch angles, it will be assumed that they are sufficiently small that their products may be neglected. The steady-state inertial angular velocities from equations (3) are

$$\left.\begin{aligned} \omega_1{}^s &= -\omega_o \sin \psi^s_{m/o} \\ \omega_2{}^s &= -\omega_o \cos \psi^s_{m/o} \\ \omega_3{}^s &= -\omega_o[-\varphi^s_{m/o} \cos \psi^s_{m/o} + \theta^s_{m/o} \sin \psi^s_{m/o}] \end{aligned}\right\} \tag{62}$$

where the superscript s means the steady-state value of the variable. Substituting for $\omega_1{}^s$, $\omega_2{}^s$, and $\omega_3{}^s$ from equations (62) into equations (1) yields

$$\omega_o{}^2 \cos \psi^s_{m/o}[-\varphi^s_{m/o} \cos \psi^s_{m/o} + \theta^s_{m/o} \sin \psi^s_{m/o}](I_3 - I_2)$$

$$= \omega_o \cos \psi^s_{m/o} h^s_{3w} - \omega_o[-\varphi^s_{m/o} \cos \psi^s_{m/o} + \theta^s_{m/o} \sin \psi^s_{m/o}](h^s_{2w} + h_{2K}) - 3\omega_o{}^2(I_2 - I_3)\varphi^s_{m/o} \tag{63}$$

$$\omega_o{}^2 \sin \psi^s_{m/o}[-\varphi^s_{m/o} \cos \psi^s_{m/o} + \theta^s_{m/o} \sin \psi^s_{m/o}](I_1 - I_3)$$

$$= \omega_o[-\varphi^s_{m/o} \cos \psi^s_{m/o} + \theta^s_{m/o} \sin \varphi^s_{m/o}]h^s_{1w} - \omega_o \sin \psi^s_{m/o} h^s_{3w} - 3\omega_o{}^2(I_1 - I_3)\theta^s_{m/o} \tag{64}$$

$$\omega_o{}^2 \sin \psi^s_{m/o} \cos \psi^s_{m/o}(I_2 - I_1) = \omega_o(h^s_{2w} + h_{2K}) \sin \psi^s_{m/o} - \omega_o h^s_{1w} \cos \psi^s_{m/o} \tag{65}$$

where misalinement errors have been assumed to be zero. The result of multiplying equation (63) by $\sin \psi^s_{m/o}$, equation (64) by $\cos \psi^s_{m/o}$, and adding is, after some rearranging,

$$[-\varphi^s_{m/o} \cos \psi^s_{m/o} + \theta^s_{m/o} \sin \psi^s_{m/o}][-\omega_o{}^2 \sin \psi^s_{m/o} \cos \psi^s_{m/o}(I_2 - I_1)$$

$$+ \omega_o(h^s_{2w} + h_{2K}) \sin \psi^s_{m/o} - \omega_o h^s_{1w} \cos \psi^s_{m/o}]$$

$$= -3\omega_o{}^2[\sin \psi^s_{m/o}(I_2 - I_3)\varphi^s_{m/o} + \cos \psi^s_{m/o}(I_1 - I_3)\theta^s_{m/o}] \tag{66}$$

hence from equation (65) it follows that equation (66) reduces to

$$\sin \psi^s_{m/o}(I_2 - I_3)\varphi^s_{m/o} + \cos \psi^s_{m/o}(I_1 - I_3)\theta^s_{m/o} = 0 \tag{67}$$

The steady-state roll and pitch inertia-wheel angular momenta h^s_{1w} and h^s_{2w} are given by equations (4) and (5), that is,

$$h_{1w}^{s} = K_{\varphi}\varphi_{m/o}^{s} \tag{68}$$

$$h_{2w}^{s} = K_{\theta}\theta_{m/o}^{s} \tag{69}$$

where, again, misalinements are assumed to be zero. Using equations (68) and (69), equation (65) can be written in the following form:

$$K_{\varphi} \cos \psi_{m/o}^{s}\varphi_{m/o}^{s} - K_{\theta} \sin \psi_{m/o}^{s}\theta_{m/o}^{s} = -\omega_{o} \sin \psi_{m/o}^{s} \cos \psi_{m/o}^{s}(I_2 - I_1) + h_{2K} \sin \psi_{m/o}^{s} \tag{70}$$

Equations (67) and (70) form two simultaneous linear equations in $\theta_{m/o}^{s}$ and $\varphi_{m/o}^{s}$ whose solution is

$$\theta_{m/o}^{s} = \frac{\omega_{o} \sin^2 \psi_{m/o}^{s}\left[(I_2 - I_1)\cos \psi_{m/o}^{s} - \frac{h_{2K}}{\omega_{o}}\right](I_1 - I_3)}{\sin^2 \psi_{m/o}^{s}(I_2 - I_3)K_{\theta} + \cos^2 \psi_{m/o}^{s}(I_1 - I_3)K_{\varphi}} \tag{71}$$

$$\varphi_{m/o}^{s} = \frac{-\omega_{o} \sin \psi_{m/o}^{s} \cos \psi_{m/o}^{s}\left[(I_2 - I_1)\cos \psi_{m/o}^{s} - \frac{h_{2K}}{\omega_{o}}\right](I_2 - I_3)}{\sin^2 \psi_{m/o}^{s}(I_2 - I_3)K_{\theta} + \cos^2 \psi_{m/o}^{s}(I_1 - I_3)K_{\varphi}} \tag{72}$$

An important property illustrated by equations (71) and (72) is that if

$$(I_2 - I_1)\cos \psi_{m/o}^{s} - \frac{h_{2K}}{\omega_{o}} = 0 \tag{73}$$

then $\theta_{m/o}^{s}$ and $\varphi_{m/o}^{s}$ are zero independent of the values of the gains K_{θ} and K_{φ}. For some mission requirements this could be a very valuable property and could be achieved for a given yaw angle $\psi_{m/o}^{s}$ simply by selecting the appropriate value of h_{2K}. (Note that equation (73) is identical to equation (32) when $\psi_{m/o}^{s} = 0$.) Another way of reducing $\theta_{m/o}^{s}$ and $\varphi_{m/o}^{s}$ is to increase the system gains K_{θ} and K_{φ} provided this does not violate any other requirement or lead to an unsatisfactory dynamic behavior.

COMPUTED RESULTS FOR A PRACTICAL EARTH-ORIENTED SATELLITE

Satellite inertias and basic control system data are given in appendix D. These data were typical of the Nimbus meteorological satellite at one stage in its development. The inertia distribution is favorable ($J_1 > 0$ and $J_2 > 0$) in the sense that the roll and pitch gravity torques are stabilizing. Identical lead-lag compensation networks are used in the pitch and roll channels. No compensation is used in the yaw channel, and no constant speed inertia wheels are used.

Studies were carried out using both digital and analog computers. Calculations on the digital computer were confined to investigations into the stability of the linearized equations describing the system. In the analog simulation, use was made of the complete equations with all the coupling and nonlinearities included. The analog study was used to determine the transient response of the system, particularly following a yaw command, and to check the validity of the stability derived from the linearized equations.

It has been demonstrated previously that the smaller the gyro time constant, the better the stability characteristics of the system and, furthermore, that it is necessary to incline the input axis of the gyro relative to the roll axis in order to avoid the possibility of instabilities being caused by gyro misalinements. It will be demonstrated subsequently that additional gyro inclination to the roll axis is necessary to avoid instabilities which can be caused by misalinements of the "marked" axes relative to the principal axes of inertia. In order to meet these desirable features, the basic control system studied is assumed to have a gyro with a time constant of 0.2 sec oriented with its input axis at an angle of -6° to the roll axis, that is, $\varphi_{c/d} = 0^\circ$, $\theta_{c/d} = -6^\circ$, and $\psi_{c/d} = 0^\circ$ (see appendix D).

Influence of Control System Gain

Root locus diagrams for the roll and yaw degrees of freedom of the basic system are shown in figures 2 and 3, respectively. It has been assumed that equation (32) is approximately satisfied, which, in this case, amounts to the statement that the pitch and roll inertias are approximately equal. The advantage of using an approximate solution of this kind for the roots of the roll-yaw characteristic equation is that it enables the stability of the roll and yaw degrees of freedom to be examined separately, thereby greatly facilitating an understanding of the influence of various system parameters, in particular, the system gains. The validity of the approximation in this case can be seen from table I, which shows a comparison of the approximate roots obtained from equations (36) and (37), an improved approximation obtained by using the true open loop poles on the imaginary axis of the roll diagram, and the exact roots. The comparison is given for two sets of the gains K_φ and K_ψ. The set with the smallest values (i.e., $K_\varphi = 0.3$ ft-lb-sec/radian, $K_\psi = 300$ ft-lb-sec^2/radian) results in a system with the greatest damping and one which therefore makes the greatest use of gravity torques to remove angular momentum from the vehicle (see fig. 2, also sketch (g) and related discussion). This system will subsequently

be referred to as the "low gain system." The other set of gains given in table I results in a system which, for all practical purposes, is undamped (see fig. 2). The gains are, however, sufficiently high to cause most of any initial angular momentum of the system to pass quickly to the inertia wheels. As a result the vehicle body angles and rates, in the residual undamped oscillation, are very small. This system will subsequently be referred to as the "high gain system." It can be seen from table I that the results of both methods are probably accurate enough for most engineering purposes. The second method of approximation produces better results for the low gain system while the first method produces better results for the high gain system. It is interesting to note that for the low gain system the coupling between roll and yaw introduced by the unequal roll and pitch inertias changes a real roll root and real yaw root into a complex pair of roots (see table I).

To complete the stability investigation, a root locus diagram for the pitch degree of freedom is shown in figure 4. This is similar to that shown in sketch (c) and discussed earlier. In order to maintain a balance in the stiffness of the control channels, the pitch gain K_θ for the low gain system is made equal to 0.3 ft-lb-sec/radian and that for the high gain system 76.4 ft-lb-sec/radian. It should be noted that, for both low and high gain systems, the channel gains have been arranged so that one unit of satellite body angle about any degree of freedom produces, in the steady state, approximately the same value of the angular momentum of the corresponding inertia wheel (i.e., $K_\theta = K_\varphi = \omega_o K_\psi$).

A comparison between the transient motion of the high and low gain systems when released from two different initial conditions is given in figures 5 and 6. It is immediately apparent that the transients of the low gain system are completely dominated by the lightly damped ($\zeta = 0.13$) mode of approximately orbital frequency. Satellite body angle, body rates, and inertia-wheel speeds all damp to zero although it takes several orbits for this to occur. Perhaps one of the most striking features of the low gain system behavior is the absence of any sharp peaks in any of the variables describing the system response. In contrast the high gain system, especially for initial conditions involving satellite body angles, exhibits rapid initial transients with relatively high peak values of body rates and inertia-wheel speeds - a behavior fully in accord with the characteristic roots of the high gain system (table I). When the rapid transients have died away, there remains, in the roll and yaw degrees of freedom, the residual undamped low-frequency mode. This shows up particularly in the inertia-wheel speeds. It does not show on the traces of the satellite body angles and body rates because the gain of the system is so high that the amplitude of the mode is below the resolution of the recorder.

It can be seen from figures 5 and 6 that there is only light coupling between both pitch and roll and pitch and yaw. To illustrate this further and to indicate the type of pitch response obtained, figure 7 shows the transients following a release of the system from an initial condition of 5° of pitch. As might be expected, the response of the low gain system is much slower than that of the high gain system although the damping remains very good.

There is no doubt that the high gain system provides a measure of control over the body rates and body angles which is far superior to that provided by the

low gain system. The principal objection to the high gain system is that accumulated system angular momentum cannot be bled off through the action of gravity torques. Instead, the only way of removing angular momentum from the system is by the expenditure of stored energy through the action of the coarse control system.

There remains the possibility that some control system with intermediate gains may provide some of the good response characteristics of the high gain system while maintaining sufficient damping of the low frequency mode to enable some degree of momentum dumping capability. An example of such an intermediate gain system is shown in figure 8. Here the gains have been set at $K_\theta = K_\Phi = 1$ ft-lb-sec/radian and $K_\psi = 1000$ ft-lb-sec^2/radian. The damping factor of the low-frequency mode is reduced from 0.13 for the low gain system to 0.055. Thus the low-frequency mode takes over twice as long to damp to a given fraction of its initial value; however, the response of the system is certainly improved.

Whether or not a compromise such as this can be regarded as satisfactory depends entirely on the design specifications. If the body angles and body angular rate specifications are not too stringent, then such a system could well provide an acceptable solution and one which requires the minimum amount of stored energy within the satellite.

Influence of Gyro Time Constant and Orientation

It has been suggested previously that, in general, it is desirable to use a gyro with a small time constant oriented to give a small positive value of $-C'_{13}/C'_{11}$. The basis for the argument is that these conditions result in the most stable roots of the yaw characteristic equation (eq. (36)). It has also been indicated that a system using an integrating gyro (very large time constant) can be made to yield reasonably stable roots of the yaw characteristic equation, provided the gyro input axis is oriented to give a large positive value of $-C'_{13}/C'_{11}$. In general these roots are not as stable as those for the system using a rate gyro. However, if these roots are such that they do not have an overwhelming influence on the transient behavior of the system, then it may be possible, especially with low control channel gains, to devise a system, using an integrating gyro, with a performance comparable to that using a rate gyro. The reason for believing this may be possible for the low gain system is that the transient response of this system has been shown to be primarily dependent on the low frequency oscillatory mode associated with stability in roll.

To check whether or not the above conjecture is valid, the system was changed in two stages. First the rate gyro (time constant of 0.2 sec) was replaced by an integrating gyro (time constant of 2000 sec), gyro orientation remaining unaltered at (0°, -6°, 0°). The main observable effect on the transient behavior of the system is an apparent increase in the coupling between roll and yaw in the sense that a disturbance introduced into one degree of freedom produces greater amplitude transients in the other (cf. figs. 5, 6, 9, 10, 11, 12, 13, 14). The initial nonlinear behavior displayed in most of the traces involving the high gain system are due to inertia-wheel motors attaining maximum

speed or maximum torque. The explanation for the coupling is that the roots of the yaw characteristic equation, which in the basic system are very damped, have had their damping reduced to the point where they materially influence the transient behavior of the system. The second change to the system involved a reorientation of the integrating gyro so that its input axis was inclined at an angle of -70° to the roll axis. Thus the value of $-C'_{13}/C'_{11}$ is increased from 0.105 to 2.748 and changes the yaw root locus diagram from the type shown in sketch (d)4 to that shown in sketch (d)3. The effect of this change on the transient behavior of the low gain system is shown in figures 9 and 10. It can be seen that the improvement in the damping of the roots of the yaw characteristic equation correspondingly improves the transient response of the system. In fact, a comparison of figures 9, 10 and 5, 6 shows that there is little to choose between the transient behavior of this system and that of the basic system employing the rate gyro. The effect of the system change on the high gain system is shown in figures 11 and 14. Although the change of gyro orientation greatly improves the transient behavior of the system, it is still considerably worse than that of the basic system. This is particularly evident when the initial conditions are in the form of angular rates, where a relatively poorly damped oscillation and a very slow convergence tend to dominate the motion.

To demonstrate the influence of gyro orientation on the behavior of the system using a rate gyro, the orientation was changed from $(0^{\circ}, -6^{\circ}, 0^{\circ})$ to $(0^{\circ}, 0^{\circ}, 0^{\circ})$; that is, the input axis of the gyro was directed along the m_1, or roll, axis. A comparison, at high gain, between this and the basic system is shown in figure 15. It can be seen that the stability of the system with gyro oriented $(0^{\circ}, 0^{\circ}, 0^{\circ})$ is much poorer than that of the basic system. The high frequency, lightly damped mode which occurs primarily in yaw can be anticipated from the arguments leading to sketch (e). A similar investigation using low gains showed no detectable differences between the behaviors of the two systems - again in general agreement with sketch (e).

Effect of Control Axes Misalinement

The effect of a $+5^{\circ}$ pitch control axis misalinement on the behavior of both low and high gain systems is shown in figure 16. It can be seen that with the low gain system the pitch inertia-wheel speed and pitch angle reach steady-state values in about 50 minutes. On the other hand, with the high gain system there is no indication of an approach to the steady-state condition even after 200 minutes. In fact, with this magnitude of pitch axis misalinement, the pitch inertia wheel of the high gain system attains its maximum design speed before a steady-state condition occurs. Thus, whereas the pitch inertia wheel of the low gain system only attains a speed of 80 rpm, that of the high gain system reaches its maximum design speed of 1800 rpm in 8 hours and must then be despun back to zero - a process which must be repeated at least every 8 hours.

A possible difficulty may occur with a low gain system because of the angle of pitch deviating from zero to a value equal to the misalinement angle. Suppose, for example, that it is desired to maintain the pitch attitude angle to within 3° of zero and that at 3° the coarse control system operates to reduce the attitude error. The coarse control system would have to come into operation at

least once every 25 minutes to maintain the pitch attitude within the specified limits. This could result in a higher rate of energy expenditure by the coarse control system than continual inertia-wheel speed desaturation with the high gain system. If, however, the specifications are such that the coarse control system threshold is greater than the anticipated pitch control axis misalinement, then the low gain system may have advantages from the point of view of expenditure of energy for control.

A series of computer runs was made wherein the systems were released from various initial conditions. It was observed that, for both low and high gain systems, the transients with and without the $+5^{\circ}$ pitch control axis misalinement were almost indistinguishable, thus verifying that small positive pitch control axis misalinements have very little influence of stability.

Shown in figure 17 is the transient behavior when the basic high gain system with a pitch control axis misalinement of -5° is released from an initial condition of 5° of roll. A comparison between figure 17 and figure 15 shows that, again, misalinements have very little influence on stability. If, however, the gyro orientation is changed from $(0^{\circ}, -6^{\circ}, 0^{\circ})$ to $(0^{\circ}, -2^{\circ}, 0^{\circ})$ then (see fig. 17) the -5° pitch control axis misalinement causes a high-frequency very lightly damped mode which appears chiefly in the yaw degree of freedom. That this loss of stability is due to the misalinement and not to the change of gyro orientation can be seen from figure 18 which shows the system behavior in the absence of misalinements. This demonstrates the importance of pitch axis misalinements on stability and indicates the sensitivity of the system to gyro orientation. A similar investigation carried out using the low gain system showed that pitch axis misalinements, of the order of magnitude considered here, have very little influence on the behavior of the system.

The effect of a $+5^{\circ}$ roll control axis misalinement on the behavior of both low and high gain systems is shown in figure 19. It can be seen that a roll axis misalinement is not so important as a pitch misalinement since it results in only relatively small variations in the orientation angles and inertia-wheel speeds. Computer runs comparing the initial transients with and without roll axis misalinements demonstrated that roll axis misalinements have a negligible influence on stability.

Yaw Channel Failure

It has been shown previously that, if the yaw channel fails, the system can be stabilized by the introduction of a constant speed pitch inertia wheel. It was also suggested that, provided the required angular momentum of the constant speed wheel is sufficiently small, biasing the speed of the pitch control inertia wheel could provide a solution. The feasibility of a scheme of this kind has been investigated for the satellite under consideration here. A value of h_{2K} equal to 0.2 ft-lb-sec was selected. This is exactly equal to one half of the assumed pitch control wheel capability (appendix D) and also satisfies the expression

$$\left(J_3 - \frac{h_{2K}}{\omega_o I_3}\right)\left(4J_1 - \frac{h_{2K}}{\omega_o I_1}\right) = 1$$

thus assuring stability. The root locus diagram for the roll-yaw stability, using this value of h_{2K}, is shown in figure 20. It can be seen that with the low gain system (i.e., K_φ = 0.3 ft-lb-sec/radian) the stability is relatively good, the damping factor for both modes of oscillation being of the order of 0.35. It should be noted that this is better than the damping factor of the low frequency mode of the fully operating system (damping factor of 0.13). The transients following initial conditions of 5° of roll and 0.005°/sec of roll rate are shown in figures 21 and 22. It can be seen that a yaw channel failure makes the system more sensitive to disturbances which influence roll rate but it operates satisfactorily and offers a method of extending the life of the satellite in the event of a yaw channel failure.

The stability of the high gain system (i.e., K_φ = 76.4 ft-lb-sec/radian) is poor, as might be expected. The root locus diagram of figure 20 shows that not only is the low-frequency mode, for all practical purposes, undamped but there is also a negative real root very close to zero (s' = -0.00255). The implication is that any disturbance to either the roll or yaw degrees of freedom will cause the yaw angle to oscillate with orbital frequency (and zero damping) while the mean angle of yaw tends to drift away from zero. This conclusion is verified by figures 23 and 24 which show the transients following initial conditions of 5° angle of roll or 0.005°/sec rate of roll. Thus this scheme when applied to a high gain system cannot be regarded as providing an adequate solution to the yaw channel failure problem.

Yaw Bias Response

The response of both the low gain and high gain systems to a yaw bias command is shown in figure 25. The command signal used is based on a Nimbus satellite requirement represented here as a change of yaw angle from +37.5° to -37.5° in about 10 minutes. With the type of time linear command signal shown in figure 25, the performance of the high gain system is undoubtedly superior. The change of angle of yaw from +37.5° to -37.5° takes about 12 minutes for the high gain system as compared with about 37 minutes for the low gain system.

Because of the coupling between the degrees of freedom, an angle of yaw produces steady-state angles of roll and pitch as discussed in earlier sections of this report. This effect is particularly evident with the low gain system where, as can be seen from figure 25, the angle of roll changes by about 8° due to the yaw bias maneuver, that is, from +4° to -4°. The effect on both roll and pitch is predicted with good accuracy by equations (71) and (72). With the high gain system the steady-state roll and pitch angles are reduced, relative to those of the low gain system, by a factor of 255 (i.e., ratio of high gain to low gain; see eqs. (71) and (72)) and are therefore too small to be detected in figure 25.

If, in the case of the satellite considered here, roll deviations of the order of 4° are tolerable during the yaw bias phase, then the yaw bias requirement can be met by reshaping the command signal. For example, if the command signal is changed to that shown in figure 26, then the low gain system meets the

requirements. The feasibility of this approach depends, of course, on the stringency of the yaw bias requirement which may, in some cases, be sufficiently severe to preclude the use of a truly low gain system.

SUMMARY OF RESULTS

A dominating feature of the dynamical behavior of the earth-oriented satellites considered is that the earth pointing axis rotates with orbital angular velocity with respect to inertial space, which results in the roll and yaw degrees of freedom being strongly coupled. This coupling, in general, precludes an analysis on a unidimensional basis. One important exception is when the condition $(I_2 - I_1) - (h_{2K}/\omega_o) = 0$ is satisfied. In this case the stability in roll and yaw are independent. An investigation of this case reveals many fundamental aspects of the dynamical behavior of earth-oriented satellites.

With the type of control system considered here, there exists a set of gains for maximum damping (termed the low gain system). An increase in the gains above those for maximum damping causes a progressive reduction of the damping of a mode of oscillation with a frequency close to orbital. This mode is closely related to the stability of the vehicle angular momentum, which in turn is dictated primarily by the gravity torques acting on the vehicle. In fact the magnitude of the gravity torques largely determines the maximum rate at which angular momentum can be dumped into the orbit.

The stability of the system is independent of whether or not the gyro input axis is located out of the satellite roll-yaw plane. A rate gyro with a small time constant oriented, relative to the roll axis, at a small angle above the satellite roll pitch plane provides the best method of controlling yaw. An integrating gyro can be used to control yaw and with the most favorable orientation results in a low gain system with a performance comparable with that using a rate gyro. Even with the most favorable orientation a high gain system using an integrating gyro has poorer stability than one with a rate gyro. One problem with the integrating gyro is that the most favorable orientation from the point of view of stability results in a reduced sensitivity to angle of yaw.

Control axes misalinements are more serious in pitch than in either roll or yaw. A pitch misalinement can cause instability if the rate gyro input axis is oriented too close to the roll axis. In addition, pitch misalinements may cause excessively high rates of expenditure of stored energy by the coarse control system for both low and high gain systems, the former because of large deviations in angle of pitch, the latter through the need for repeated inertia-wheel despinning. The low gain system could show advantages if the anticipated pitch control axis misalinement angle were less than the satellite coarse control system pitch attitude threshold limit.

Yaw bias requirements are most easily met by the high gain system, but the low gain system in many cases can be made to operate satisfactorily by suitable shaping of the yaw command signal. One problem with the low gain system is that large steady-state angles of yaw produce steady-state angles of pitch and roll.

A constant speed pitch wheel will stabilize the system when the yaw channel fails and is particularly satisfactory when the system gains are low. The system is still theoretically stable when high gains are used, but it is so poorly damped that it cannot be regarded as satisfactory. A constant speed pitch wheel will not stabilize the system when the roll channel fails.

Ames Research Center
National Aeronautics and Space Administration
Moffett Field, Calif., Feb. 13, 1963

APPENDIX A

DERIVATION OF THE GYRO TRANSFER FUNCTION

The expression for the gyro gimbal angle θ_g (eq. (2)) may be rewritten in the form

$$\begin{aligned} I_g\ddot{\theta}_g + C_o\dot{\theta}_g = &-I_g(C'_{21}\dot{\omega}_1 + C'_{22}\dot{\omega}_2 + C_{23}\dot{\omega}_3) \\ &+ H_r[(C'_{11} - C_{31}\theta_g)\omega_1 + (C'_{12} - C_{32}\theta_g)\omega_2 + (C'_{13} - C_{33}\theta_g)\omega_3] \\ &+ \Delta M_g - K\theta_g \end{aligned} \tag{A1}$$

where K is the torque generator feedback constant ($K = 0$ for a gyro operating in the integrating mode, ΔM_g is any spurious torque acting about the gyro gimbal axis and C'_{11}, C'_{12}, etc.,[1] are related to C_{11}, C_{12}, etc., by the following expressions

$$\left.\begin{aligned} C'_{21} &= C_{21} - \psi_{d/m}C_{22} + \theta_{d/m}C_{23} \\ C'_{22} &= C_{22} + \psi_{d/m}C_{21} - \varphi_{d/m}C_{23} \\ C'_{23} &= C_{23} - \theta_{d/m}C_{21} + \varphi_{d/m}C_{22} \\ C'_{11} &= C_{11} - \psi_{d/m}C_{12} + \theta_{d/m}C_{13} \\ C'_{12} &= C_{12} + \psi_{d/m}C_{11} - \varphi_{d/m}C_{13} \\ C'_{13} &= C_{13} - \theta_{d/m}C_{11} + \varphi_{d/m}C_{12} \end{aligned}\right\} \tag{A2}$$

Note that if there are no misalinements, $C'_{11} = C_{11}$, etc.

In the case of small satellite body angles and rates, the relationship between the inertial angular velocities and Euler angles and rates as expressed by equations (3) becomes, to a first approximation,

$$\left.\begin{aligned} \omega_1 &= \dot{\varphi}_{m/o} - \omega_o\psi_{m/o} \\ \omega_2 &= \dot{\theta}_{m/o} - \omega_o \\ \omega_3 &= \dot{\psi}_{m/o} + \omega_o\varphi_{m/o} \end{aligned}\right\} \tag{A3}$$

---

[1]Note that the quantities C'_{11}, C'_{12}, etc., are the direction cosines relating the $\bar{c}_i$ axes to the $\bar{m}_i$ axes.

Substituting equation (A3) into equation (A1), rearranging the terms, and deleting those involving products of small quantities results in the following expression:

$$I_g\ddot{\theta}_g + C_D\dot{\theta}_g + (K - H_r\omega_{2o}C_{32})\theta_g = H_r[(C'_{11}\varphi_{m/o} + C'_{13}\omega_o\varphi_{m/o}) + C'_{12}(\dot{\theta}_{m/o} - \omega_o) + (C'_{13}\dot{\psi}_{m/o} - C'_{11}\omega_o\psi_{m/o})] + \Delta M_g \qquad (A4)$$

where the terms in I_g on the right side of equation (A1) have been omitted because H_r is numerically very much greater than I_g (the ratio is usually of the order of 10^3).

Equation (A4), written in terms of the Laplace transform variable s, becomes

$$[I_gs^2 + C_Ds + (K - H_r\omega_oC_{32})]\theta_g = H_r[(C'_{11}s + C'_{13}\omega_o)\varphi_{m/o} + C'_{12}s\theta_{m/o} + (C'_{13}s - C'_{11}\omega_o)\psi_{m/o}] + \Delta M_g - H_rC'_{12}\omega_o \qquad (A5)$$

Since, in general, $I_g/C_D \ll C_D/(K-H_r\omega_oC_{32})$ the expression $I_gs^2+C_Ds+(K-H_r\omega_oC'_{32})$ can be written, with good accuracy, in the form

$$(K - H_r\omega_oC_{32})\left(\frac{I_gs}{C_D} + 1\right)\left(\frac{C_Ds}{K - H_r\omega_oC_{32}} + 1\right)$$

The time constant I_g/C_D is usually extremely small, that is, of the order of 0.001 second. It can therefore be assumed that the term $[(I_gs/C_D) + 1]$ does not significantly affect the system dynamics. Equation (A5) can then be written in the following form:

$$\theta_g = \frac{H_r}{K-H_r\omega_oC_{32}}\left[\frac{(C'_{11}s+C'_{13}\omega_o)\varphi_{m/o}+C'_{12}s\theta_{m/o}+(C'_{13}s-C'_{11}\omega_o)\psi_{m/o}+\frac{\Delta M_g}{H_r}-C'_{12}\omega_o}{\tau_gs + 1}\right] \qquad (A6)$$

where

$$\tau_g = \frac{C_D}{K - H_r\omega_oC_{32}}$$

It can be seen from equation (A6) that the only difference between the dynamic behavior of gyros operating in the rate or the integrating mode arises through differences in the time constant τ_g. As might be expected, the differences in τ_g can be very large. For example, a typical gyro has a value of τ_g in the integrating mode of about 2000 seconds, while in the rate mode it can be made, say, 0.2 second or even smaller, if desired, simply by choosing the appropriate value for the torque generator feedback constant K. The value of τ_g in the integrating mode can be changed by changing the value of the damping constant C_D, although this may involve major design changes in the gyro.

It should be noted here that the gyro used in the integrating mode is stable only if $H_r\omega_o C_{32}$ is negative. Since ω_o is positive and H_r is positive, this implies that C_{32} must be negative. This means that the positive direction of the gyro spin reference axis must make an angle of less than 90^o with respect to the negative $\bar{d}_2$ direction of the gyro reference frame. This condition is not generally necessary in the case of the rate gyro since K is normally much greater than $H_r\omega_o C_{32}$.

APPENDIX B

ALTERNATIVE DERIVATION OF THE CHARACTERISTIC EQUATION

In the section of the report dealing with the stability of the linearized equations, the characteristic equation is derived by the usual method of taking the determinant of the coefficients. The disadvantage of this approach is that it is a purely formalistic procedure which, in some cases, can obscure some of the physical facts related to the final form of the characteristic equation. It is proposed here to use an alternative method of derivation to reveal some of these physical implications.

The set of linearized homogeneous equations is given below in terms of the Laplace transform variable s' appropriate to a time scale $\tau = \omega_o t$.

$$\left[I_1 s'^2 - 4(I_3 - I_2) - \frac{h_{2K}}{\omega_o}\right]\Phi + \left[-(I_1 - I_2 + I_3)s' - \frac{h_{2K}}{\omega_o}\right]\Psi + \frac{s'h_{1W}}{\omega_o} - \frac{h_{3W}}{\omega_o} = 0 \tag{B1}$$

$$[I_2 s'^2 + 3(I_1 - I_3)]\Theta + \frac{s'h_{2W}}{\omega_o} = 0 \tag{B2}$$

$$\left[(I_1 - I_2 + I_3)s' + \frac{h_{2K}}{\omega_o}\right]\Phi + \left[I_3 s'^2 + (I_2 - I_1) - \frac{h_{2K}}{\omega_o}\right]\Psi + \frac{h_{1W}}{\omega_o} + \frac{s'h_{3W}}{\omega_o} = 0 \tag{B3}$$

$$\frac{-K_\Phi F_\Phi(\omega_o s')\Phi}{\omega_o} + \frac{h_{1W}}{\omega_o} = 0 \tag{B4}$$

$$\frac{-K_\Theta F_\Theta(\omega_o s')\Theta}{\omega_o} + \frac{h_{2W}}{\omega_o} = 0 \tag{B5}$$

$$K_\Psi F_\Psi(\omega_o s')(C'_{11}s' + C'_{13})\Phi + K_\Psi F_\Psi(\omega_o s')C'_{12}\Theta + K_\Psi F_\Psi(\omega_o s')(C'_{13}s' - C'_{11})\Psi + \frac{h_{3W}}{\omega_o} = 0 \tag{B6}$$

where Φ, Θ, and Ψ are the Laplace transforms of $\varphi_{m/o}$, $\theta_{m/o}$, $\psi_{m/o}$. It follows immediately from equations (B2) and (B5) that

$$\left[I_2 s'^2 + 3(I_1 - I_3) + \frac{K_\Theta F_\Theta(\omega_o s')s'}{\omega_o}\right]\Theta = 0 \tag{B7}$$

Consider the two quantities ζ and η defined by the following equations

$$\zeta = I_1 s'\Phi + \frac{h_{1W}}{\omega_o} + \left[(I_2 - I_1) - \frac{h_{2K}}{\omega_o}\right]\Psi \tag{B8}$$

$$\eta = I_3 s'\Psi + \frac{h_{3W}}{\omega_o} + \left[(I_3 - I_2) + \frac{h_{2K}}{\omega_o}\right]\Phi \tag{B9}$$

The quantities ζ and η are, in reality, the components of angular momentum about the $\bar{b}_1$ and $\bar{b}_3$ axes, respectively. Substituting equations (B8) and (B9) into equations (B1) and (B3) yields

$$s'\zeta - \eta - 3(I_3 - I_2)\Phi = 0 \tag{B10}$$

$$s'\eta - \zeta = 0 \tag{B11}$$

Substituting for Φ from equation (B10) into equations (B4) and (B8) and for h_{1W}/ω_o from equation (B4) into equation (B8) yields

$$s'^2\zeta - s'\eta + 3J_1\zeta + \frac{K_\varphi F_\varphi(\omega_o s')(s'\zeta - \eta)}{I_1\omega_o} - 3J_1\left[(I_2 - I_1) - \frac{h_{2K}}{\omega_o}\right]\Psi = 0 \tag{B12}$$

Substituting for ζ from equation (B11) into equation (B12)

$$\left[s'(s'^2 + 1 + 3J_1) + \frac{K_\varphi F_\varphi(\omega_o s')(s'^2 + 1)}{I_1\omega_o}\right]\eta + 3J_1\left[(I_2 - I_1) - \frac{h_{2K}}{\omega_o}\right]\Psi = 0 \tag{B13}$$

Substituting for Φ from equation (B10) into equations (B9) and (B6), and for h_{3W}/ω_o from equation (B6) into equation (B9)

$$\eta + \left[(I_3 - I_2) + \frac{h_{2K}}{\omega_o}\right]\frac{(s'\zeta - \eta)}{3J_1I_1} - K_\psi F_\psi(\omega_o s')(C'_{11}s' + C'_{13})\frac{(s'\zeta - \eta)}{3J_1I_1}$$

$$+ K_\psi F_\psi(\omega_o s')C'_{12}\Theta - [I_3 s' - K_\psi F_\psi(\omega_o s')(C'_{13}s' - C'_{11})]\Psi = 0 \tag{B14}$$

Substituting for ζ from equation (B11) into equation (B14) and rearranging

$$-\frac{1}{3J_1}\left\{3J_1 - \left[(I_3 - I_2) + \frac{h_{2K}}{\omega_o}\right]\frac{(s'^2 + 1)}{I_1} + K_\psi F_\psi(\omega_o s')(C'_{11}s' + C'_{13})\frac{(s'^2 + 1)}{I_1}\right\}\eta$$

$$- K_\psi F_\psi(\omega_o s')C'_{12}\Theta + I_3\left[s' - \frac{K_\psi F_\psi(\omega_o s')(C'_{13}s' - C'_{11})}{I_3}\right]\Psi = 0 \tag{B15}$$

Now if $(I_2 - I_1) - (h_{2K}/\omega_o) = 0$, equation (B13) reduces to

$$\left[s'(s'^2 + 1 + 3J_1) + \frac{K_\varphi F_\varphi(\omega_o s')(s'^2 + 1)}{I_1\omega_o}\right]\eta = 0 \tag{B16}$$

thus demonstrating that with $[(I_2 - I_1) - (h_{2K}/\omega_o)] = 0$ the equation

$$s'(s'^2 + 1 + 3J_1) + \frac{K_\Phi F_\Phi(\omega_o s')(s'^2 + 1)}{I_1 \omega_o} = 0 \qquad (B17)$$

governs the stability of the yaw component of angular momentum η and, by equations (B11) and (B10), the stability of the roll component of angular momentum ζ and the roll angle Φ. Thus equation (B17) provides all the necessary information for deciding whether or not the system is capable of "dumping" its angular momentum (roll-yaw) into the orbit.

A disturbance introduced through the angle of yaw Ψ cannot influence Θ nor, if $(I_2 - I_1) - (h_{2K}/\omega_o) = 0$, can it influence η, since both of these variables are uniquely determined by equations (B7) and (B16). It follows that the stability in yaw is governed only by the term in Ψ in equation (B15); that is,

$$s' - \frac{K_\Psi F_\Psi(\omega_o s')(C'_{13}s - C'_{11})}{I_3} = 0 \qquad (B18)$$

This argument also shows that since C'_{12} only occurs in equation (B14) it can have no influence on the stability of the system. However, while the terms in Θ and η in equation (B15) do not influence the stability of the system, they do have an influence on the transient motion in yaw; that is, a disturbance in either Θ or η produces a disturbance in Ψ.

APPENDIX C

SOME PROPERTIES OF THE DENOMINATOR POLYNOMIAL IN EQUATION (59)

Consider the polynomial

$$s'^4 + s'^2\left[1 + 3J_1 + \left(J_3 - \frac{h_2K}{\omega_o I_3}\right)\left(J_1 - \frac{h_2K}{\omega_o I_1}\right)\right] + \left(J_3 - \frac{h_2K}{\omega_o I_3}\right)\left(4J_1 - \frac{h_2K}{\omega_o I_1}\right) = 0$$

when

$$J_1 \geq 0$$

To ease the subsequent discussion, the polynomial will be written

$$s'^4 + Bs'^2 + C = 0 \tag{C1}$$

where

$$B = \left[1 + 3J_1 + \left(J_3 - \frac{h_2K}{\omega_o I_3}\right)\left(J_1 - \frac{h_2K}{\omega_o I_1}\right)\right] \tag{C2}$$

$$C = \left(J_3 - \frac{h_2K}{\omega_o I_3}\right)\left(4J_1 - \frac{h_2K}{\omega_o I_1}\right) \tag{C3}$$

It is well known that the most stable set of roots[1] which can be possessed by a polynomial of the form given in equation (C1) is when all the roots are imaginary. The necessary and sufficient conditions for this are:

$$B \geq 0 \tag{C4}$$

$$C \geq 0 \tag{C5}$$

$$B^2 - 4C \geq 0 \tag{C6}$$

Equation (C3) can be written in the following form:

$$\left(\frac{h_2K}{\omega_o I_3}\right)^2 - \frac{h_2K}{\omega_o I_3}\left(J_3 + 4J_1\frac{I_1}{I_3}\right) + \frac{I_1}{I_3}(4J_1J_3 - C) = 0 \tag{C7}$$

---

[1]The term "most stable set of roots" is defined to mean the set of roots with the least upper bound for the real parts.

and has real roots provided

$$\left(J_3 + 4J_1 \frac{I_1}{I_3}\right)^2 - 4 \frac{I_1}{I_3} (4J_1J_3 - C) \geq 0$$

or

$$\left(J_3 - 4J_1 \frac{I_1}{I_3}\right)^2 + 4 \frac{I_1}{I_3} C \geq 0 \tag{C8}$$

Thus if condition (C5) is satisfied, then equation (C7) always has two real roots (i.e., $(h_{2K}/\omega_o I_3)_1$ and $(h_{2K}/\omega_o I_3)_2$). These roots clearly satisfy the following conditions:

$$\left.\begin{aligned} \left(\frac{h_{2K}}{\omega_o I_3}\right)_1 &\geq J_3 \\ \left(\frac{h_{2K}}{\omega_o I_1}\right)_1 &\geq 4J_1 \end{aligned}\right\} \tag{C9}$$

and

$$\left.\begin{aligned} \left(\frac{h_{2K}}{\omega_o I_3}\right)_2 &\leq J_3 \\ \left(\frac{h_{2K}}{\omega_o I_3}\right)_2 &\leq 4J_1 \end{aligned}\right\} \tag{C10}$$

Equation (C2) can be written in the following form

$$B = 1 + 3J_1 \left[1 - \left(J_3 - \frac{h_{2K}}{\omega_o I_3}\right)\right] + C \tag{C11}$$

Thus if a value of h_{2K} is selected which satisfies condition (C9) and, therefore condition (C5), then it follows from equation (C11) that

$$B \geq 1 + C > 0 \tag{C12}$$

so that condition (C4) is satisfied. Furthermore it follows from conditions (C12) and (C5) that

$$B^2 - 4C \geq B^2 - 4(B - 1) = (B - 2)^2 > 0 \qquad (C13)$$

so that condition (C6) is satisfied.

The solution of equation (C1) in terms of s'^2 is

$$s'^2 = \frac{-B \pm \sqrt{B^2 - 4C}}{2}$$

Considering first the positive value of the square root and using condition (C12)

$$(s'^2)_1 = \frac{-B + \sqrt{B^2 - 4C}}{2} \geq \frac{-B + \sqrt{B^2 - 4(B - 1)}}{2} = -1$$

Thus

$$\left.\begin{aligned} s'_{11} = -s'_{12} = Kj \\ \text{where} \quad K \leq 1 \end{aligned}\right\} \qquad (C14)$$

The remaining roots are derived by taking the negative value for the square root, that is,

$$(s'^2)_2 = \frac{-B - \sqrt{B^2 - 4C}}{2} \leq \frac{-B - \sqrt{B^2 - 4(B - 1)}}{2} = -(B - 1) \leq -C$$

Thus

$$\left.\begin{aligned} s'_{21} = -s'_{22} = Lj\sqrt{C} \\ \text{where} \quad L \geq 1 \end{aligned}\right\} \qquad (C15)$$

To sum up, therefore, for every value of h_{2K}/ω_o which satisfies the condition

$$\frac{h_{2K}}{\omega_o} \geq [\text{both } (I_2 - I_1) \text{ and } 4(I_2 - I_3)]$$

all the roots of equation (C1) lie on the imaginary axis. Furthermore the roots are symmetrically disposed relative to the real axis and the two on the positive imaginary axis are located so that one is always equal to or less than j and the other always greater than or equal to $j\sqrt{C}$.

APPENDIX D

SATELLITE BASIC DATA

Inertias

Principal inertia in roll I_1	190 slug-ft^2
Principal inertia in pitch I_2	146 slug-ft^2
Principal inertia in yaw I_3	120 slug-ft^2

Inertia Parameters

$$J_1 = \frac{I_2 - I_3}{I_1} \qquad 0.137$$

$$J_2 = \frac{I_1 - I_3}{I_2} \qquad 0.480$$

$$J_3 = \frac{I_2 - I_1}{I_3} \qquad -0.367$$

Control-System Transfer Functions

$$F_\varphi(S) = \frac{1 + \tau_\varphi s}{(1 + \alpha\tau_\varphi s)(1 + \tau_m s)}$$

$$F_\theta(s) = \frac{1 + \tau_\theta s}{(1 + \alpha\tau_\theta s)(1 + \tau_m s)}$$

$$F_\psi(s) = \frac{1}{(1 + \tau_g s)(1 + \tau_m s)}$$

where the time constants, etc., have the following values:

Motor time constant τ_m	38.4 sec
Gyro time constant τ_g (rate mode)	0.2 sec
Gyro time constant τ_g (integrating mode)	2000 sec
Compensation network time constant $\tau_\varphi = \tau_\theta$	7 sec
Compensation network lead-lag constant α	0.1

Additional Motor Flywheel Characteristics

Maximum flywheel speed	1800 rpm
Stall torque	0.0104 ft-lb
Maximum momentum	0.4 ft-lb-sec

Gyro Orientation Matrix

Since for a gyro working in the integrating mode, it is essential that C_{32} be negative (see appendix A). The $\bar{c}_i$ and $\bar{d}_i$ reference frames are initially alined so that the spin reference axis of the gyro lies along the negative $\bar{d}_2$ axis, that is, initially,

$$\begin{bmatrix} \bar{C}_1 \\ \bar{C}_2 \\ \bar{C}_3 \end{bmatrix} = \begin{bmatrix} 1 & 0 & 0 \\ 0 & 0 & 1 \\ 0 & -1 & 0 \end{bmatrix} \begin{bmatrix} \bar{d}_1 \\ \bar{d}_2 \\ \bar{d}_3 \end{bmatrix}$$

The Euler sequence orienting the $\bar{c}_i$ frame relative to the $\bar{d}_i$ frame is pitch, yaw, roll, that is, $\theta_{c/d}$, $\psi_{c/d}$, $\varphi_{c/d}$. This yields the following relationships for those elements of the [C] matrix which enter into the gyro equations:

$$C_{11} = \cos \psi_{c/d} \cos \theta_{c/d}$$

$$C_{12} = \sin \psi_{c/d}$$

$$C_{13} = \sin \theta_{c/d} \cos \psi_{c/d}$$

$$C_{32} = -\cos \psi_{c/d} \cos \varphi_{c/d}$$

It is assumed throughout that the orbit is circular and the orbital rate ω_o is 0.001 radian/sec. This is equivalent to a satellite altitude of about 580 statute miles.

REFERENCES

1. Roberson, Robert E.: Methods for the Control of Satellites and Space Vehicles. WADD Tech. Rep. 60-643, vol. 2, July 1960.

2. Roberson, R. E.: Torques on a Satellite Vehicle From Internal Moving Parts. Jour. Appl. Mech., vol. 25, no. 2, June 1958, pp. 196-200.

3. Cannon, Robert H., Jr.: Some Basic Response Relations for Reaction-Wheel Attitude Control. American Rocket Society Jour., vol. 32, no. 1, Jan. 1962, pp. 61-74.

TABLE I.- COMPARISON BETWEEN APPROXIMATE AND EXACT ROOTS OF ROLL-YAW CHARACTERISTIC EQUATION

Low gain K_φ = 0.3 ft-lb-sec/radian, K_ψ = 300 ft-lb-sec^2/radian

Principal degree of freedom	Approximation (1) Derived from equations (36) and (37)		Approximation (2) Equations (36) and (37) with true open loop imaginary poles		Exact	
	Real	Imaginary	Real	Imaginary	Real	Imaginary
Roll	-0.1009	-1.062	-0.1242	-1.077	-0.1376	-1.052
Roll	-.1009	1.062	-.1242	1.077	-.1376	1.052
Roll	-24.61		-24.61		-24.76	
Roll	-1430		-1430		-1430	
Roll	-1.469		-1.422		-1.468	-.9164
Yaw	-2.133		-2.133		-1.468	.9164
Yaw	-30.76		-30.76		-31.20	
Yaw	-4993		-4993		-4993	
High gain K_φ = 76.4 ft-lb-sec/radian, K_ψ = 76,400 ft-lb-sec^2/radian						
Roll	-.0005105	-1.000	-.0006210	-1.000	-.0005162	-1.000
Roll	-.0005105	1.000	-.0006210	1.000	-.0005162	1.000
Roll	-48.17	-93.26	-48.17	-93.26	-46.90	-93.43
Roll	-48.17	93.26	-48.17	93.26	-46.90	93.43
Roll	-1360		-1360		-1360	
Yaw	-2508	-1588	-2508	-1588	-2509	-1593
Yaw	-2508	1588	-2508	1588	-2509	1593
Yaw	-9.461		-9.461		-9.490	

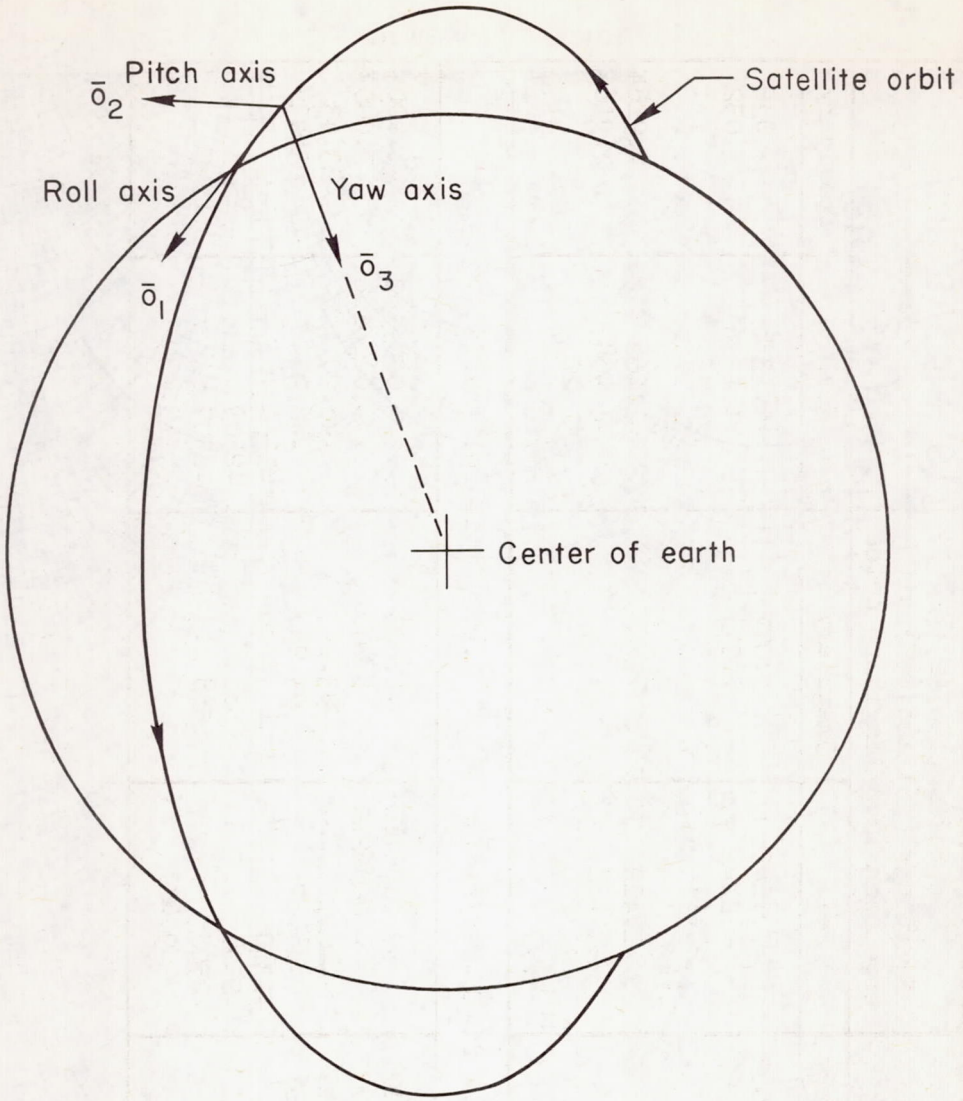

$\bar{o}_3$ is along a line from the vehicle center of mass to the center of the earth.

$\bar{o}_2$ is perpendicular to the orbital plane (measured positive in the reverse direction to the orbital angular momentum vector).

$\bar{o}_1$ is perpendicular to $\bar{o}_3$ and $\bar{o}_2$ and completes the right handed axes system.

Figure 1.- Orbital reference frame.

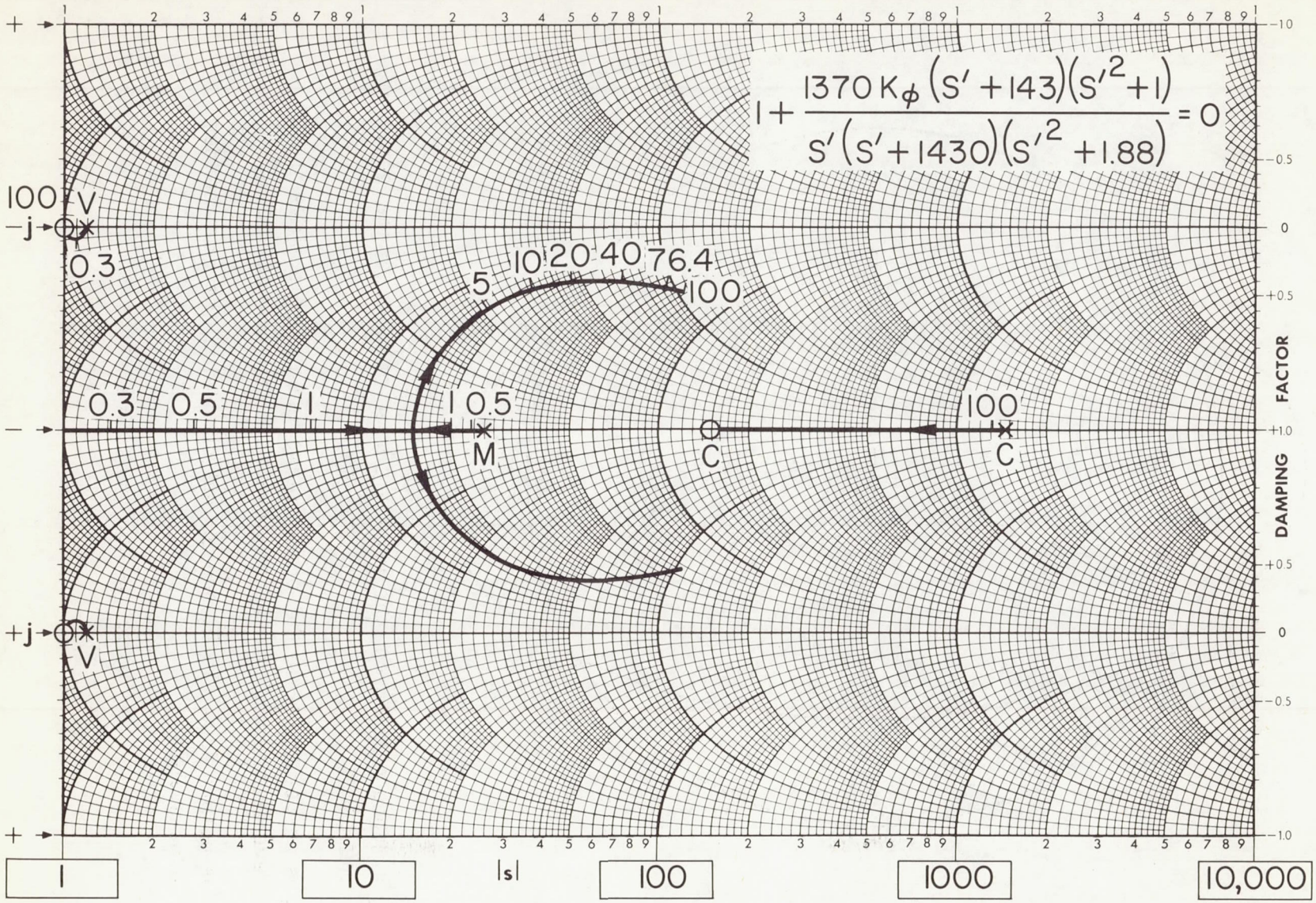

Figure 2.- Roll stability.

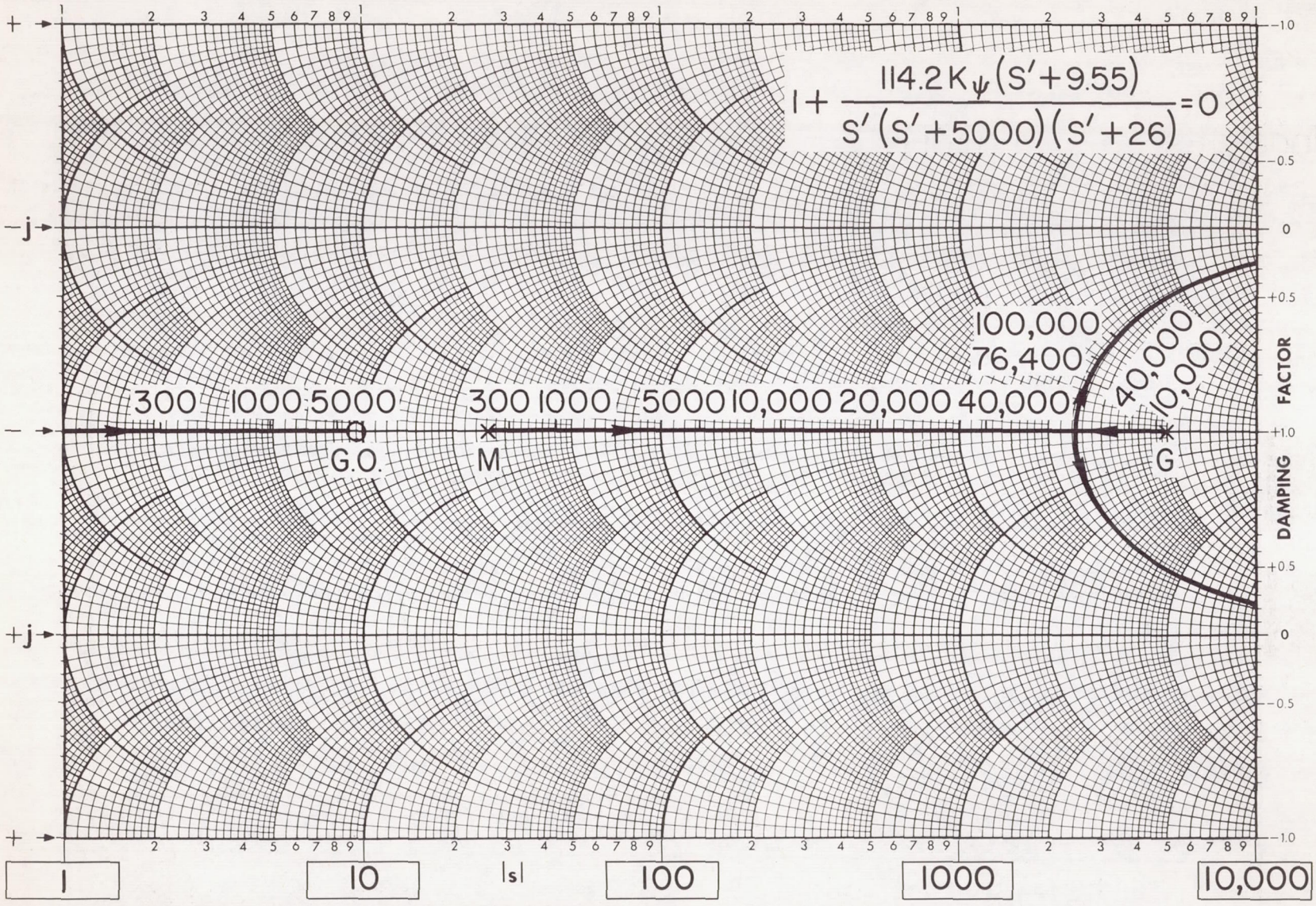

Figure 3.- Yaw stability.

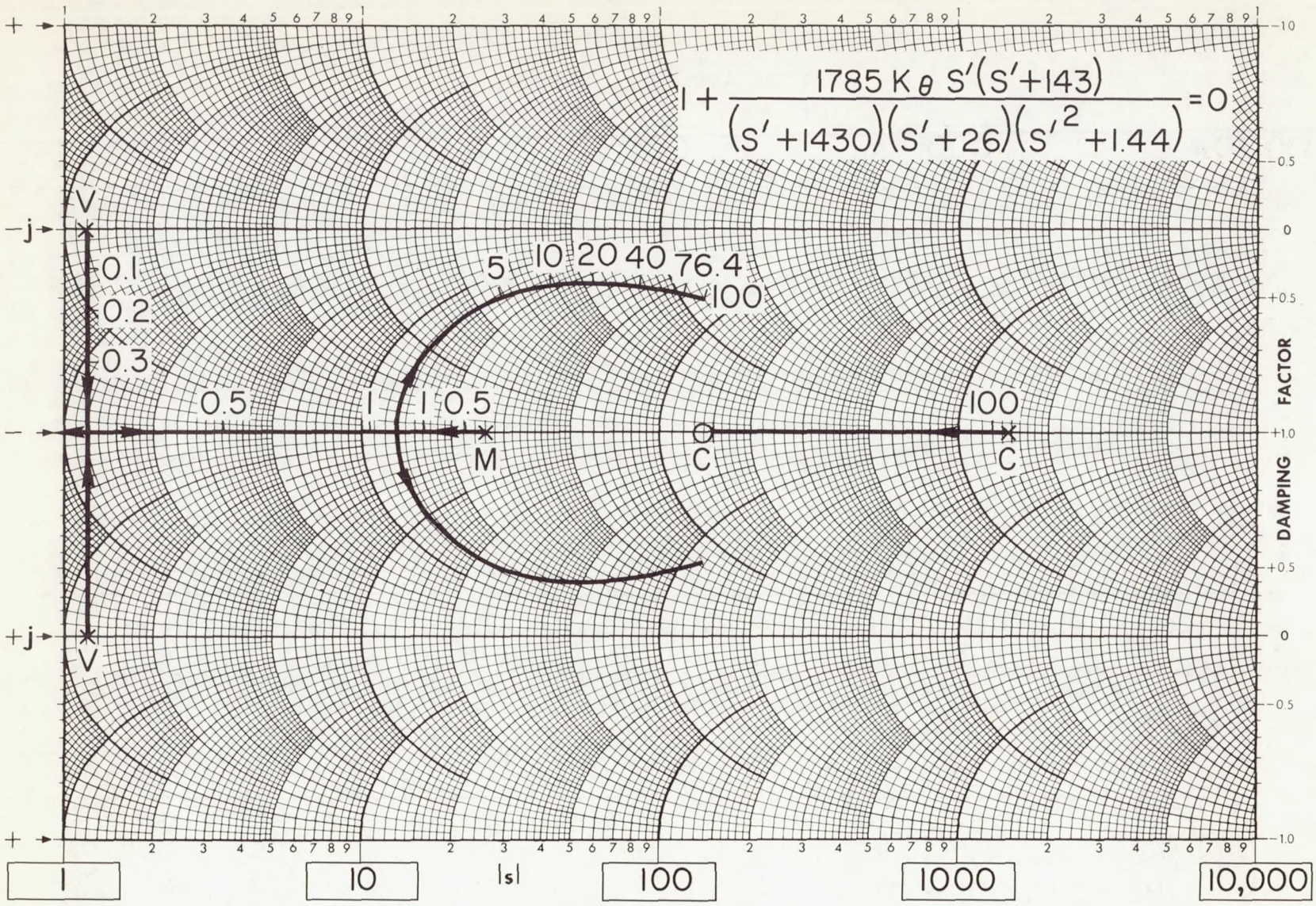

Figure 4.- Pitch stability.

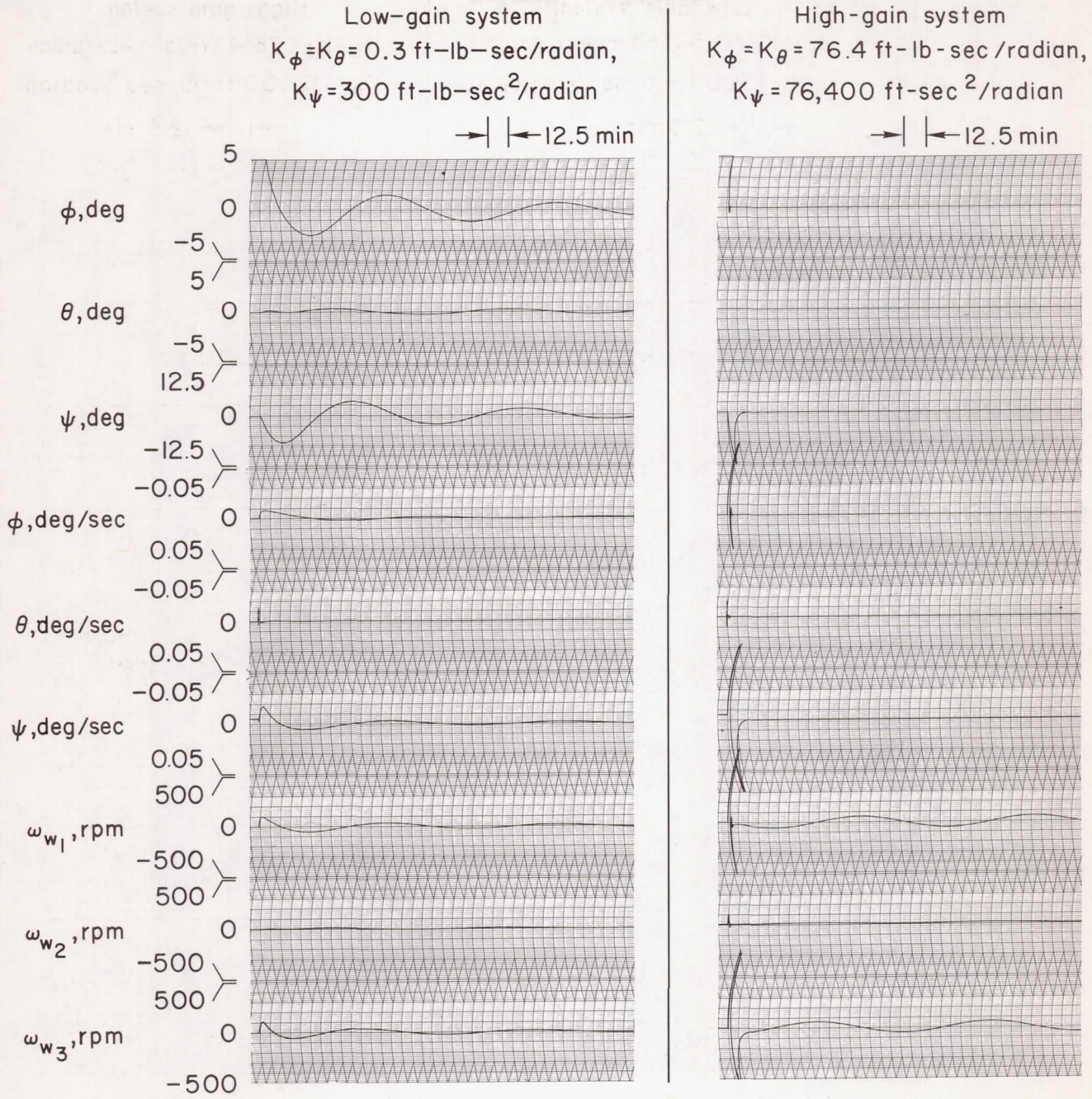

Figure 5.- Response from initial condition $\varphi = 5^\circ$; rate gyro ($\tau_g = 0.2$ sec) with orientation (0°, -6°, 0°).

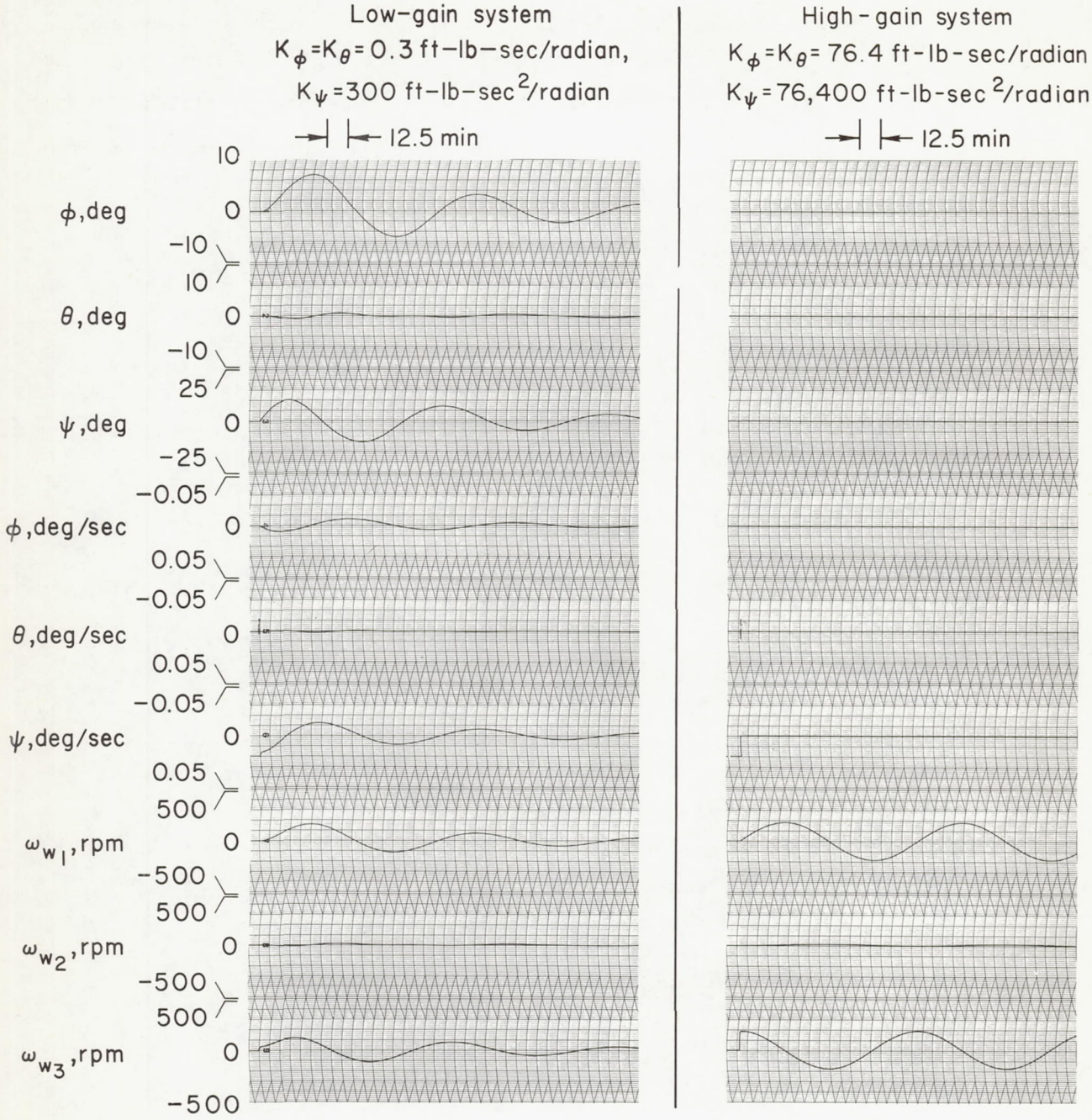

Figure 6.- Response from initial condition $\dot{\psi} = 0.02^\circ$/sec; rate gyro ($\tau_g = 0.2$ sec) with orientation (0°, -6°, 0°).

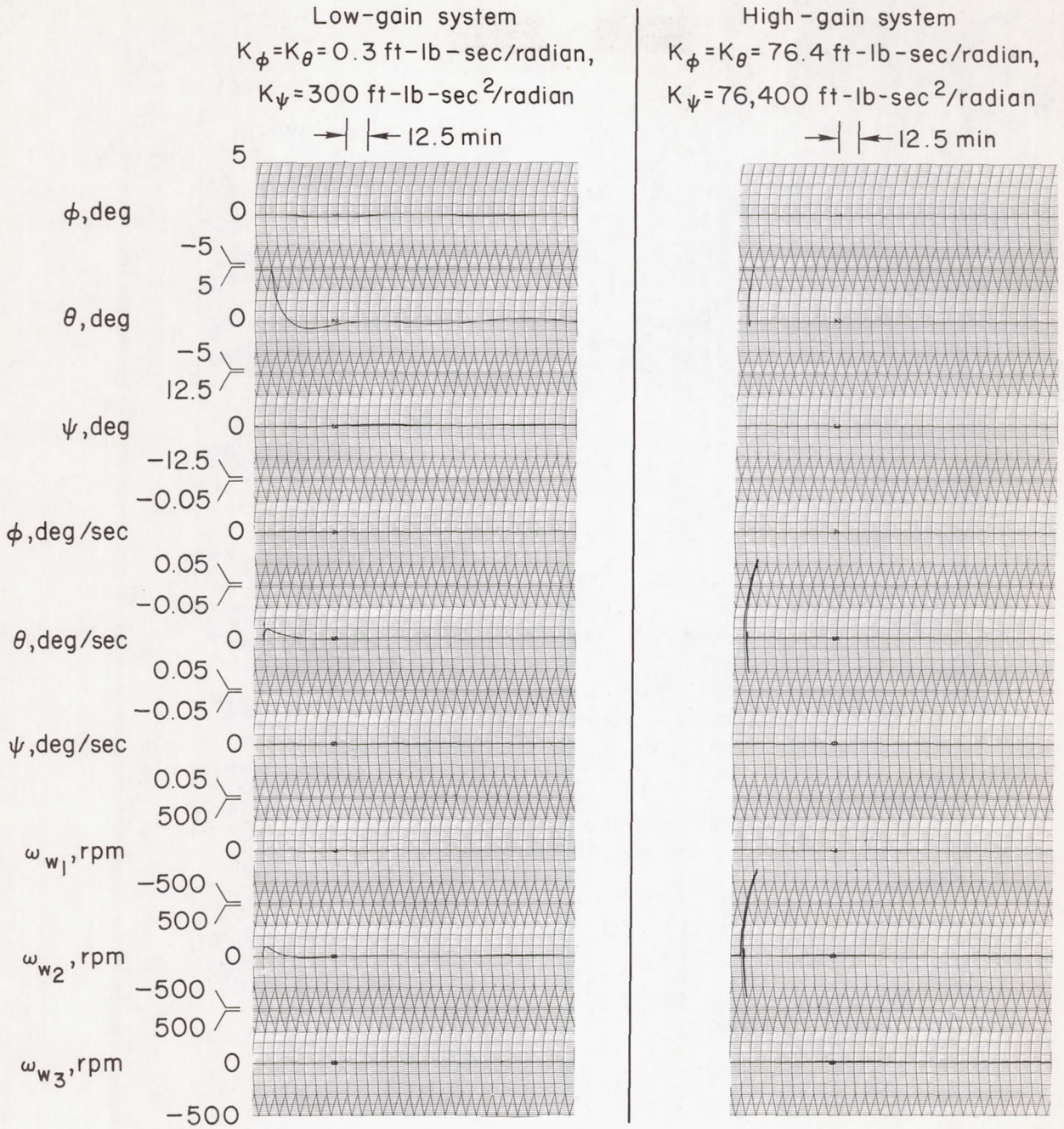

Figure 7.- Response from initial condition $\theta = 5^\circ$; rate gyro ($\tau_g = 0.2$ sec) with orientation (0°, -6°, 0°).

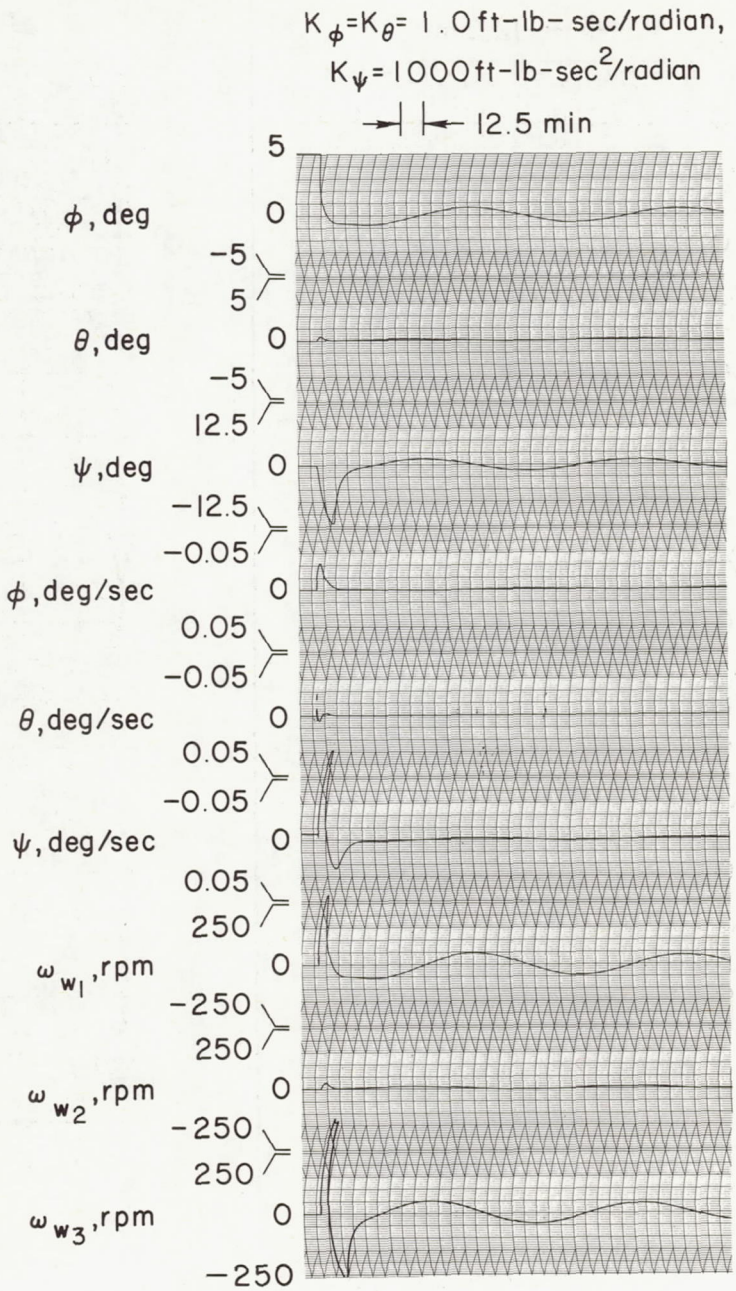

Figure 8.- Response from initial condition $\varphi = 5^\circ$; rate gyro ($\tau_g = 0.2$ sec) with orientation (0°, -6°, 0°).

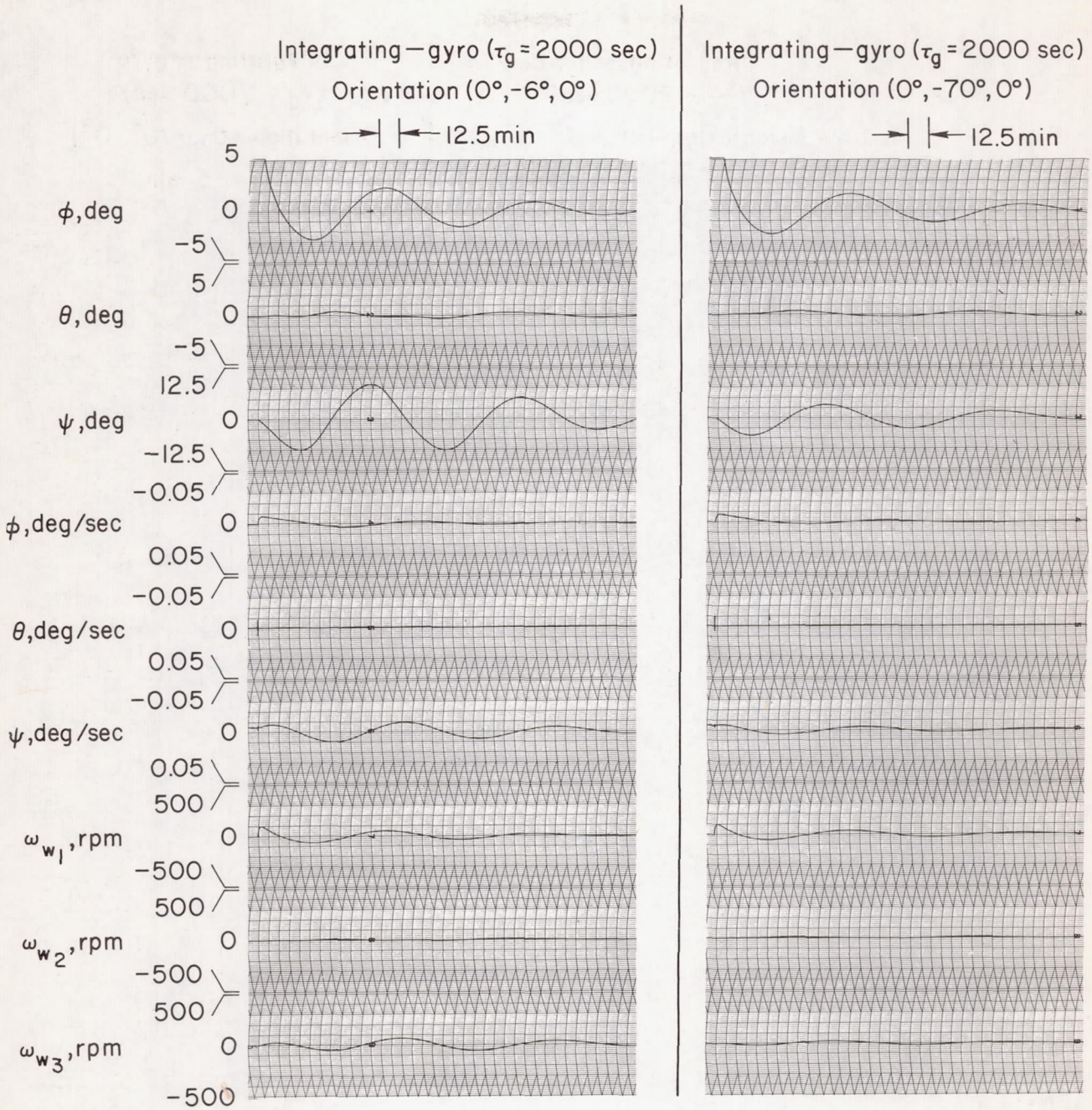

Figure 9.- Response from initial condition $\varphi = 5^{o}$; low-gain system $K_{\varphi} = K_{\theta} = 0.3$ ft-lb-sec/radian, $K_{\psi} = 300$ ft-lb-sec^2/radian.

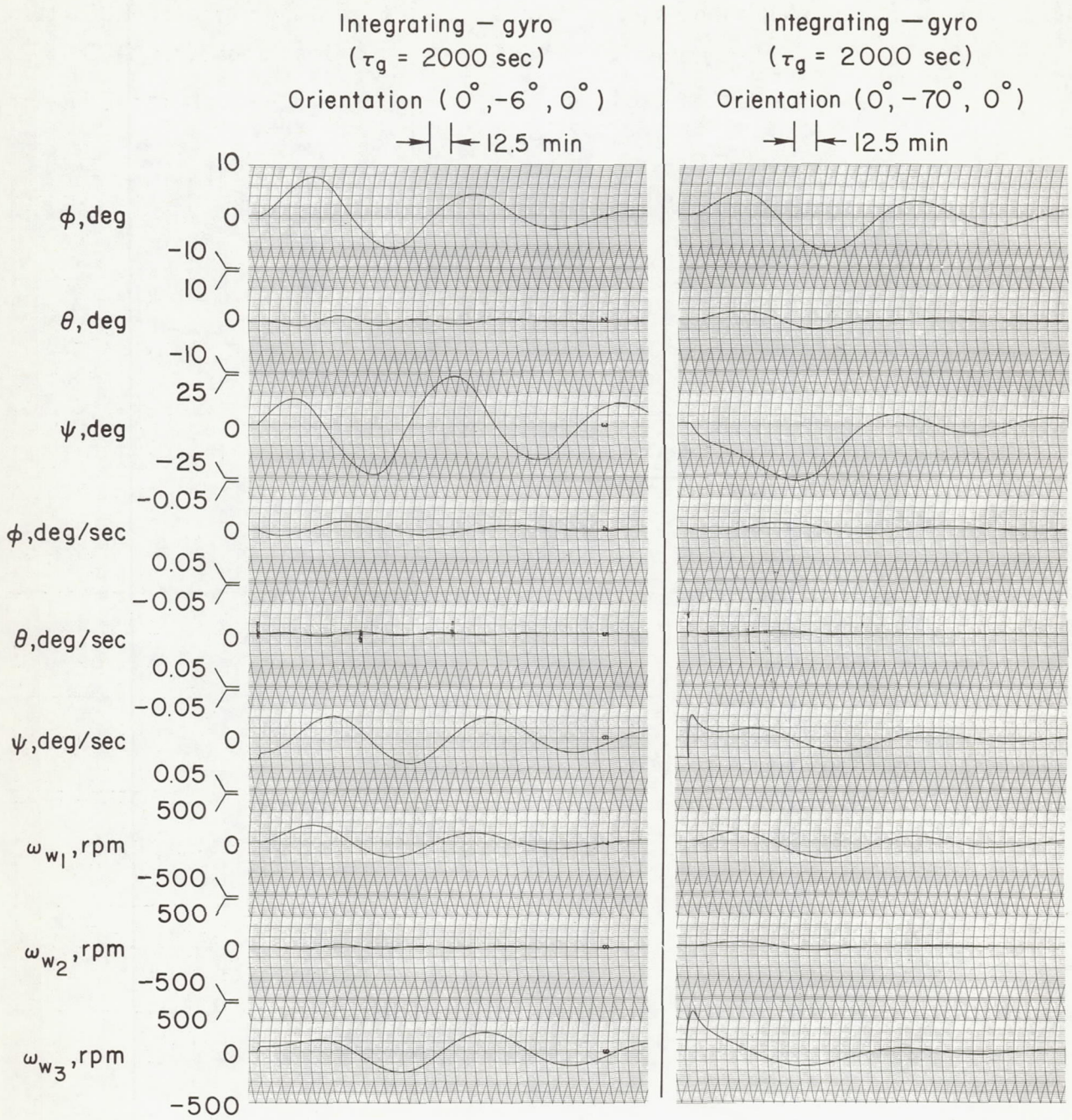

Figure 10.- Response from initial condition $\dot{\psi}$ = 0.02°/sec; low-gain system $K_\varphi = K_\theta$ = 0.3 ft-lb-sec/radian, K_ψ = 300 ft-lb-sec^2/radian.

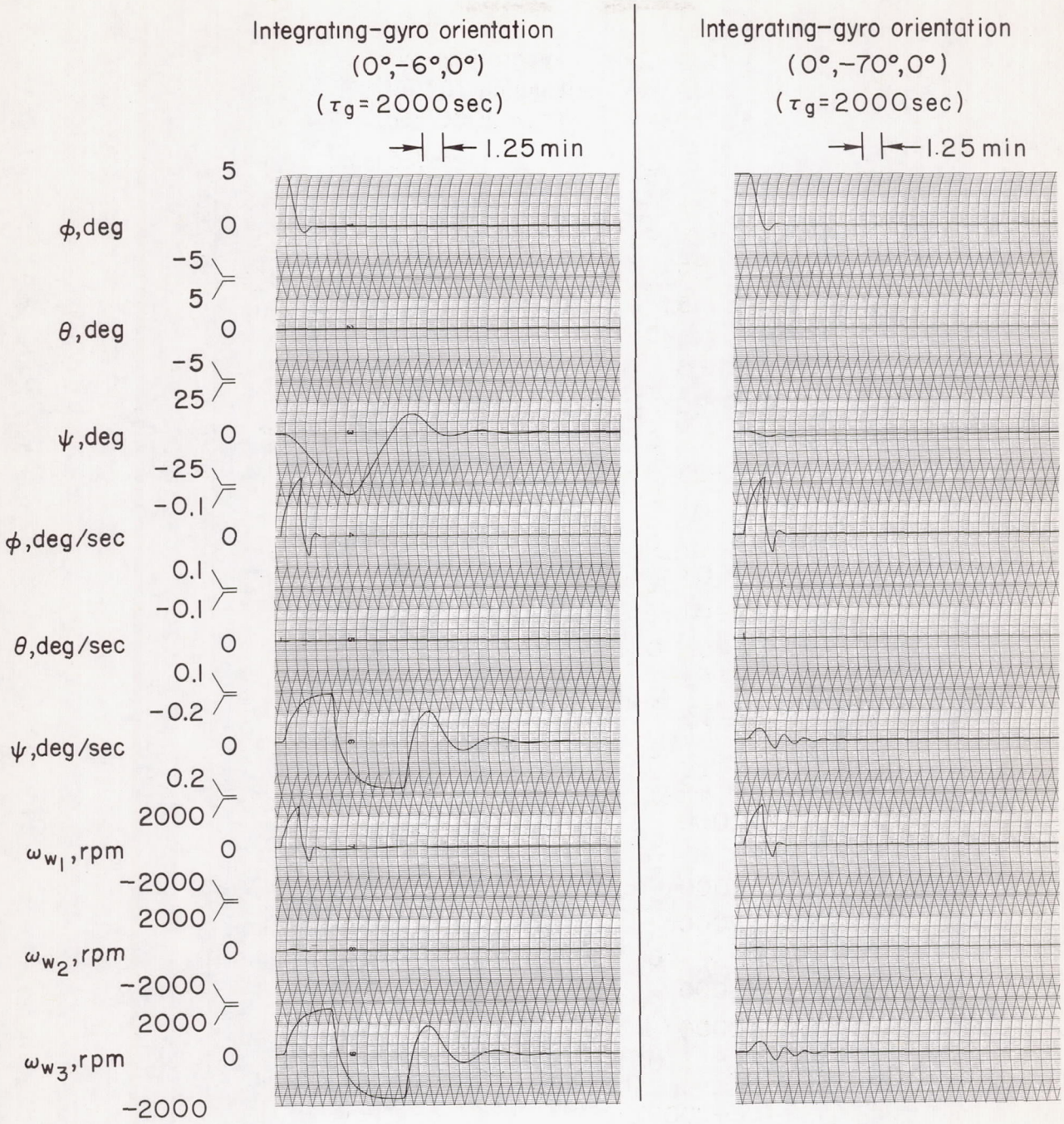

Figure 11.- Response from initial condition $\varphi = 5^{\circ}$; high-gain system $K_{\varphi} = K_{\theta} = 76.4$ ft-lb-sec/radian, $K_{\psi} = 76{,}400$ ft-lb-sec^2/radian.

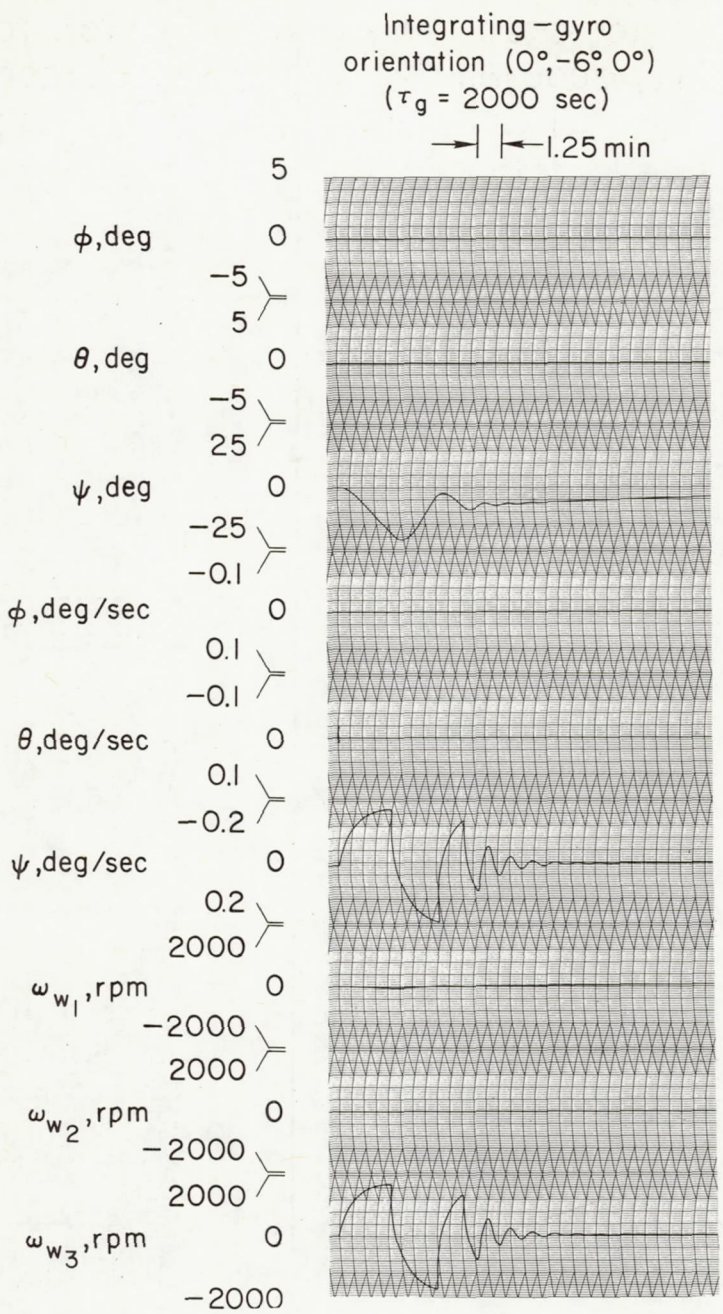

Figure 12.- Response from initial condition $\dot{\psi}$ = 0.005°/sec; high-gain system $K_\varphi = K_\theta$ = 76.4 ft-lb-sec/radian, K_ψ = 76,400 ft-lb-sec^2/radian.

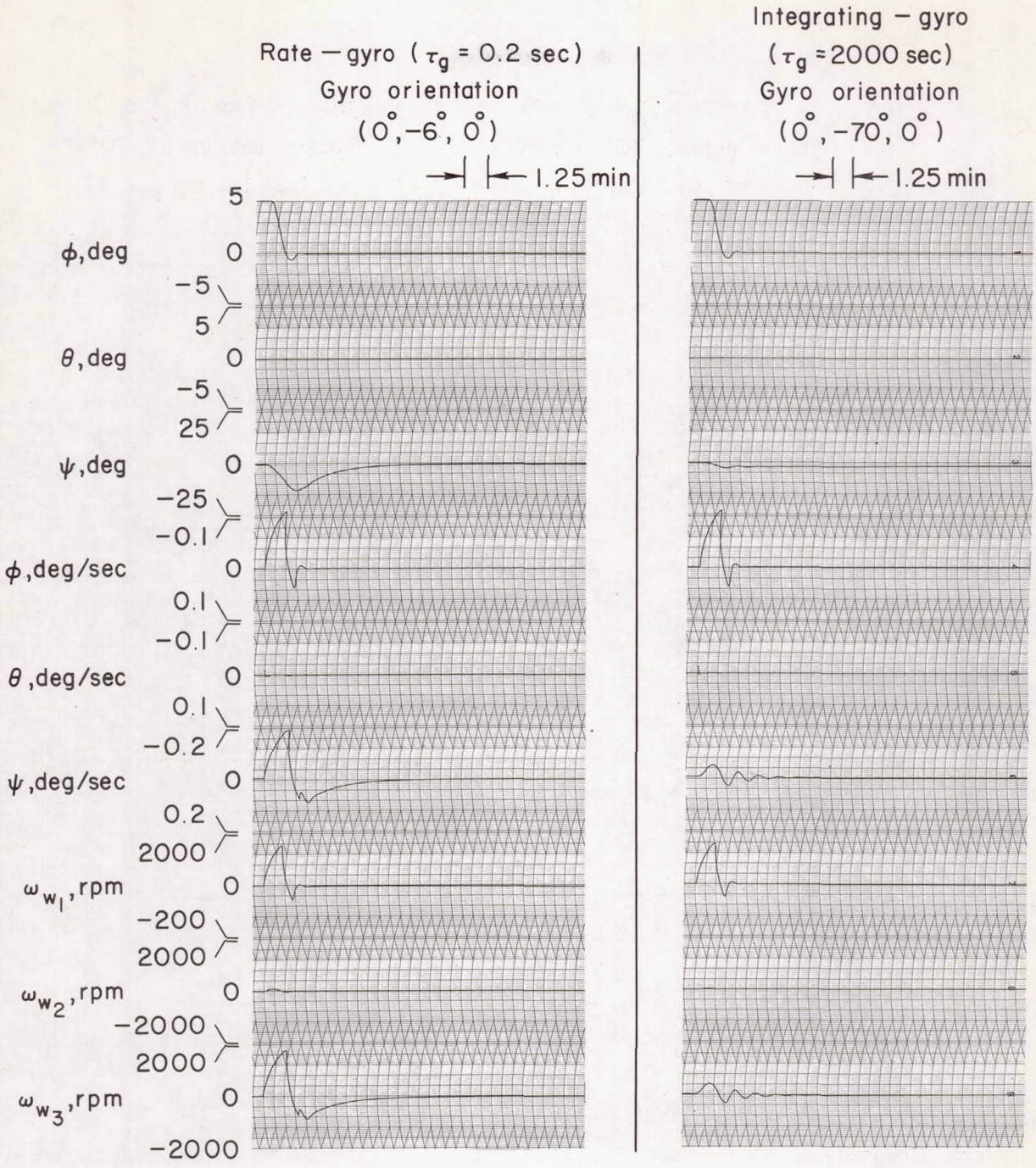

Figure 13.- Response from initial condition $\varphi = 5^{\circ}$; high-gain system $K_{\varphi} = K_{\theta} = 76.4$ ft-lb-sec/radian, $K_{\psi} = 76{,}400$ ft-lb-sec^2/radian.

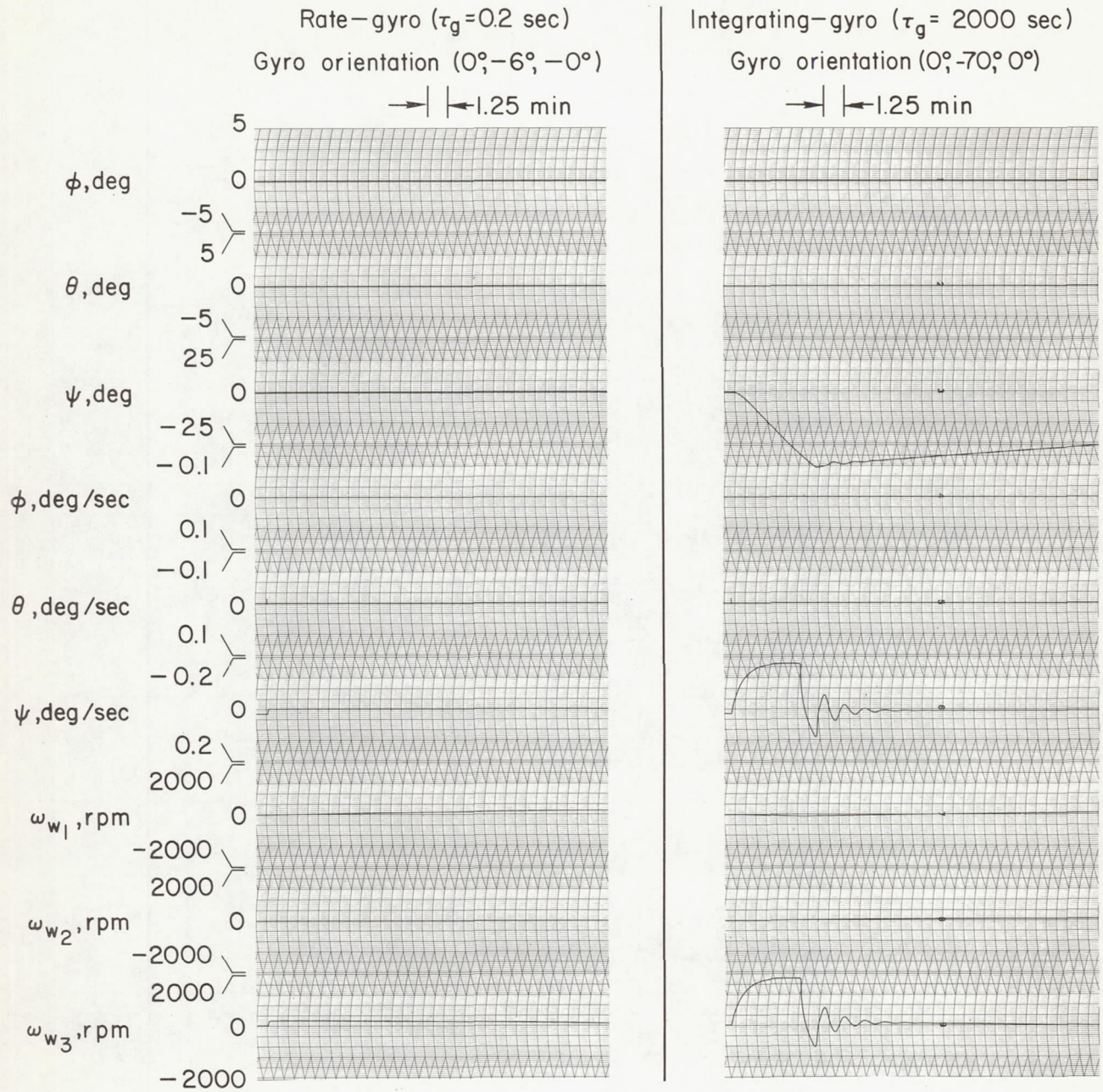

Figure 14.- Response from initial condition $\dot{\psi}$ = 0.02°/sec; high-gain system $K_\varphi = K_\theta$ = 76.4 ft-lb-sec/radian, K_ψ = 76,400 ft-lb-sec^2/radian.

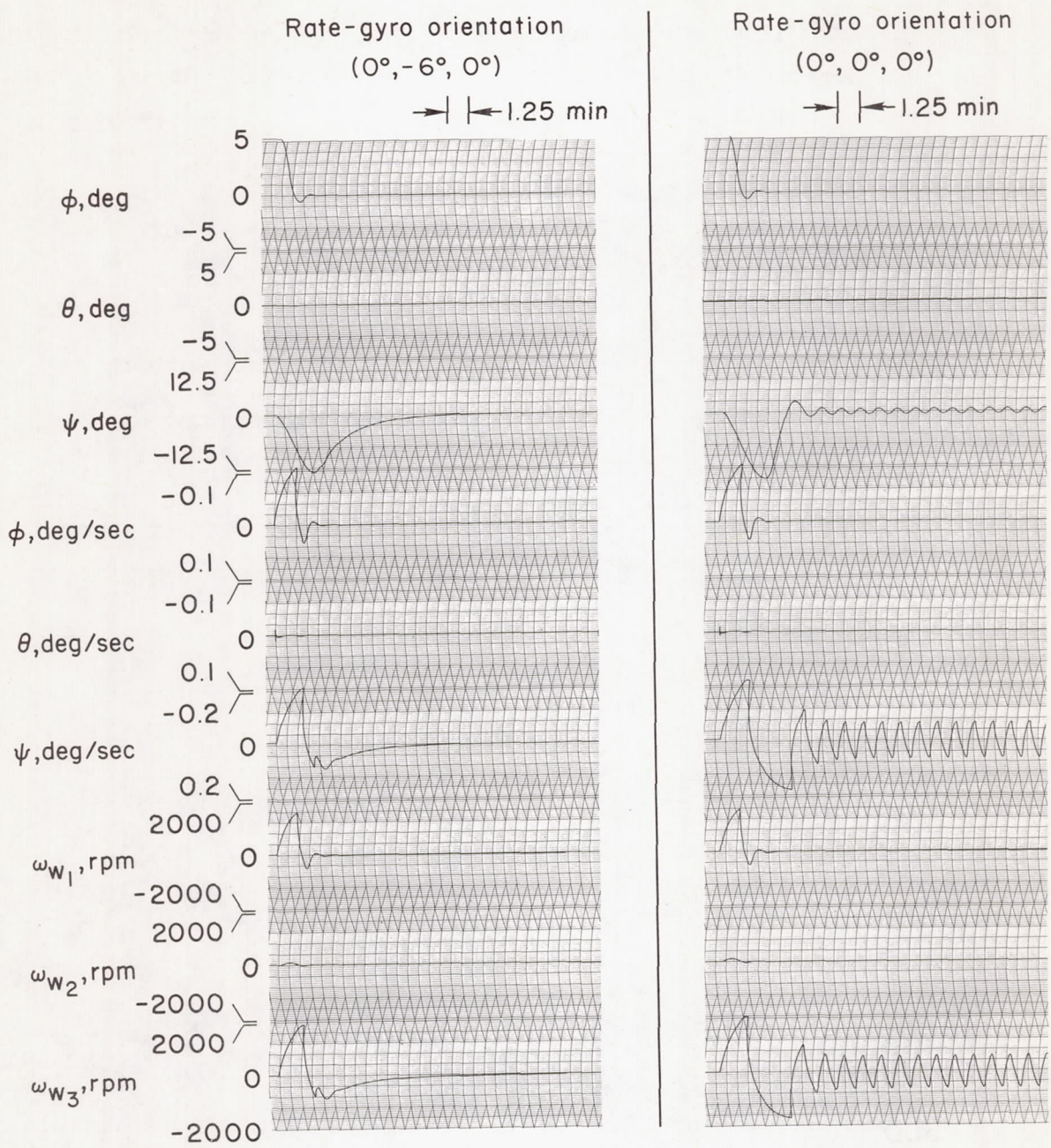

Figure 15.- Response from initial condition $\varphi = 5^{\circ}$; high-gain system $K_{\varphi} = K_{\theta} = 76.4$ ft-lb-sec/radian, $K_{\psi} = 76{,}400$ ft-lb-sec^2/radian.

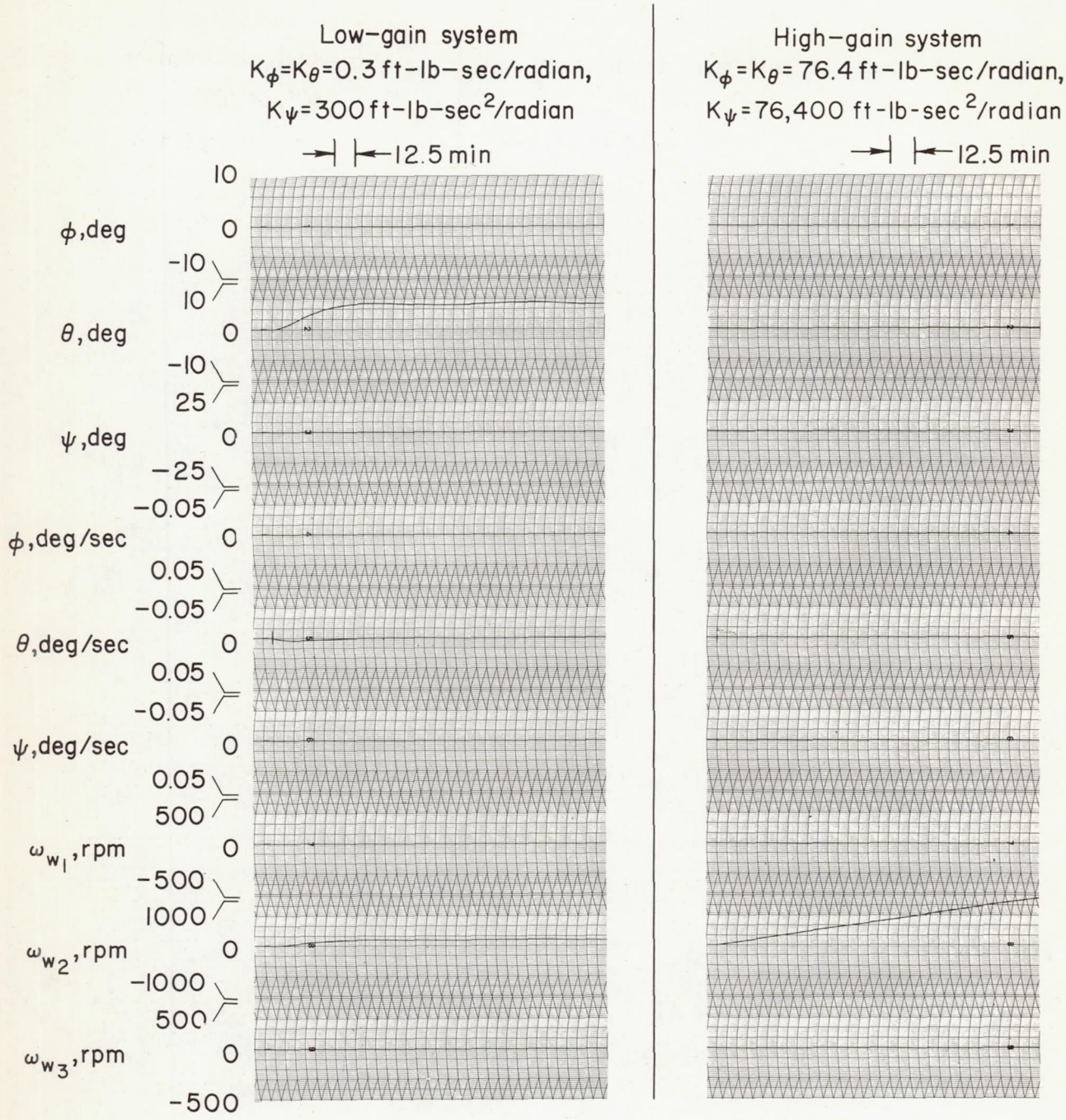

Figure 16.- Effect of 5° axis misalinement in pitch (initial orientation angles and rates zero); rate gyro (τ_g = 0.2 sec) with orientation (0°, -6°, 0°).

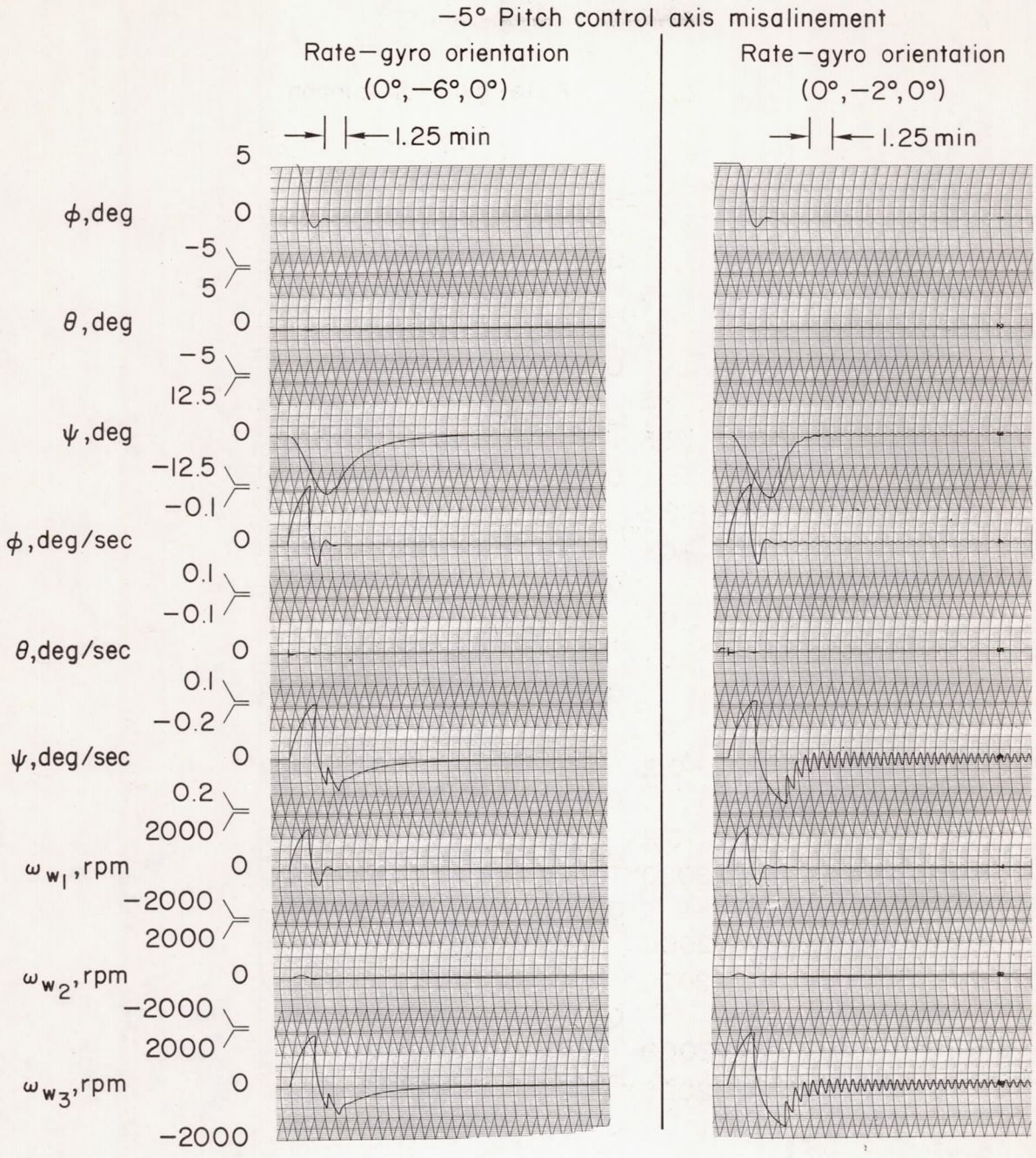

Figure 17.- Response from initial condition $\varphi = 5^{\circ}$; high-gain system $K_{\varphi} = K_{\theta} = 76.4$ ft-lb-sec/radian, $K_{\psi} = 76{,}400$ ft-lb-sec^2/radian.

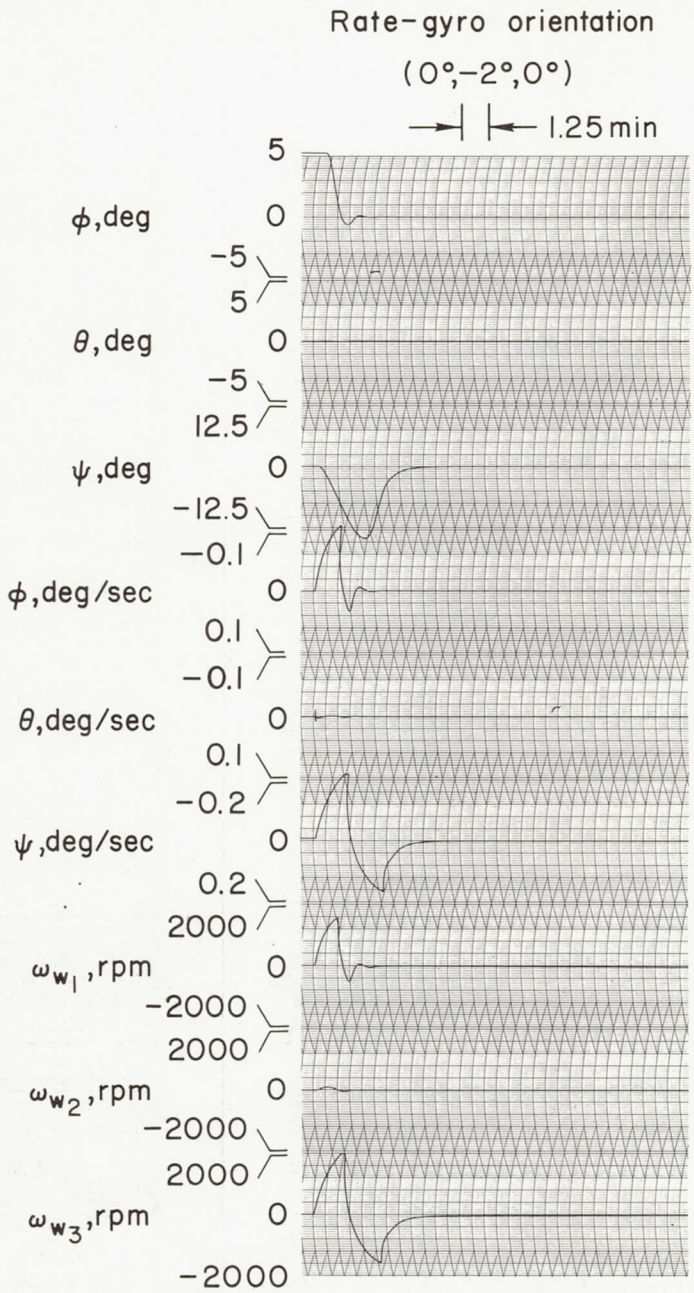

Figure 18.- Response from initial condition $\varphi = 5^{\circ}$; high-gain system $K_{\varphi} = K_{\theta} = 76.4$ ft-lb-sec/radian, $K_{\psi} = 76{,}400$ ft-lb-sec^2/radian.

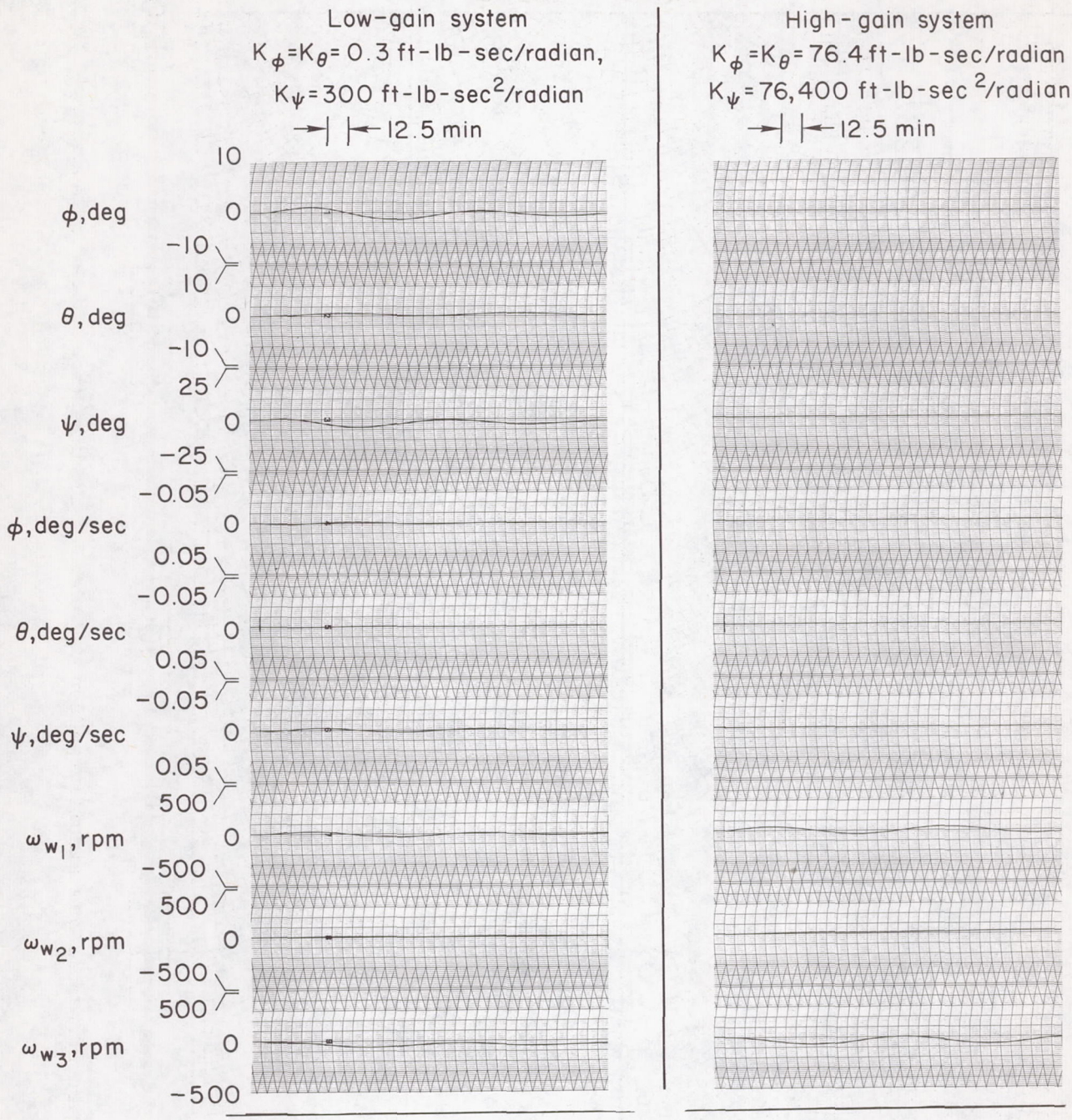

Figure 19.- Effect of 5° axis misalinement in roll (initial orientation angles and rates zero); rate gyro (τ_g = 0.2 sec) with orientation (0°, -6°, 0°).

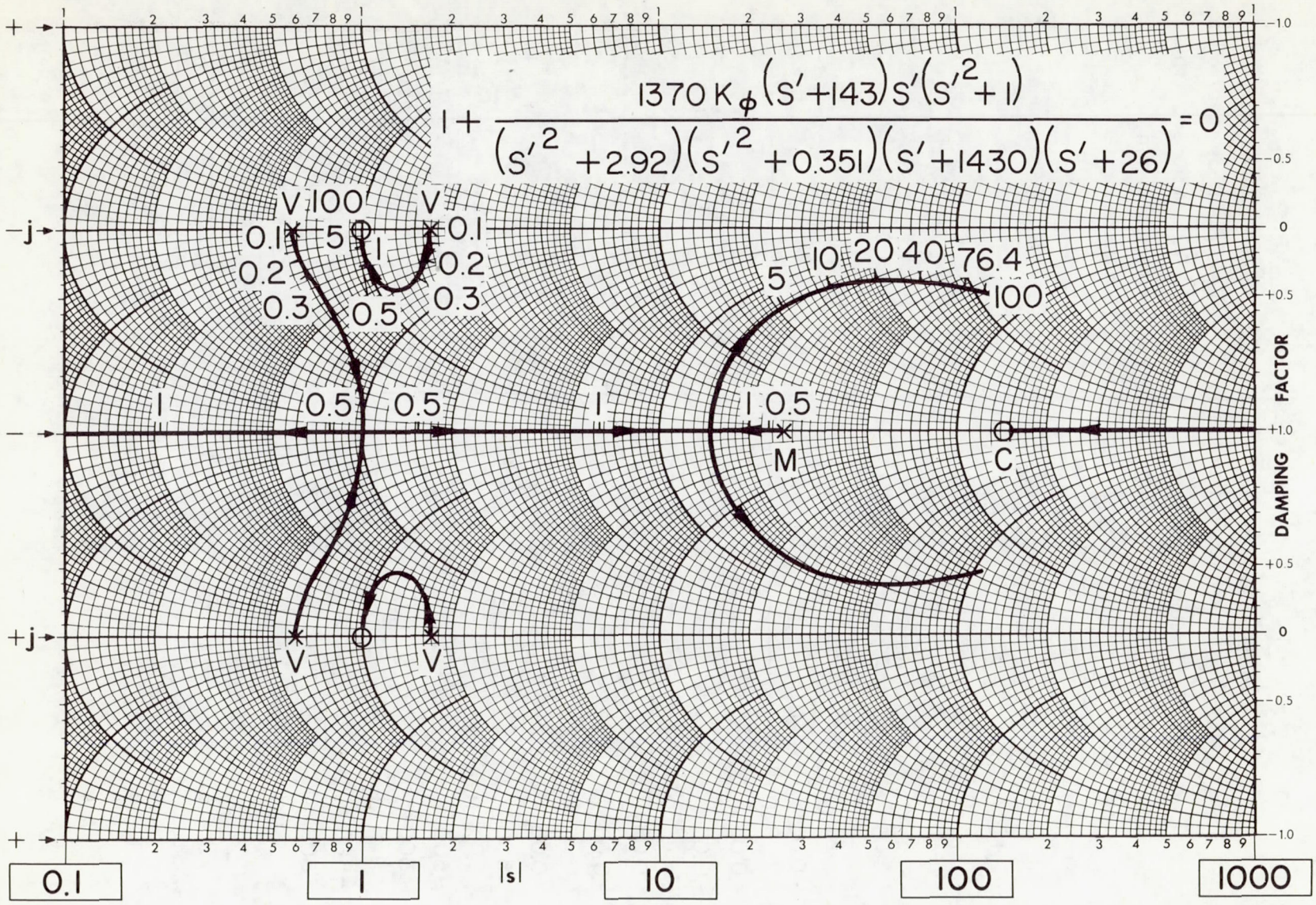

Figure 20.- Roll-yaw stability after yaw channel failure (h_{2K} = 0.2 ft-lb-sec).

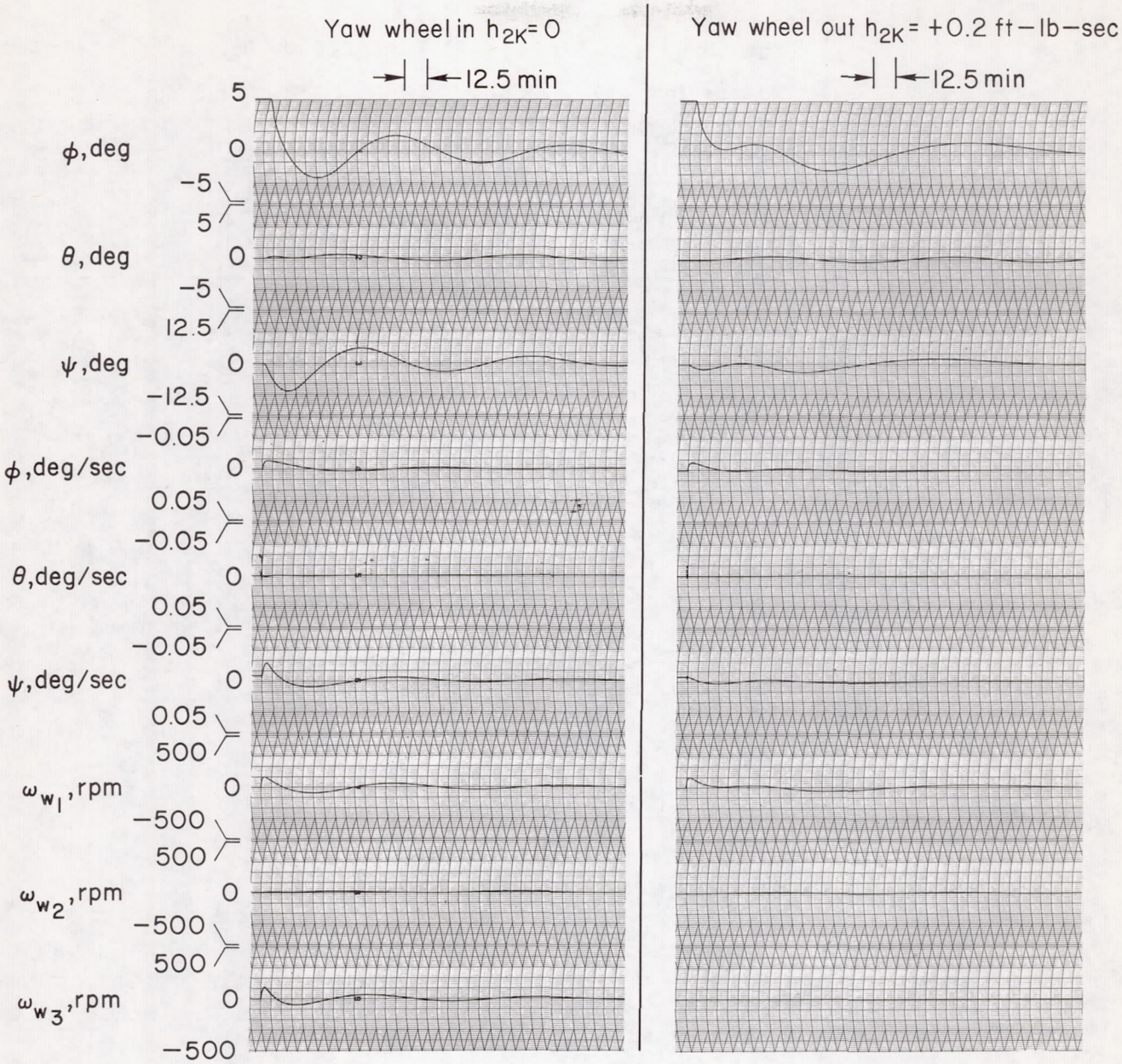

Figure 21.- Response from initial condition $\varphi = 5^{\circ}$; low-gain system $K_{\varphi} = K_{\theta} = 0.3$ ft-lb-sec/radian, $K_{\psi} = 300$ ft-lb-sec^2/radian; rate gyro ($\tau_g = 0.2$ sec) with orientation (0°, -6°, 0°).

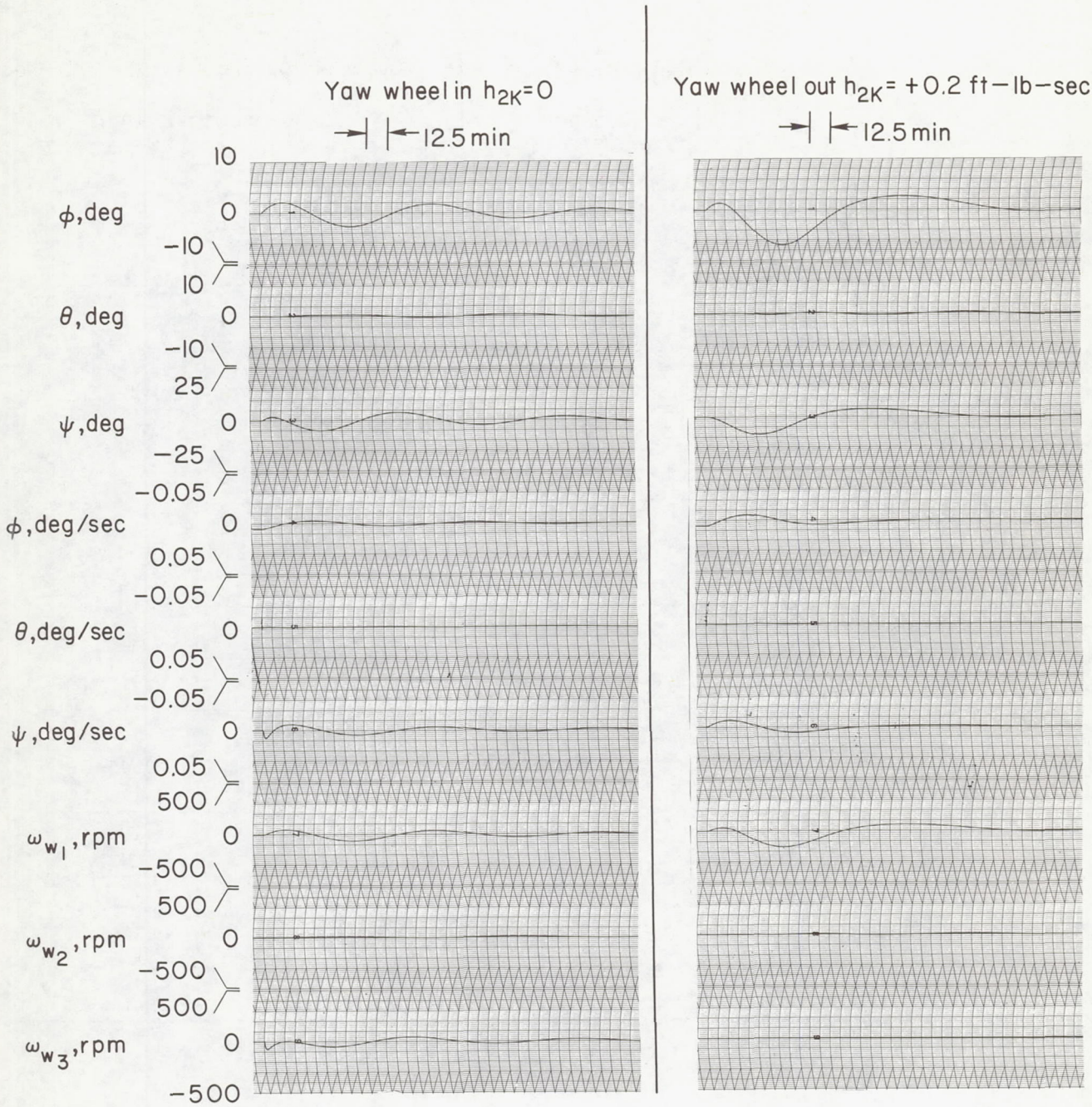

Figure 22.- Response from initial condition $\dot{\phi}$ = 0.005°/sec; low-gain system $K_\varphi = K_\theta$ = 0.3 ft-lb-sec/radian, K_ψ = 300 ft-lb-sec^2/radian; rate gyro (τ_g = 0.2 sec) with orientation (0°, -6°, 0°).

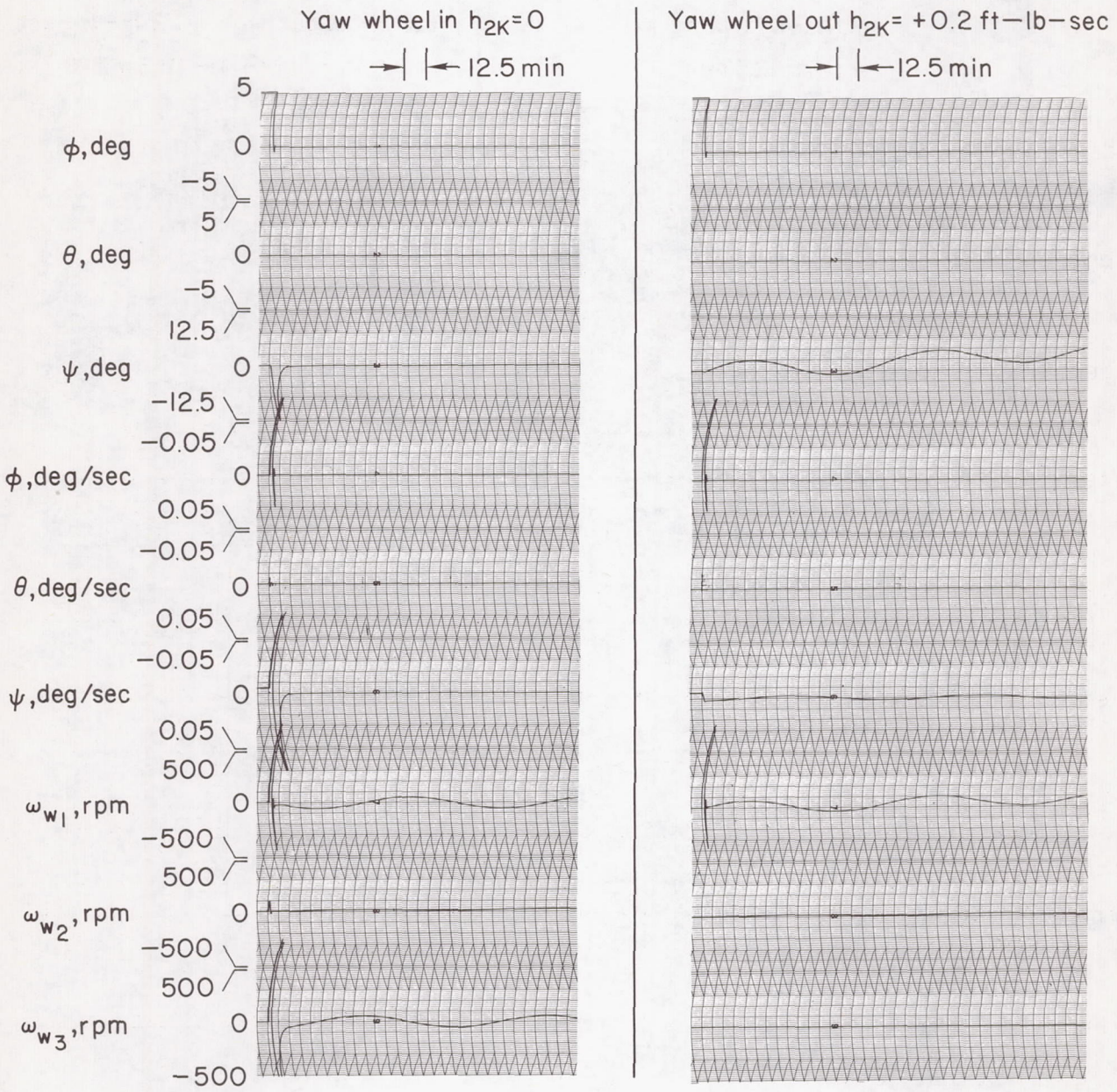

Figure 23.- Response from initial condition $\varphi = 5^{\circ}$; high-gain system $K_{\varphi} = K_{\theta} = 76.4$ ft-lb-sec/radian, $K_{\psi} = 76{,}400$ ft-lb-sec^2/radian; rate gyro ($\tau_g = 0.2$ sec) with orientation (0°, -6°, 0°).

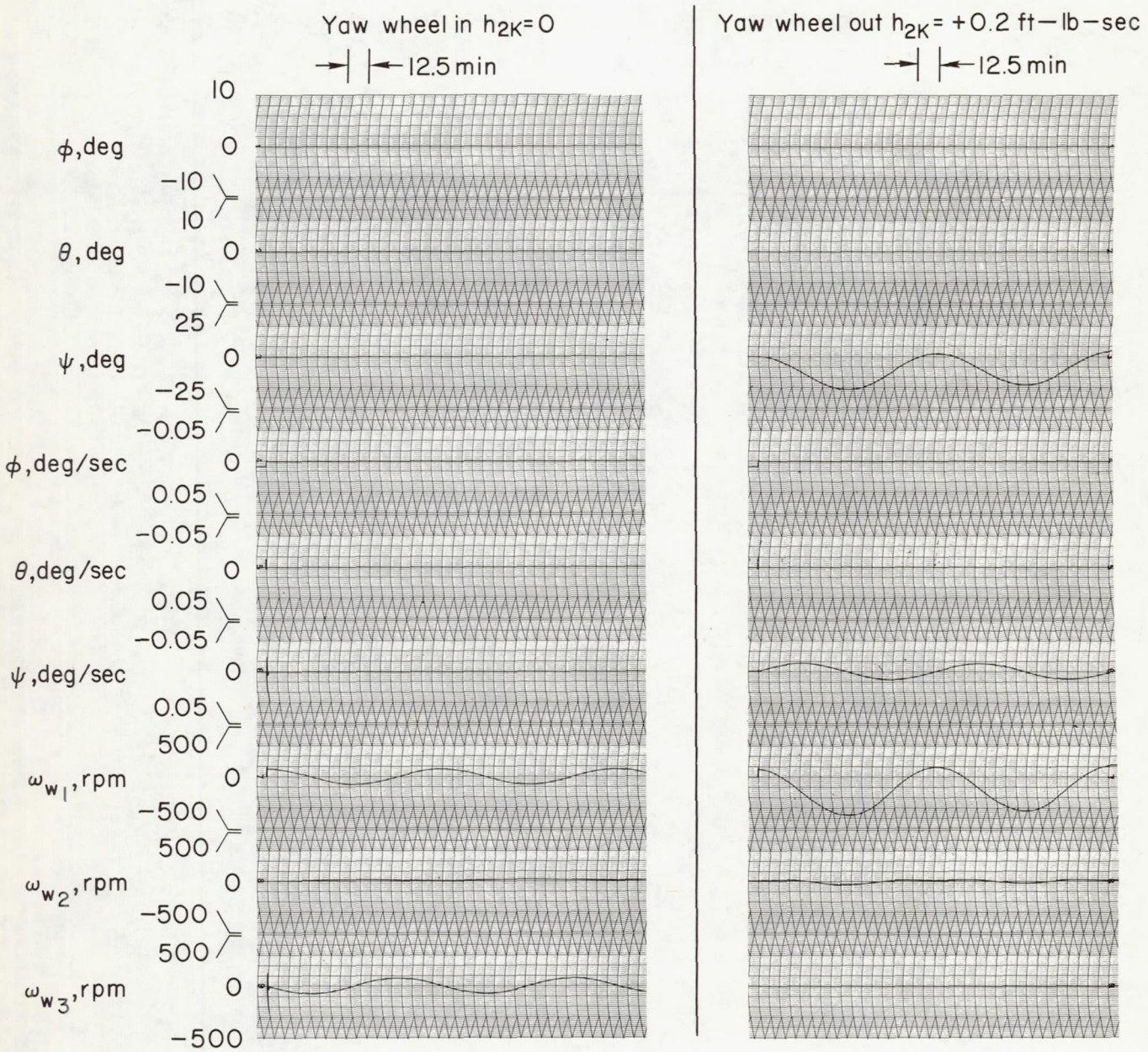

Figure 24.- Response from initial condition $\dot{\phi} = 0.005^{\circ}$/sec; high-gain system $K_{\phi} = K_{\theta} = 76.4$ ft-lb-sec/radian, $K_{\psi} = 76{,}400$ ft-lb-sec^2/radian; rate gyro ($\tau_g = 0.2$ sec) with orientation (0°, -6°, 0°).

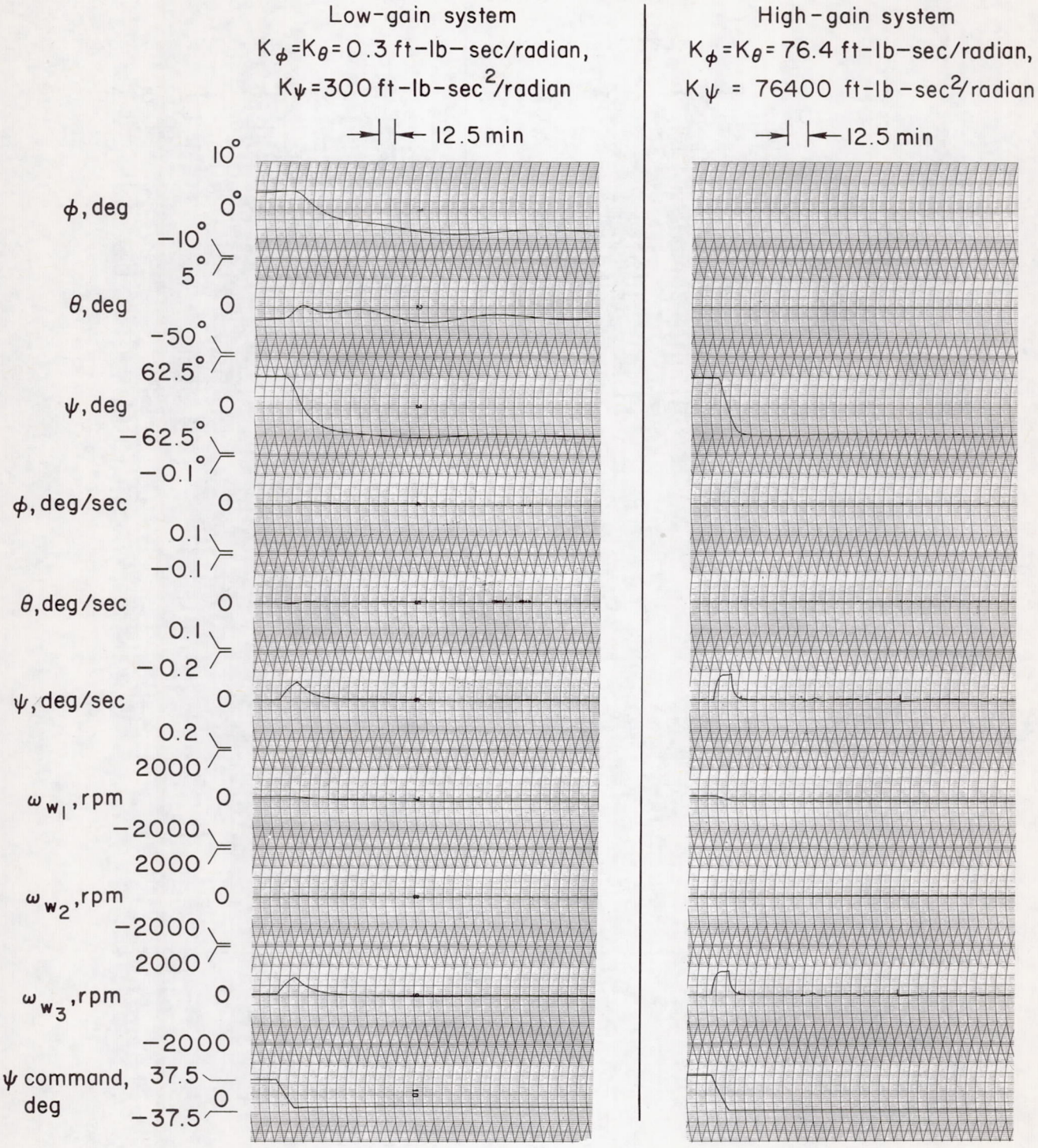

Figure 25.- Response to yaw bias signal (rate-gyro orientation 0°, -6°, 0°).

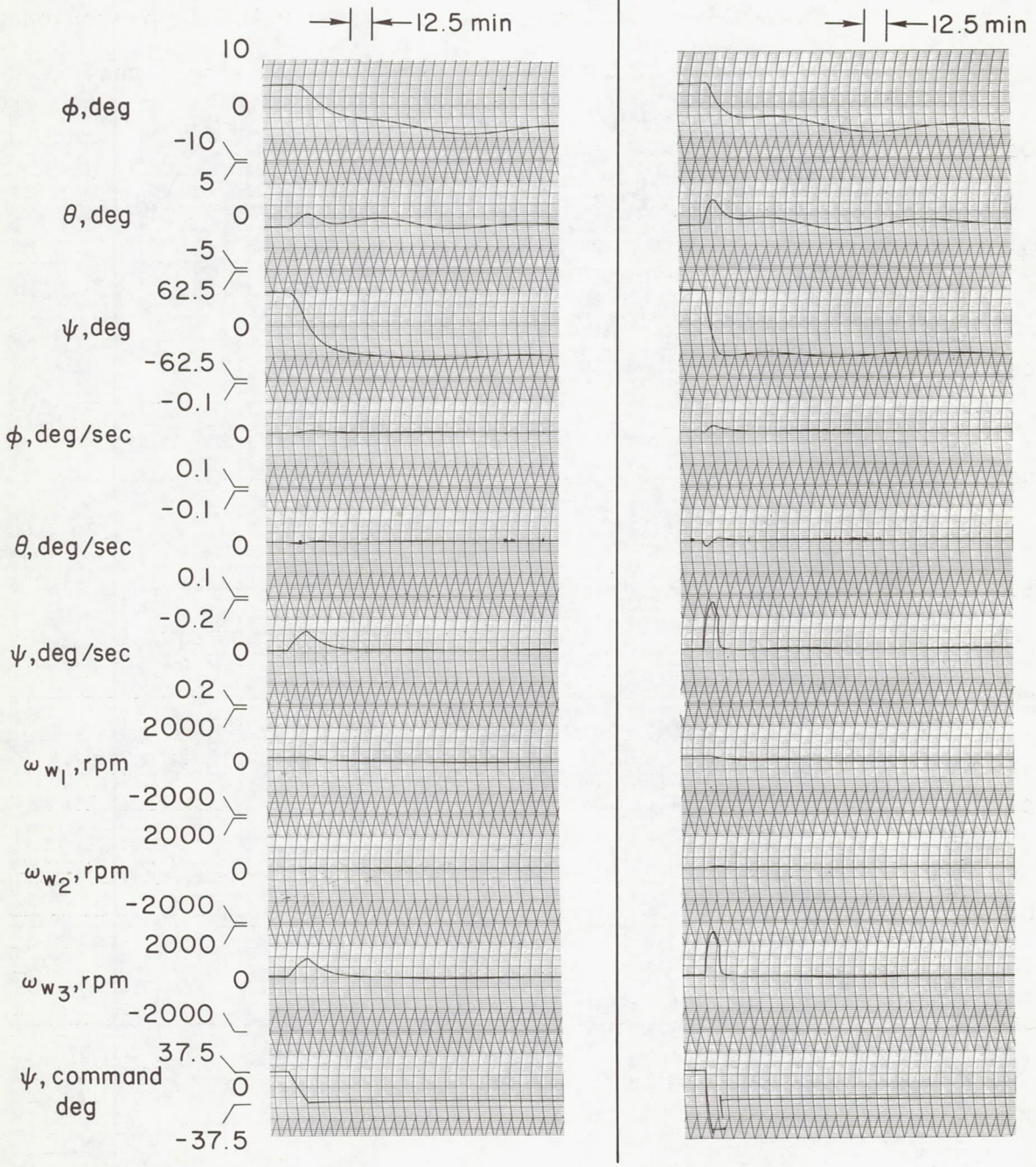

Figure 26.- Response to yaw bias signal (low-gain system $K_\varphi = K_\theta = 0.3$ ft-lb-sec/radian, $K_\psi = 300$ ft-lb-sec^2/radian); rate-gyro orientation (0°, -6°, 0°).